Molecular mechanisms that control synapse number and activity

Elena Santana Martín

Universidad Autónoma de Madrid

Programa de doctorado en Biociencias Moleculares

Departamento de Biología Molecular
Facultad de Ciencias
Universidad Autónoma de Madrid

Molecular mechanisms that control synapse number and activity

Elena Santana Martín licenciada en Biologñia por la Universidad Autónoma de Madrid.

Directores de tesis: Sergio Casas-Tintó y Alberto Ferrús

Tesis realizada en el Departamento de Neurobiología Molecular, Celular y del Desarrollo del Instituto Cajal

Abbreviations

Upstream Activation Sequence (UAS)
Neuromuscular junction (NMJ)
Segmental nerves (SN)
Transverse nerve (TN)
Active zone (AZ)
Action potential (AP)
Discs large (Dlg)
Leucine-rich repeat (LRR)
Dally-like (Dlp)
Fasciclin (Fas)
Bone Morphogenetic Protein (BMP)
Wingless (wg)
Connectin (Con)
Microtubule cytoskeleton (MT)
Arrow (arr)
Frizzled2 (Fz2)
Dishevelled (dsh)
Bruchpilot (Brp)
Ubiquitin-proteasome system (UPS)
Highwire (Hiw)
Wallenda (Wnd)
Mitogen-activated protein kinase (MAP kinase)
LIM kinase (LIMK)
Wishful thinking (Wit)
Phosphatidylinositol-4,5-biphosphate 3-kinase (PI3K)
mammalian Target of Rapamycin (mTOR)
Protein Kinase B (AKT)
CAST (CAZ-associated structural protein)
ERC (ELKS-Rab6-interacting protein)
Soluble NSF Attachment Protein (SNARE)
Synaptobrevin (Syb)
Vesicle associated membrane protein (VAMP2)
Guanosine-5’-triphosphate (GTP)
Guanosine-5’-diphosphate (GDP)
Calcium Binding Proteins (CBP)
Calcium sensor proteins (CSP)
Neural Calcium Sensor 1 (NCS-1)
Frequenin (Frq)
Calcium/calmodulin-dependent protein kinase II (CaMKII)
Messenger ribonucleoprotein complexes (mRNP)
mRNA binding proteins (RBPs)
Fragile X Mental Retardation Protein (FMRP)
Processing bodies (P bodies)
microRNAs (miRNAs)
Glutamate Receptor (GluR)
Autism Spectrum Disorders (ASD)
Homeotic (Hox)
Antennapedia (Antp)
Ultrabithorax (Ubx)
Abdominal (abd)
Self-righting node neurons (SNR)
Acyl protein thioesterase 1(APT1)
Cytoplasmic Polyadenylation element binding protein (CPEB)

Contents

1. Summary

Synapse contacts are the primary form of communication between neurons. In this work, we explore how synapses are created, maintained and dismantled. We studied three different signaling mechanisms which induce changes at the larval neuromuscular junction of *Drosophila melanogaster*. We focused on two major aspects of neural function, synapse number and transmission.

The study on PI3K signaling has revealed the functional hierarchical order of up- and down-stream components of the pathway. In addition, that study uncovered a second, antagonistic signaling pathway. Elements of the pro- and anti-synaptogenic pathways cross-regulate each other suggesting that the actual number of synapses that a neuron establishes results from a delicate equilibrium between synapse formation and elimination.

The second study which composes this PhD project addresses the functional interaction between the Guanine Exchange Factor Ric8a and the calcium sensor Frq2, known in vertebrates as NCS-1. It describes how these two proteins contribute to determine the number of synapses and the probability of neurotransmitter release per synapse. Interestingly, these two synaptic features are regulated in opposite directions by the interaction Ric8a/Frq.

Finally, the third study relates to Orb2, a protein involved in learning and memory in the adult, which acts as a pro-synaptogenic signal during developmental stages. Orb2 induces local translation of one of its target mRNA, the one that encodes the transcription factor Brat, through its structural transition from monomer (repressor) to oligomers (activator). Finally, Brat modulates synapse number, presumably through the regulation of genes encoding synapse components.

1. Resumen

Los contactos sinápticos constituyen la principal forma de comunicación entre neuronas. En este trabajo, exploramos cómo se crean, mantienen y destruyen las sinapsis. Para ello utilizamos tres mecanismos de señalización diferentes que inducen cambios en la terminación neuromuscular de *Drosophila melanogaster.* Nos centramos en los dos aspectos principales que definen la función neural, número de sinapsis y transmisión.

El estudio sobre la vía de PI3K muestra una relación funcional jerárquica entre elementos de la vía. Además, este estudio explora una segunda vía antagónica de la primera. Los elementos pro y anti-sinaptogénicos se regulan entre ellos, sugiriendo que el número de sinapsis de una neurona es el resultado de un delicado equilibrio entre formación y eliminación de sinapsis.

El segundo trabajo que compone este proyecto de doctorado determina la relación funcional entre el factor de intercambio de Guanina Ric8 y el sensor de calcio Frq2, conservado en vertebrados como NCS-1. El estudio describe cómo dos proteínas contribuyen al establecimiento de sinapsis y la probabilidad de liberación de neurotransmisor por sinapsis.

Finalmente, el tercer estudio describe el papel de Orb2, una proteína relacionada con aprendizaje y memoria en el adulto, como elemento pro-sinaptogénico durante estadios larvarios.

Orb2 induce la traducción local del RNA mensajero de una de sus proteínas diana, que codifica el factor de transcripción Brat, a través del cambio conformacional de Orb2 de monómero (represor) a oligómero (activador). Además, Brat regula el número de sinapsis, probablemente regulando la transcripción de genes sinápticos.

2. Introduction

Neuronal function is the major determinant of behavior and changes deviant from normalcy lead to neural diseases and cognitive impairments. This neuronal function is highly determined by the synapse number. Synapses are dynamic structures which constitute the contact points between neurons or neurons with their target tissue.

Synapse number can be influenced by several factors such day/light cycle, learning experiences or age [1-4]. Relatively small changes in synapse number can induce remarkable changes in behavior [5]. Moreover, synapse loss is one of the early events in many neurodegenerative diseases such Alzheimer and Parkinson diseases [6]. Schizophrenia patients exhibit a mild loss of inhibitory synapses [7]. But not only synapse loss is necessary to induce neural impairments. Modifications in glutamatergic circuits which increase the synapse number can lead to epilepsy episodes [8]. An excess of dendritic spines or lack of maturation results in Fragile-X syndrome or Down syndrome [9, 10]. These features underscore the importance of an accurate equilibrium between excitatory and inhibitory inputs for normal function.

The second major aspect that affects neuron activity is neurotransmitter release. The neuronal language is encoded by spikes and transmitted through synaptic contacts. After neuronal stimulation Ca^{+2} enters to the presynaptic site triggering the release of neurotransmitters stored in synaptic vesicles. Neurotransmitters bind to ligands and induce responses at the postsynaptic site. This is considered a fast (1 millisecond) and primary form of communication between neurons. Changes in the probability of neuron firing determines long-term potentiation and depression [11, 12], which represent the basis for memory formation.

Mutations in the *presenilin* genes, which cause familial Alzheimer's disease, induce vesicle defects [13]. Other pathologies such mental retardation and autism have mutations in genes regulating Ca^{+2} influx at the presynaptic site [14]. These evidences sustain the relevance of a proper regulation of the synapse.

Synapses are complex structures and its components are tissue or process-specific. Nevertheless, most synapses have common elements and are suitable to be modified by similar mechanisms. These modifications are conserved among species which allows us the study of complex pathways in relatively simple models. In this context, we took advantage of the neuromuscular junction of *Drosophila melanogaster* to study synapse dynamics.

2.1. Drosophila melanogaster as an experimental model

Many non-mammalian species such as *Drosophila melanogaster, Aplysia californica, Caenorhabditis elegans* or *Danio Rerio* have been used to study the nervous system [15-18].

Common advantages of using these models are their relative simplicity, reduced number of cells and less complex neural centers. This is complemented by their small size, rapid cell cycle and abundant progeny.

In *Drosophila melanogaster,* the development of the binary expression system Gal4/UAS [19] allows the genetic manipulation of gene expression. The first component of this binary system is represented by fly lines that express Gal4, a yeast transcription factor [20, 21] containing a DNA-binding domain and a transcription activation domain. The second component is represented by constructs of the desired gene under the control of Gal4-targetted UAS (Upstream Activating Sequences) (Figure 1).

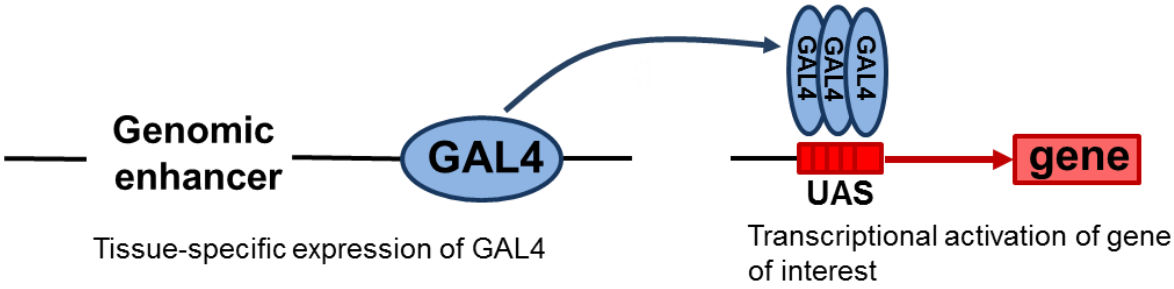

Figure 1: Gal4/UAS system: Schematic representation of expression system. Gal4 is located under a tissue-specific enhancer. Gal4 binds to UAS which precedes the gene of interest.

This system allows expressing our protein of interest under an specific promoter, in a spatio-temporal manner.

The wide battery of Gal4 and UAS constructs has rendered *Drosophila melanogaster* a useful model for studies on developmental biology, organogenesis and neuroscience.

2.2. Third instar larval NMJ

The *Drosophila* larval body, especially its muscles and neuromuscular junctions (NMJs) are a convenient site where to apply the powerful genetic tools including the Gal4/UAS system. In this context, the larval NMJ is a perfect structure for the study of mechanisms of neurotransmitter release, synapse physiology, vesicle trafficking, structural and functional synaptic changes.

2.2.1. NMJ morphology

Motor neurons are individually specified and generated in lineages deriving from identified neuroblasts [22]. During embryonic stages 13-15, motor neurons extend their axons towards their corresponding muscle targets. Each motor axon follows a determined pathway specific for a muscle or group of muscles [23].

From the neuron somata located in the ventral ganglia, cells extend axons through the bilateral segmental nerves (SN) and transverse nerves (TN) to the muscle fibers [24]. Motor neurons branch over the muscle in characteristic and most important, stereotyped patterns forming synaptic boutons (Fig.2). Most motor neurons are excitatory (glutamatergic) and their varicosities come in two major classes, type-Ib (big boutons) and type-Is (small boutons) [25, 26].

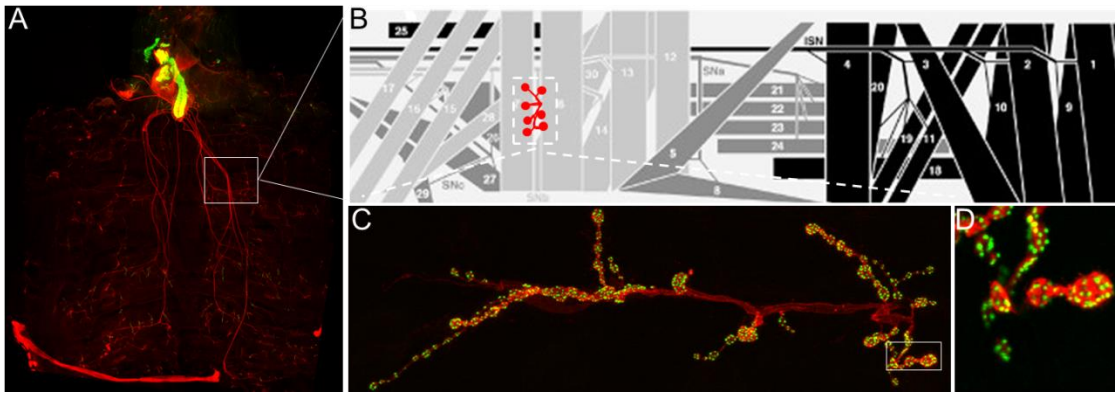

Figure 2:Anatomy of the NMJ: A)Confocal image of third instar larva body wall. B)Scheme of abdominal muscles. NMJ in red. C)Confocal image of an NMJ. Membrane is stained with anti-Hrp(red). Synapses stained with anti-Bruchpilot (green). D) Magnification of synaptic boutons

Inside these boutons we observe the active zones (AZs), single functional transmission units characterized by electro dense T-bar structures [27]. On the presynaptic site (NMJ), AZs are composed by Ca^{+2} channels, machinery of release and recycling of vesicles and vesicles pools. Otherwise the postsynaptic site (muscle) is composed by transmitter receptors and second messenger systems [28, 29]. Each synaptic terminal contains 20-50 synaptic boutons with a variable number of AZs per bouton (Fig.2).

At the NMJ Ca^{+2}- signaling initiates intercellular communication between the presynaptic (bouton) and the postsynaptic side (muscle). Ca^{+2} triggers synaptic vesicle exocytosis that mediates neurotransmitter release at the AZs [30, 31] (Fig.3).

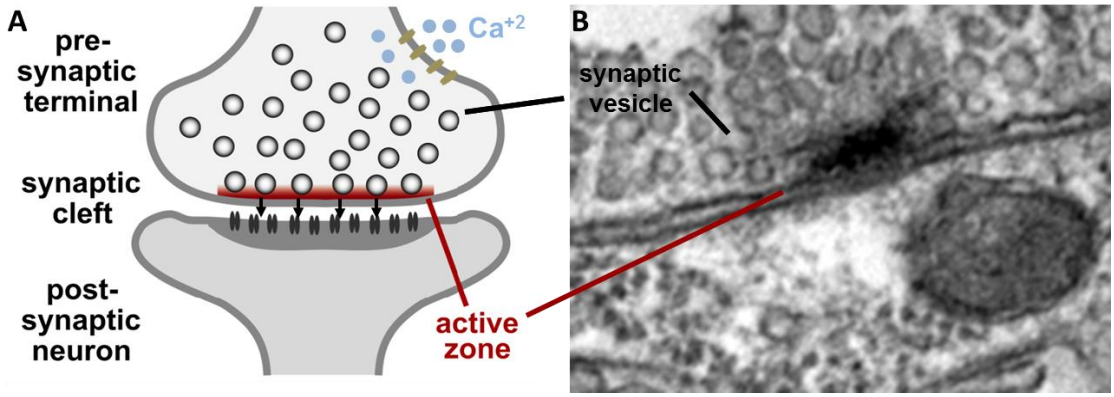

Figure 3: Active zone in a synapse: A) Representation of a synaptic contact. Ca^{+2} entry at the pre-synaptic terminal induces neurotransmitter release at the synaptic cleft. B) Electron microscopy image of synaptic contact. Pre- and post- synaptic specializations in black zones.

Three different modes of neurotransmitter release exist and can be monitored by electrophysiological recordings: 1) evoked synchronous release that initiates after action potential (AP) and it is induced by Ca^{+2} entry in the synaptic bouton [32], 2) evoked asynchronous release characterized by a delay with respect to the AP [33], and 3) spontaneus 'mini' release, which represents the exocytosis of single vesicles and it is tightly correlated with Ca^{+2} influx [34]. Each type of release leads to specific responses at the postsynapsis.

2.2.2. NMJ development

Genetic screenings have revealed several signaling pathways involved in synaptogenesis and synapse stabilization. One needs to discriminate between two processes: 1) synapse formation, and 2) synapse maturation and maintenance. Each process has characteristic signals while others are common.

Examples of components involved in the development of the NMJ include Bone Morphogenetic Proteins (BMPs) and wingless (wg), synaptic adhesion molecules such as Conectin (Con) or Fasciclin (Fas) and extracellular matrix proteins such Syndecan and Dally-like [35].

During normal development, the axonal growth cone (NMJ precursor) contacts with its target muscle. Postsynaptic Glutamate Receptor (GluR) and Discs large (dlg) accumulates at contact sites and this process leads to the differentiation of the growth cone into a presynaptic terminal [36]. At early stages of NMJ development, motor neurons innervate more than one muscle to restrict later on their contacts to specific muscles [37]. Among the discriminatory molecules, we find mostly adhesion molecules such as LRR (Leucine-rich repeat) proteins Con and Capricious or Fas3. These proteins are both expressed in specific subsets of muscles and in the NMJ facilitating recognition [38, 39]. Mutants which ectopically express these molecules alter their targets [40] underscoring the specificity of the mechanism.

Immature NMJs need to increase their branching to accommodate the expansion that muscles suffer during larval moltings.

During NMJ development, many transient structures are eliminated. The mechanisms that underlie a correct synapse formation are not fully understood.

One major aspect of NMJ development is growth. Concerning this, we can divide molecules in two main groups, growth promoters and growth inhibitors.

2.2.2.1. Genes promoting synaptic growth

In this group we distinguish two additional sub-categories: those that alter microtubule cytoskeleton (MT) and increase NMJ size, and genes related with AZs formation.

In the MT dynamics, the Wnt family plays an essential role. The *Drosophila* Wnt homolog, wg, is expressed at, and secreted from, glutamatergic NMJ. Wg

triggers signals, both in the presynaptic and postsynaptic site. The loss of wg leads to the reduction of boutons and causes aberrant morphology [41]. In the cascade of Wg signaling pathway other genes affect the MT cytoskeleton integrity. Arrow (arr) is a co-receptor of Frizzled2(Fz2) receptor for the ligand wg; while dishevelled (dsh) is a phosphoprotein functionally downstream of Fz2. Downregulation of both proteins, Arr and Dsh, affects the MT cytoskeleton leading to decrease in the number of boutons but increase in size of the remaining ones [42].

The assembly of AZs requires gene transcription and translation followed by the protein transport along the axon and finally depositing at the nascent AZ site. In this complex process, scaffold proteins such as ELKS (Bruchpilot in *Drosophila*) and Liprin-alpha are critical for the establishment and maintenance of normal AZs. These proteins form a multi-domain but they function in a hierarchical manner and they appear in a specific temporal sequence (Fig.4). Liprin is deployed early during AZ formation and it locates opposite to Bruchpilot (Brp), which appears later and it is responsible of the T-bar formation [43].

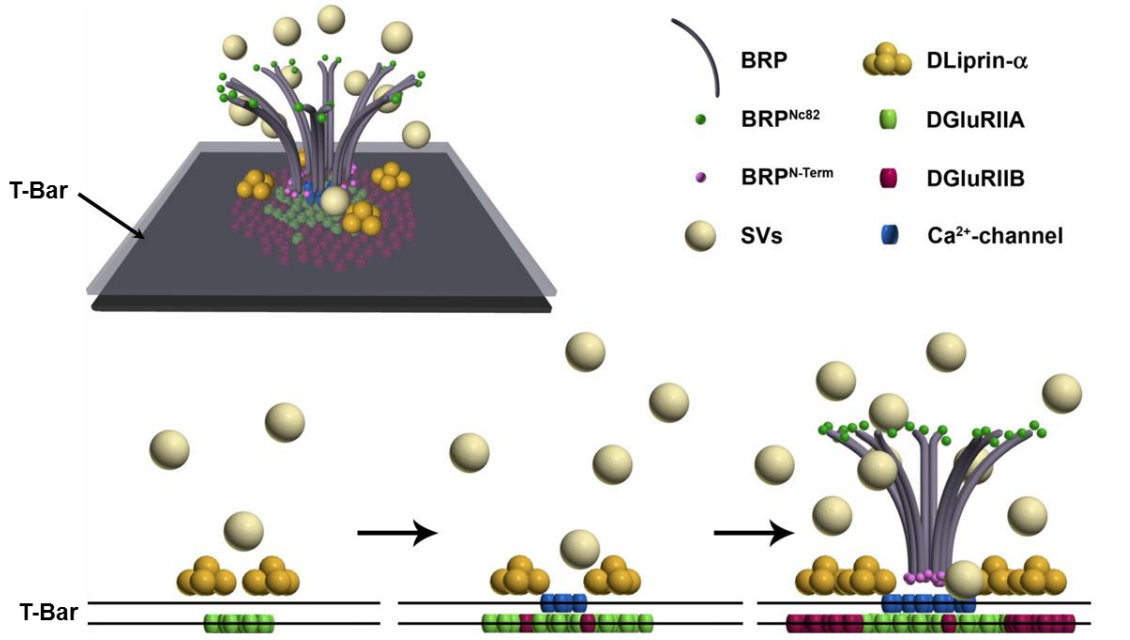

Figure 4: Spatiotemporal model of AZ assembly at the NMJ: A) Schematic representation of components of the AZs at the T-Bar. B) Sequential appearance of AZ components at the T-Bar.SVs synaptic vesicles. Modified from Fouquet 2009.

Despite the temporal difference in synthesis, these proteins bind each other and assure the efficiency of AZs formation and neurotransmitter release. Depletion of Brp, leads to lack of T-bars and Ca^{+2} channels and, as a consequence,

inefficient vesicle release [44]. Liprin mutants exhibit reduced number of synaptic boutons, enlarged active zones and defective synaptic transmission [45]. This mechanisms is conserved across invertebrates and vertebrates [43, 46].

2.2.2.2. Genes that restrict synaptic growth

The NMJ suffers three different processes of elimination of synapses during the life cycle. First, the NMJ is induced during late-stage embryo in a Ca^{+2} dependent manner [47] to eliminate ectopic contacts of non-target muscles. This mechanism of elimination or pruning is conserved in humans, where lack of synapse elimination on dendritic spines leads to mental retardation and autism [48]. Another refinement occurs after embryogenesis and is related with the gain of boutons proportional to the increase in muscles size during larval moltings [49]. The last round of massive elimination of synapses occurs during metamorphosis [50]. Akin to *Drosophila* metamorphosis, pruning also occurs in mammalian brain during puberty which is a requirement for optimal cognition [51]. Genes that negatively regulate fly´s NMJ growth include another cytoskeletal modulator, Spastin, whose mutants show aberrant number of boutons [52].

The NMJ growth is also regulated by protein elimination through the ubiquitin-proteasome system (UPS). An example is Highwire (Hiw), an ubiquitin ligase required for bouton growth control. Hiw regulates Mitogen-activated protein kinase (MAP kinase) signaling through Wallenda (Wnd). Loss of *hiw* function yields expanded NMJ arborizations while the same effect is achieved by the overexpression of *wnd*. This antagonistic effect suggests that *hiw* could be a negative regulator of *wnd* [53].

2.2.3. NMJ maintenance

To consider ‘stable’ a fully developed NMJ is not a correct concept because synapses are constantly changing in number and, to some extent, in functional status. These changes seem to result from displacements of an equilibrium between growth and retraction signaling, and are elicited by the functional demands of the target cell or organ [54]. Major mechanisms of stability and

maintenance are: 1) transport of proteins to the synaptic terminals, and 2) subsequent dynamics of the cytoskeleton.

2.2.3.1. Genes contributing to synapse maintainment

Several proteins are involved in the regulation of synaptic stability. Fasciclin II, a cell adhesion molecule, is located both pre and postsynaptically. Lack of FasII yields a phenotype where NMJ in embryonic stages is normal but, in late larval development, it leads to a reduction of boutons [55], revealing a role in stability but not during development. In the case of LIMK (LIM domain kinase) protein, DLIMK1 binds to Wishful thinking (Wit), a BMP receptor, and this binding is critical for synaptic stability but not for Smad-mediated synaptic growth [56]. This evidence suggests a dual role for DLIMK1 first during development of the NMJ and later in maintainence.

Phosphatidylinositol-4,5-biphosphate 3-kinase (PI3K) is a member of a kinase family involved in cellular growth, proliferation, differentiation, cellular survival and intracellular trafficking [57-59]. These properties render PI3K as a major player in cancer progression [60-62]. The canonical PI3K pathway and its relation with other proliferating proteins, such mammalian Target of Rapamycin (mTOR) or Protein Kinase B (AKT), are well known [63]. The effect of PI3K as a pro-synaptogenic signal and the use of its overexpression as an approach to increase synapse number in aged neurons has been described [64]. Furthermore, pathological conditions which lead to synapse loss, such as that caused by human Aß42 expression in flies, can be suppressed by the co-overexpression of PI3K [65].

This effect of PI3K in Drosophila seems conserved in vertebrate neurons [66]. However, we are still far from knowing the complete molecular cascade which triggers the normal and precise NMJ formation.

2.2.4. NMJ dynamics

Despite its stereotyped pattern, the NMJ is constantly changing. These changes can be observed at the level of efficiency of neurotransmitter release, morphology, number of boutons, number of active zones. These features have been well documented during the different larval stages [55, 67, 68].

The stereotyped pattern of NMJ is critical to detect changes in synapse number and morphology.

Although dynamic, the number of synapses of a given motorneuron and at a specific developmental stage, is reproduced across individuals. Since we can genetically alter the desired synaptic proteins, the modifications observed can be attributed to our manipulations.

Most proteins involved in synapse biology are conserved across species including humans, making these studies very useful for answering basic questions in neurosciences.

Among these synaptic proteins, we have CAZ-associated structural protein (CAST) and ELKS-Rab6-interacting protein (ERC) [69]. A fly ortholog of CAST is Brp, that localizes in the active zones (AZs) [70]. Mutants of Brp show fewer T-bar specializations and Ca^{+2} channels. As a consequence, these mutants exhibit changes in synaptic short-term plasticity and impairments in vesicle trafficking [71].Due to the intimate relation between the NMJ formation and the stabilization of Brp, we find this evolutionary conserved protein as an excellent candidate to visualize, and hence count, synapse .

The use of single neurons to study synapses becomes feasible in the abdominal body wall muscles of the larvae.Recordings from single boutons (Fig.5) have revealed differences in the release efficiency and the protein components between Ib and Is boutons [72, 73].

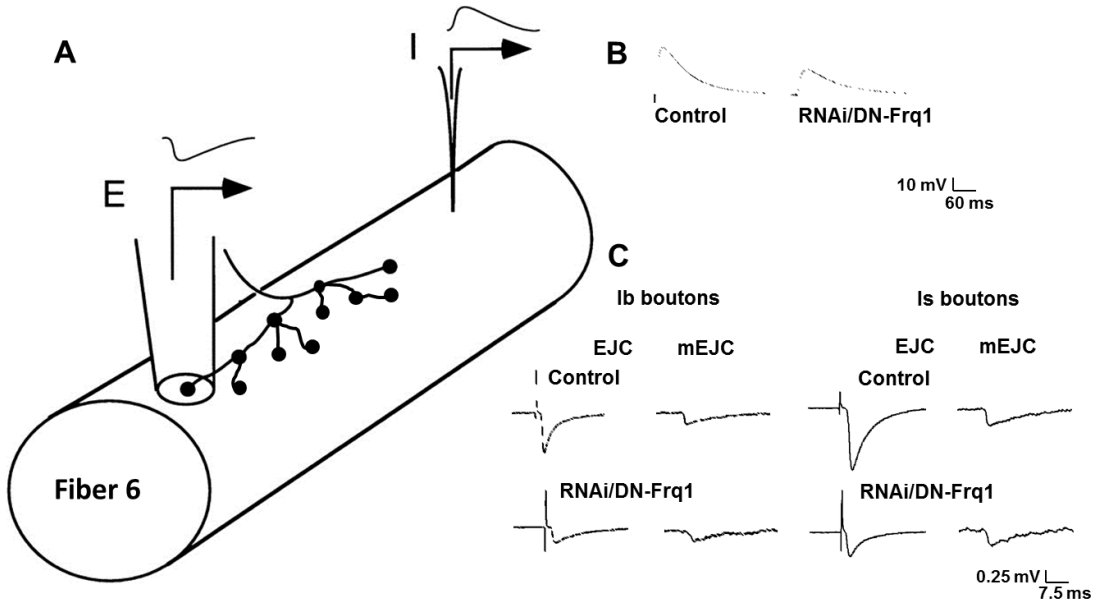

Figure 5: Electrophysiology at the NMJ:A) Scheme of an NMJ over the muscle. **I:** intracellular recordings. **E:** extracellular recordings (Macropatch). **B)** Excitatory Junction Potential (EJPs) of intracellular recordings for Control and RNAi/DN-Frq1. **C)** Excitatory Junction Currents (ECJ) of single bouton recordings of Ib and Is boutons for Control and RNAi/DN-Frq1.

Neurotransmission is characterized by a fast recycling of presynaptic vesicles. Endo- and exocytosis of vesicles are mediated by Soluble NSF Attachment Protein (SNARE) complexes [74]. After Ca^{+2} influx, SNARE protein Synaptobrevin (Syb), vesicle associated membrane protein (VAMP2) in other species, induces membrane fusion and, hence, neurotransmitter release [75]. Mutants for synaptobrevin lead to vesicle docking and synaptic transmission defects [76].

2.3. Neurotransmitter release

Fast changes that characterize neural plasticity depend largely on the ability of neurons to transmit information within milliseconds. At the dendrites, an AP induces a cascade of signals which lead to neurotransmitter release down the axon to reach the presynaptic site [77].

We find two types of neurotransmission in the brain, chemical and electrical. Most extended is the chemical, while electrical is restricted to specific pairs of neurons.

2.3.1. Calcium and synaptic transmission

The intracellular Ca^{+2} signaling is involved in many regulatory functions in different cell types [78].

In neurons, Ca^{+2} controls vesicle trafficking and neurotransmitter release. In the chemical transmission, an AP induces the activation of specific proteins. Among them are voltage-gated Ca^{+2} channels which, once they open due to the change in the membrane potential, allow an inflow of this ion into the cell. Intracellular Ca^{+2} modulates the binding of neurotransmitter containing vesicles to the plasma membrane of the active zone of the synapse with the concourse of the SNARE protein complex. This interaction is required for positioning (docking) the synaptic vesicles ready for exocytosis [79]. Vesicles release neurotransmitter in the synaptic cleft. Finally, neurotransmitters bind to the receptor located in the membrane of the postsynaptic side. This sequence of

events induces postsynaptic membrane modifications which initiate signaling cascades that cause short or long term changes in the receiving cell [80].

The wide diversity of mechanisms regulated by Ca^{+2} depends on magnitude, speed, and time. These events are controlled by two types of proteins, intracellular signals controlling the Ca^{+2} intake to the presynaptic site, and calcium binding proteins which respond differently depending on the calcium intracellular levels.

2.3.2. Calcium influx control

Ca^{+2} entry has to be strictly regulated, not only to generate different signals, but to prevent the collapse of the cell cytoskeleton [81].

In this context, G proteins are negative modulators of calcium channels. G proteins are guanine nucleotide-binding proteins that act as molecular switches between Guanosine-5'-triphosphate (GTP)-bound and Guanosine-5'-diphosphate (GDP)-bound states. G proteins are heterotrimers constituted by Gα, Gβ and Gγ subunits. Stimuli induce the switch from GDP (inactive) to GTP (active) bound states of the Gα subunit. The GTP state leads to the dissociation of the trimer into a monomer of Gα and a dimer composed by Gβγ subunits (Fig.4).

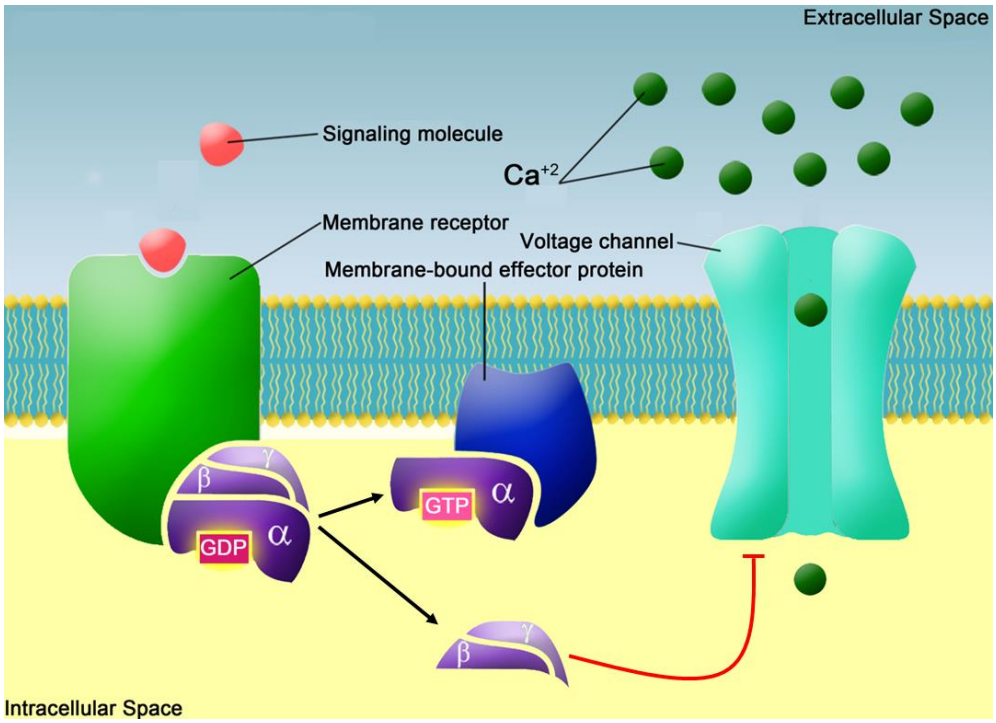

Figure 4: G-protein gated Ca^{+2} channel. Schematic representation of G protein controlling Ca^{+2} voltage-dependent channels. Gα is bound to Gßɣ. Molecular switch of GDP for GTP releases Gα and Gßɣ which blocks the associated channels.

In humans, at least 16 genes codify Gα monomers and are classified in Gαs, Gαi/o and Gαq. Five genes encode subunit Gβ and 12 Gγ [82].

In neurons, these G proteins are involved in inhibition of calcium channels, either voltage-dependent or independent. The most well-known inhibition mechanism mediated by G protein includes Gβγ heterodimer. This heterodimer specifically binds to the α1 subunit of Ca_V2 channels blocking its activity [83] and, thus, Ca^{+2} entry through a shift in the voltage dependence [84]. This is a faster membrane depolarization-dependent process and there are no second messengers involved.

In addition, Gα subunit can lead to Ca^{+2} channel inhibition but in a depolarization-resistant mechanism and, consequently, voltage-independent. Several signaling steps are involved in this process, including channel phosphorylation [85], activation of phospholipase C [86] and a secondary process which includes the dimer subunit Gβγ [87]. Increase in signaling steps render this process slower than the voltage-dependent inhibition.

2.3.3. Calcium binding proteins

Intracellular calcium has a crucial role in activating neurotransmitter release.

How a single ion type induces different outcomes such apoptosis, hormone secretion or neurotransmitter release is due in part to the Calcium Binding Proteins (CBP).CBP are a group of proteins that participate in Ca^{+2} storage and signaling pathways. Although CBPs are heterogeneous in properties and structure a common feature is the ability of binding Ca^{+2} in specific domains.

Differences in frequency of the AP lead to Ca^{+2} level changes in the synaptic terminals. CPB can be divided in high affinity proteins/low capacity or low affinity/high capacity proteins for Ca^{+2}. Depending on the Ca^{+2} concentration, these proteins will bind or not Ca^{+2} ions triggering a response.

The structure of domains is critical for accurate binding. We distinguish here between proteins with EF-hand motifs such as calmodulin,troponin C or calcineurin, and CBPs without EF-domains such as calsequestrin and calreticulin [88].

Among the CBPs with EF-motif we have to distinguish:

-CBP modulating Ca^{+2} concentration which transport Ca^{+2} ion across membranes acting as Ca^{+2} buffers

-Calcium sensor proteins (CSP) which additionally can be modulated by calcium inducing a cellular response

2.3.3.1. Calcium sensor proteins

CSPs characterize for their ability to bind $Ca^{+2}$and change their conformation to bind specific targets and modify their function.

A well-studied pathway involves Calmodulin. After calcium entry, it may be captured by Calmodulin. This event triggers a signaling cascade through calmodulin-dependent protein kinases (CaMKs). Activation of this cascade enhances the efficacy of synaptic transmission and, eventually, may lead to long-term memory [89].

The CSP Neural Calcium Sensor 1 (NCS-1) controls Ca^{+2} levels through modulation of calcium channels. It was first discovered in *Drosophila* as Frequenin (Frq) [90] and its sequence and function are conserved in vertebrates [91]. Frq/NCS-1 is exclusive of the nervous system where it controls Ca^{+2} influx and neurotransmitter release. Frq/NCS-1 is also involved in synaptic terminal growth [92] and learning and memory acquisition [93]. Calcium/calmodulin-dependent protein kinase II (CaMKII) is another target of NCS-1 [94].

Drosophila mutants of Frq exhibit phenotypes that, in humans, are observed in schizophrenia, bipolar disorder or X-linked mental retardation [95-97]. These include abnormal synapse number and probability of release [92, 98].

Here, we explored the role of Frq in two different, but closely related, processes: specification of synapse number and control of neurotransmission. Specifically, we aim to elucidate whether Frq acts in a single mechanism for both processes, or if it acts through two separated pathways involving distinct proteins.

2.4. Translational control at the NMJ

The morphological complexity of neurons is a challenge for the transport of mRNAs from the soma to the synapses. Given the speed at which axon transport systems operate (about 1-10 microns /h) and the length that some axons may reach (from millimeters to over a meter), it is challenging to explain the high turn-over rate of synapses (hours). The solution is to transport mRNA to the synapses and locally maintain a pool of messengers tightly regulated by translational controls.

These translational mechanisms that respond to synaptic stimulation constitute the basis of molecular changes and plasticity which characterizes short and long-term memory.

2.4.1. Local translation at the synapses

At the synapses, mRNAs distribute forming granules called Messenger ribonucleoprotein complexes (mRNP). These complexes contain mRNA binding proteins (RBPs) which regulate localization, stability and translation of mRNAs through binding to their untranslated regions (3'UTR or 5'UTR) [99].

RNA granules contain different populations of proteins depending on its function. Some of them, such Fragile X Mental Retardation Protein (FMRP), regulates translational activity during development of the nervous system [100] and remains in mature synapses. Processing bodies (P bodies) regulate mRNA degradation working with micro-RNA,non-coding RNAs that act as post-transcriptional regulators of gene expression, and microtubules [101]. In mature synapses prion-like proteins such Orb2 localizes in RNA granules and promotes or block translation depending on stimuli [102].

Thus, FMRP, miRNA and prion-like proteins among others are the main regulators of local translation.

2.4.1.1. FMRP as modulator of translation

FMRP is a translational repressor. This protein is a RBP located in dendritic spines associated with ribosomes or forming RNPs in the cytoplasm where the local RNAs are normally translated [103].

FMRP acts as a dual protein blocking or promoting translation according to its phosphorylation status [104]. Recent studies have shown that FMRP represses translation in association with microRNAs (miRNAs). Phosphorylation of FMRP induces binding of miR-125a to the target mRNA, blocking its translation. Activation of neurotransmitter receptors via mGluR signaling induces FMRP dephosphorylation leading to destabilization of miR-125-mRNA binding, thus permitting mRNA translation [105].

The aberrant expression of FMRP causes trinucleotide repeat expansions which leads to loss of function. Misregulation of FMRP induces loss of the translational brake on synthesis of synaptic proteins leading to abnormal growth of spines. This is the major cause of Fragile X Mental Retardation Syndrome and Autism Spectrum Disorders (ASD) [106].

2.4.1.2. miRNAs and local regulation at synapses

MicroRNAs regulate translation independently of FMRP in many processes such as circadian clock activity [107], apoptosis and cell proliferation [108]. Its role is remarkable in development and synapse maturation. In early stages of development, miRNAs such as *iab-4* (conserved in vertebrates as miRNA-196) interact with Homeotic (Hox) genes modulating the expression of Antennapedia (Antp), Ultrabithorax (Ubx) and abdominal (abd) proteins abd-A and abd-B [109]. Impairments in this miRNA lead to misregulation of Ubx in the self-righting node neurons (SNR) triggering to left-right orientation defects in larva and adult locomotion [110].

Classical genetic studies revealed different subsets of miRNA regulating maturation versus formation of synapses. For example, members of let-7 family and miR-125 are required for maturation, but not formation, of NMJ. Mutants for these genes exhibit locomotion and behavioral impairments in the adult [111].

Concerning synapse number, miR-138 has been identified as a negative regulator of spine size due to its control over the expression of acyl protein thioesterase 1(APT1). This enzyme regulates the palmitoylation status of proteins related with neurotransmitter release such as G Proteins [112].

In mature synapses, the main role of miRNAs is the control of local synaptic changes that underlie learning and memory.

For example, studies placed miRNA to control the abundance of glutamate receptor subunits (GluRA and GluRB) at the fly NMJ, thus controlling synaptic transmission [113].

miRNA alterations leads to abnormal development of spines and dendrites and are related with psychiatric diseases such schizophrenia [114].

Recent studies relate miRNA impairments with epilepsy which presents abnormal electric activity in the brain. In this case, up or downregulation of certain miRNAs are associated to epilepsy progression and their expression serves as biomarkers of the disease [115].

2.4.1.3. Prion-like proteins

For a normal development and maintenance of synapses, beyond the proper levels and types of proteins, we find the prion-like or conformational regulators.

Cytoplasmic Polyadenylation element binding protein (CPEB) acts as a conserved translational regulator activating mRNAs [116, 117]. In addition, CPEB show prion-like properties. Studies of *Aplysia* memory formation reveal that two different conformational stages of CPEB contribute to induce synaptic changes [118].

Orb2 is the fly homolog of neural CPEB of *Aplysia*, and the prionic characteristics and function are conserved among both species [119].

Orb2 is a major player in long-term memory. Orb2 is located in AZs at the synapses under two different isoforms, Orb2A and Orb2B. Each isoform have different properties, Orb2A is less abundant but triggers the oligomerization process. Following synaptic stimulation,Orb2A changes its conformational state (monomer to oligomer) and induces Orb2B oligomerization (Fig.5) [102].

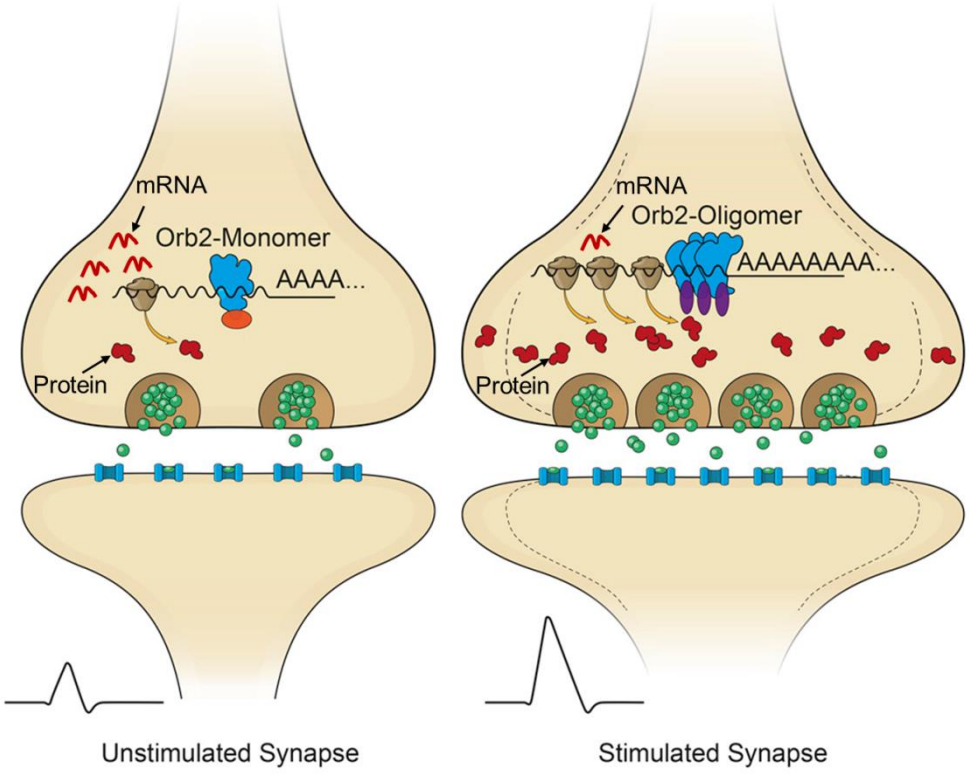

Figure 5: **Orb2 changes its conformational state under synapse stimulation.** The Scheme represents monomeric Orb2 repressing translation, oligomerization and protein synthesis after stimulation. Modified from

Orb2 oligomers bind to certain mRNAs related with neuronal growth, synapse formation and turnover and proteolysis (Table 1) [120].The conformational state is critical because Orb2 oligomers are activators while Orb2 monomers are repressors of translation [121].

Synaptic growth/stability	Synaptic activity	Proteolysis	Unknown
Neuroligin	N-Syb	Uch	CG30193
Still life	Pka-R2	Rpt1	CG14528
Brain tumor	Widerborst	Rpt4	CG6891
Capulet	Pathetic	Rpn9	CG12769
Glaikit		Unkempt	CG31300
Act5c		Tequila	CG6129
Branchless		Murashka	CG4306
DaPKC			CG10824
Orb2			

Table 1: Orb2 Synaptic targets

The Orb2 localization in the adult brain and its role in short and long-term memory has been widely studied [102, 120, 122]. Orb2 is also required for spermatogenesis, its expression in the germline of adult males is essential in the process of meiosis and differentiation [123].

Furthermore, Orb2 is critical during embryogenesis where it plays a role in asymmetric cell division of precursors of neuroblasts [124]. Otherwise, its role in the development and maintenance of NMJ remains unknown. Our goal here is to explore the role of Orb2 in synapses and to determine whether rapid changes in translation conformation-dependent can lead to synaptic changes.

3. Aim of this thesis

Synapse formation and stabilization is the result of a delicate equilibrium among different molecular mechanisms. We explore in this work the two major mechanisms which characterize the function of a neuron, its number of synapses and the probability of neurotransmitter release. Furthermore, we use different strategies in order to elucidate which is the minimal intervention we can make to elicit a change in synapse stability. For that, we explore diverse possibilities, genetic manipulation of genes through their up or downregulation in order to stablish their functional hierarchy. In addition, we aim to investigate how changes in the conformational state of certain proteins relate to post-translational mechanisms.

4.Objectives

- To identify candidates of the PI3K signaling pathway which establish the number of synapses.
- To elucidate the functional interactions between pro and anti-synaptogenic signals.
- To unravel the mechanism by which the Ca^{2+}-binding protein Frq2 regulates synapses.
- Once an interacting partner for Frq2 had been identified, Ric8a, to elucidate the relevance of this interaction in the joint regulation of synapse number and activity.
- To study the structural transitions of Orb2 as a regulator of mRNA translation in neurons.
- To analyze the case of Brat, a target of Orb2, in the regulation of synapses.

These three studies had been published independently and, all together, constitute the research towards the PhD.

5. Chapter I:*The equilibrium between antagonistic signaling pathways determines the number of synapses in Drosophila*

5.1. Introduction

Este capítulo está constituido por el manuscrito:

-*The equilibrium between antagonistic signaling pathways determines the number of synapses in Drosophila.* Sheila Jordán-Álvarez*, **Elena Santana***, Sergio Casas-Tintó, Ángel Acebes, Alberto Ferrús.

*Co-autoría

PLoSOne.2017Sep11;12(9):e0184238 doi:10.1371/journal.pone.0184238

Elena Santana Martín participó en este estudio planificando y realizando los experimentos, adquisición y posterior procesamiento de imágenes, realización de parte de análisis estadístico y elaboración de parte del material gráfico. La redacción, elaboración del material gráfico y discusión del trabajo se realizó en colaboración con todos los autores.

La formación de sinapsis funcionales implica un delicado equilibrio entre señales moleculares. Su desregulación en las neuronas puede inducir a serios problemas cognitivos. En este trabajo se estudia la vía de PI3K, proteína quinasa relacionada con crecimiento y proliferación celular. La quinasa PI3K y elementos relacionados como AKT o GSK3 han sido caracterizados por su relación con proliferación celular en procesos tumorales. Nosotros abordamos una nueva aproximación y estudiamos el efecto de estas proteínas en la formación de sinapsis. Concretamente, estudiamos el efecto que la modulación que esta quinasa tiene en la formación de sinapsis en la terminación neuromuscular de Drosophila.

Además de PI3K se analizan candidatos susceptibles de modular sinapsis, resultado de una búsqueda racional de elementos que interaccionan con PI3K u otros elementos de la vía.

Entre estos candidatos encontramos receptores tirosina quinasa (RTKs), receptores serina/treonina quinasa (RSTK) y o proteínas quinasa activadas por mitógeno (MAPKs), considerados elementos pro-sinaptogénicos.

Dado que nuestra hipótesis se basa en un equilibrio entre elementos pro y anti-sinaptogénicos, en nuestro análisis incluimos elementos conocidos por bloquear la diferenciación celular como las proteínas Mad y Medea. Analizamos el efecto de estas proteínas en el número de sinapsis.

Ciertas proteínas como Jun/Fos forman heterodímeros por lo que en algunos casos analizamos su efecto por separado o conjunto. En estos casos se observa que proteínas por separado no producen efecto mientras que la combinación si lo hace, sugiriendo la delicada complejidad funcional entre los elementos propuestos. Mediante diferentes combinaciones genéticas entre los candidatos propuestos se estudiaron relaciones de epistasia.

Para ello analizamos el número de sinapsis en la terminación neuromuscular de *Drosophila* utilizando un programa informático que nos permite establecer de forma inequívoca el número de sitios activos.

En nuestros experimentos combinamos diferentes elementos pro y anti-sinaptogénicos intentando obtener un número de sinapsis similar a los controles. En algunos casos obtuvimos este resultado mientras que ciertas combinaciones seguían manteniendo un fenotipo pro o anti-sinaptogénico.

Nuestros resultados sugieren que existe una relación jerárquica entre los elementos analizados.

Además demostramos que elementos tanto pro- como anti-sinaptogénicos son necesarios para el correcto establecimiento de las sinapsis.

PLOS ONE

RESEARCH ARTICLE

The equilibrium between antagonistic signaling pathways determines the number of synapses in *Drosophila*

Sheila Jordán-Álvarez[☯¤a], Elena Santana[☯], Sergio Casas-Tintó, Ángel Acebes[¤b]*, Alberto Ferrús*

Institute Cajal C.S.I.C., Madrid, Spain

☯ These authors contributed equally to this work.
¤a Current address: Centro de Biología Molecular "Severo Ochoa" (CSIC-UAM), Madrid, Spain
¤b Current address: Centre for Biomedical Research of the Canary Islands, Institute of Biomedical Technologies, University of La Laguna, La Laguna, Tenerife, Spain
* aferrus@cajal.csic.es (AF); aacebesv@ull.es (AA)

Check for updates

OPEN ACCESS

Citation: Jordán-Álvarez S, Santana E, Casas-Tintó S, Acebes Á, Ferrús A (2017) The equilibrium between antagonistic signaling pathways determines the number of synapses in *Drosophila*. PLoS ONE 12(9): e0184238. https://doi.org/10.1371/journal.pone.0184238

Editor: Marie-Laure Parmentier, Institut de genomique fonctionnelle, FRANCE

Received: April 4, 2017

Accepted: August 21, 2017

Published: September 11, 2017

Copyright: © 2017 Jordán-Álvarez et al. This is an open access article distributed under the terms of the Creative Commons Attribution License, which permits unrestricted use, distribution, and reproduction in any medium, provided the original author and source are credited.

Data Availability Statement: All relevant data are within the paper and its Supporting Information files.

Funding: Research was funded by a grant from the Ministry of Economy (BFU2012-3819 to AF) and a PhD fellowship (BES-2007-1659 to SJA). S.C.-T. holds a contract from the Ramón y Cajal program RYC-2012-11410. The funders had no role in study design, data collection and analysis, decision to publish, or preparation of the manuscript.

Abstract

The number of synapses is a major determinant of behavior and many neural diseases exhibit deviations in that number. However, how signaling pathways control this number is still poorly understood. Using the *Drosophila* larval neuromuscular junction, we show here a PI3K-dependent pathway for synaptogenesis which is functionally connected with other previously known elements including the Wit receptor, its ligand Gbb, and the MAPkinases cascade. Based on epistasis assays, we determined the functional hierarchy within the pathway. Wit seems to trigger signaling through PI3K, and Ras85D also contributes to the initiation of synaptogenesis. However, contrary to other signaling pathways, PI3K does not require Ras85D binding in the context of synaptogenesis. In addition to the MAPK cascade, Bsk/JNK undergoes regulation by Puc and Ras85D which results in a narrow range of activity of this kinase to determine normalcy of synapse number. The transcriptional readout of the synaptogenesis pathway involves the Fos/Jun complex and the repressor Cic. In addition, we identified an antagonistic pathway that uses the transcription factors Mad and Medea and the microRNA bantam to down-regulate key elements of the pro-synaptogenesis pathway. Like its counterpart, the anti-synaptogenesis signaling uses small GTPases and MAPKs including Ras64B, Ras-like-a, p38a and Licorne. Bantam downregulates the pro-synaptogenesis factors PI3K, Hiw, Ras85D and Bsk, but not AKT. AKT, however, can suppress Mad which, in conjunction with the reported suppression of Mad by Hiw, closes the mutual regulation between both pathways. Thus, the number of synapses seems to result from the balanced output from these two pathways.

Introduction

Synapses are dynamic neural structures that can exhibit a turnover of hours [1–3] and are influenced by day/light cycle, age, and learning [4–8] among other physiological processes.

Competing interests: The authors have declared that no competing interests exist.

Molecular mechanisms that could account for building/removal of synapses within these short times are largely unknown. Changes in synapse number, even if relatively small, can elicit notable changes in behavior [9, 10], or result in neural disorders [11]. For example, a mild 16% loss of inhibitory synapses has been reported in the cortex of schizophrenia patients [12]. Also, subtle perceptual and cognitive impairments manifest as a consequence of changes in the number of synapses well before cells are definitively lost by irreversible neurodegeneration [13, 14].

Extensive previous studies have identified proteins and processes that mediate synapse development and turnover. These include neurotrophins and neuropeptides [15–17], trafficking of receptors to and from the synapse [18], components such as N-cadherin [19], CaMKII [20, 21] or PSD-95 [22]. Also, synapse activity contributes to refine the number of synapses in a relatively long term basis [23, 24]. However, prior to these mechanisms of synapse maintenance, a different set of signals are required to initiate synaptogenesis and to cancel it when the appropriate number of them is reached. Different neuron types have characteristic numbers of synapses. In general, neuron size and synapse number correlate positively [25, 26]. Nonetheless, the neuron-type specific number of synapses, "the correct number", can fluctuate according to normal physiology, and these fluctuations can occur in the range of hours [27, 28]. Several proteins have been reported to signal for synaptogenesis in *Drosophila* [2, 29, 30] and vertebrates [31–33]. However, their hierarchy has not been established yet, nor a regulatory mechanism that could account for a rapid change in the number of synapses has been proposed.

As it is well known, different signaling pathways may share components depending on the cell type, physiological process or developmental context [34, 35]. For example, PI3K has been identified in multiple pathways downstream of various receptor types including tyrosine-kinase, G-protein-coupled and integrins [36, 37]. This scenario justifies the need to study a signaling pathway in a defined cell type rather than assuming that interactions described in a given context will apply to all cell types. Also, the biological relevance of molecular interactions requires to be validated under *in vivo* conditions. Here, we set out to identify the up- and down-stream components from PI3K, a key factor that we previously identified as a modulator of synaptogenesis in identified *Drosophila* neurons [2] and which is conserved in mammalian hippocampal cells [32]. We revisited other elements known to be involved in synaptogenesis, and analyzed their functional hierarchy by epistasis assays. In the course of our study, however, we identified and characterized an antagonistic signaling that counterbalances the pro-synaptogenesis pathway. Both pathways cross-regulate each other suggesting that the final number of synapses result from the equilibrium between their respective signaling activities.

Neurites, varicosities (a.k.a. boutons) and synapses are morphologically different features in a neuron and, consequently, the signaling for their genesis is also different. For example, while AKT promotes collateral branching and synapse formation [2, 38], FAK reduces branching but promotes synapses [39]. Also, small GTPases show differential localization in postsynaptic spines *vs* axon collateral branches [40]. Even collaterals from the same axon exhibit different ways of branching (reviewed in [41, 42]). These facts, justify to count synapses directly in this study, rather than using bouton number as a proxy.

Material and methods

Fly stocks

The class I phosphoinositide kinase PI3K is represented in *Drosophila* by Dp110. All fly constructs used here correspond to Dp110 but, for simplicity, we refer to them as PI3K. The pan-neural driver *elav-Gal4* (*w*; P{w[+mC] = GAL4-elav.L}3*) [43] and those affecting motor

neurons, *D42-Gal4 (w*; P{w[+mW.hs] = GawB}D42)* [44], as well as lines *myc-PI3K (w^{1118};P{w[+mC] = Myc-Dp110}1)*, *myc-PI3K$^{\Delta RBD}$ (w^{1118};P{w[+mC] = Myc-Dp110[RBD]}1)*, *UAS-PI3K$^{92E.CAAX}$ (P{w[+mC] = Dp110-CAAX}1, y^1 w*)* [45], *UAS-Bsk (w*; P{w[+mC] = UAS-bsk.B}2)*, *UAS-Bsk$^{DN.}$ (w^{1118} P{w[+mC] = UAS-bsk.DN}2)* [46], *UAS-hep ($w^{[*]}$; P{w[+mC] = UAS-hep.B}2)* [47], *UAS-htl (y^1 w*; P{w[+mC] = UAS-htl.M}YYDFR-F16)*, *htl^{AB42} (w*; htl^{AB42}red e/TM3, P{ry[+t7.2] = ftz/LacZ}SC1, ry^{RK} Sb^1 Ser^1)*, *btl^{dev1} (btl^{dev1}/TM1, T(2;3)D^7, red^1 D^7)* [48], *UAS-Fos (w^{1118}; P{w[+mC] = UAS-Fra}2)*, *UAS-Jun (y^1 w^{1118}; P{UAS-Jra}2)* [49], *UAS-Fos^{DN} (w^{1118}; P{w[+mC] = UAS-Fra.Fbz}5)*, *UAS-Jun^{DN} (w^{1118}; P{w[+mC] = Jbz}1)* [50], *UAS-Ras85D (w*; P{w[+mC] = UAS-Ras85D.K}5–1)*, *UAS-Ras^{DN} (P{w[+mC] = UAS-ras.N17}TL1, w^{1118})* [51, 52], *UAS-Ras64B (w[*]; P{w[+mC] = UAS-Ras64B.V14}1)*, *UAS-Ask1^{RNAi} (y^1 sc* v^1; P{y[+t7.7] v[+t1.8] = TRiP.GL00238}attP2)*, *UAS-Mad^{RNAi} (y^1 v^1; P{y[+t7.7] v[+t1.8] = TRiP.JF01263}attP2)*, *UAS-Licorne (y^1 w^{67c23} P{y[+t7.7] = Mae-UAS.6.11}lic[GG01785])*, *UAS-Rala^{DN} (w*; P{w[+mC] = UAS-Rala.S25N}2)*, *UAS-Slpr^{RNAi} (y^1 sc* v1; P{TRiP.HMS00742}attP2)*, *UAS-put^{RNAi} (y^1 sc* v1; P{TRiP.HMS01944}attP40)*, *actin-Gal4* (*P{Act5C-GAL4}*) and *tub^{LL7}-Gal4* (*P{tubP-GAL4}*) were from Bloomington Stock Center (NIH P40OD018537) (http://flystocks.bio.indiana.edu/). The other driver used in motor neurons, *OK6-Gal4*, was a gift from Cahir J. O'Kane (University of Cambridge, United Kingdom) [53]. Strains *UAS-PI3K (y^1 w^{1118};P{w[+mC] = UAS-PI3K92E.Exel}2)* and *UAS-PI3K^{DN} (y^1 w*; P{w[+mC] = Dp110[D954A]}2)* [54] were provided by Dr. J. Botas (Baylor College of Medicine, Houston, TX). Strains *UAS-Hiw* (*P{UAS-hiw.W}*) [55], *UAS-wit* (*P{UAS-wit.M}*), *wit^{B11}* (*bw^1; wit^{B11} st^1/TM6B, Tb^1*), *wit^{A12}* (*bw^1; wit^{A12} st^1/TM6B, Tb^1*) [56], *UAS-gbb* (*P{UAS-gbb.K}*) [57], *gbb^1*, *gbb^2* [58] *UAS-Mad$^{\#2A3}$* and *UAS-Medea$^{\#5.13A3}$* [59] were a gift from Dr. G. Marqués (University of Minnesota). Strains *UAS-Wnd (w*; P{w[+mC] = UAS-wnd.C}2)* (50), H*iw^{ND8}* (*w* hiw^{ND8}*) [60] and H*iw$^{\Delta E3}$* (55) were kindly provided by Dr. A. DiAntonio (University of Washington in St. Louis, USA). Driver *Mhc-Gal4* (*P{Mhc-GAL4.U}*) [61] was used to target the postsynaptic cell. The *puc^{RNAi}* (GD3018), *p38a^{RNAi}* (KK102484), *Medea^{RNAi}* (GD19689) and *Mad^{RNAi}* (KK110517) strains were from the Vienna Stock Center (http://stockcenter.vdrc.at/control/main). The microRNA *UAS-bantamA* strain (*M{UAS-ban.S}ZH-86Fb*) [62] was provided by Dr. M. Milán (IRB, Barcelona, Spain), and line *UAS-cic(3xHA) att86Fb* (F001848) was from Dr. G. Jiménez (IBMB, Barcelona).

Validation of genetic tools and procedures

For down-expression experiments, mutants or dominant negative forms were used when available. In a few cases, RNAi constructs were employed as an alternative. All RNAi lines used in this study do not have reported off-targets. In addition, their effectiveness was tested with general Gal4 drivers (*gmr-Gal4*, *tub^{LL7}-Gal4* or *actin-Gal4*) under the criterion of morphological or adult viability phenotypes. Furthermore, some genetic combinations were also tested for protein effects in Western blots (see main Text). The RNAi that, having passed the previous criteria, failed to yield a synaptic phenotype constitute an innocuous RNAi control (see S1 Table). The synaptic value of reference corresponds to genotypes in which the Gal4 drives neutral *UAS-GFP* or *UAS-LacZ* constructs. To count synapses, the *D42-Gal4* driver was used throughout, while for qPCR assays, we used the *elav-Gal4*. All synapse counts correspond to the larval motor neuron 6/7 from abdominal segment A3. Only one neuromuscular junction per crawling LIII larvae was used in order to maximize the stochastic variability and, hence, to increase the biological relevance of the statistical differences. Cultures were kept at 25˚C and reared under non-crowding conditions, 10–15 males and 20–30 females per vial changed every other day. All genotypes were obtained from crosses repeated over a two years period.

Experimental cell system

The neuromuscular junction (NMJ) of third larval instar [63] was used as experimental system. Boutons are often used as a surrogate of synapses in quantitative studies of synaptogenesis. However, common experience shows that synapses are not confined to boutons, and boutons can be devoid of synapses. To avoid these caveats, we adopted the criterion of counting the total number of mature active zones per neuromuscular junction irrespective of their bouton allocation. Genetic manipulations were driven to selected motor neurons using the binary Gal4/UAS system [64]. Synapses were visualized under confocal microscopy by the monoclonal antibody nc82 (1:10, DSHB, IA) which identifies the Bruchpilot protein, homolog to the mammalian CAST [65], and serves as an active zone-specific marker [2, 66–68] located at the edge of the characteristic T bar specialization of fly synapses [69]. The neuronal membrane was labeled with rabbit anti-HRP (1:200, Jackson ImmunoResearch). The secondary antibodies used were Alexa 488 (goat anti-mouse, 1:500, Molecular Probes) and Alexa 568 (goat anti-rabbit, 1:500, Molecular Probes). Larvae were mounted in Vectashield (Vector Labs).

Image acquisition and synapse number quantification

Confocal Images were acquired with a Leica Confocal Microscope TCS SP5 II (Mannheim, Germany). Synapse number was determined in all genotypes using the IMARIS software (Bitplane). Since IMARIS performs 3D reconstructions of the neuromuscular junction, the identification of synapses can be considered as reliable. Finally, to avoid misidentification of synapses, a threshold was stablished and a quality filter of shape and size was applied in all cases to unambiguously count synapses independently of changes of branching, length or area in the selected motor neurons. To stablish the threshold, we choose a confocal plane to measure the size of the nc82-positive spots present in that plane irrespective of whether they are contained within a bouton or along the axon. These measurements provide an average value that, for the acquisition conditions at 63x magnification (1024x256 pixels), corresponds to 0.5μm. This value is consistent with the synapse size as determined by transmission electron microscopy, and was fed to the software to count rounded spots of that size. Parameters were kept constant throughout the study of all genotypes.

Quantitative PCR

mRNA extractions from third instar larvae were obtained through standard protocols using TRIZOL (Invitrogen) and kept frozen at -80˚C. SuperSCript II Reverse Transcriptase (*Invitrogen*) was used with 5 μg of mRNA of each sample following the manufacturer instructions. Quantification of gene expression was determined using specific Taqman probes (*Applied Biosystems*). Each reaction was done in triplicate and with at least three different samples of each genotype.

Western blotting

For biochemical assays, 5–10 fly heads were homogenized in 20 μl of lysis buffer containing NaCl 150 mM, 0.05% Tween-20 and TBS pH 7.5. For detection of pAKT protein, approximately 5–10 head equivalents of protein extract were analyzed on a 4%–12% gradient SDS-PAGE and electro-blotted onto nitrocellulose 0.45 μM (GE Healthcare) 100V for 1 h. The membranes were blocked in 5% BSA in TBS-Tween-20 buffer and incubated with pAKT antibody (1:3000) (Cell Signaling) and anti-tubulin (1:10000) (Sigma-Aldrich) overnight at 4˚C with constant agitation. The antibody-antigen interaction was visualized by chemiluminescence using HRP-coupled secondary antibody and developed with ECL (Pierce).

Statistics

Statistical significance was calculated using one way ANOVA test. Synapse number comparisons were always performed between experimental conditions *vs* their corresponding control in each experiment. Female larvae were used throughout unless otherwise indicated. Data are plotted as whisker diagrams indicating the maximum and minimum values (vertical line), the 25% and 75% values (box) and the median value (horizontal line within the box). An ANOVA test was used also to compare mRNA levels in qPCR assays. The software GraphPad Instat 3 was used throughout. Significant differences between groups were indicated by $^{*}p<0.05$, $^{**}p<0.001$ and $^{***}p<0.0001$.

Results

Synapses were visualized from the presynaptic active zone (AZ) as nc82 immuno-positive spots which identifies the CAST-type protein Brp. These spots are located opposite to glutamate receptors (GluR) [3, 70] (S1A Fig). The levels of Brp have been related to the type of neurotransmitter release mechanism, spontaneous *vs* inducible [71]. In our study we do not make a distinction between these two types of AZs. A 3D reconstruction of a normal A3 NMJ is shown in S1 Movie. Using the binary UAS/Gal4 expression system [64], we manipulated genetically the motor neuron that innervates muscles 6/7 of the larval abdominal segment A3. For brevity, the symbols ↓ and ↑ are used to indicate elicited down- and over-expression, respectively. Genotypes are indicated in the figure legends and synapse number raw data are shown in S2 Table.

Receptors and ligands in the pro-synaptogenesis pathway

The receptor Wit and its ligand Gbb modulate the number of boutons and their growth [72–74]. Boutons and synapses, however, are two different neuronal processes which are not causally related (see below). Thus, we assayed here the potential relationship of PI3K with Gbb and Wit in the context of synaptogenesis.

The ligand Gbb is expressed in, and secreted from, the muscle [59, 75]. The selective overexpression of Gbb in the muscle (*Mhc-Gal4*) had no effect on the number of AZ in the genetically normal presynaptic motor neuron (Gbb↑, Fig 1A). This lack of effect may reflect a down-titration of the excess of Gbb by Crimpy [73, 76] although we did not explore this possibility further. The *gbb* attenuation by an RNAi (Gbb↓), however, reduces AZ number (Fig 1A). Heterozygous mutant larvae for *gbb* exhibit a mild reduction of synapses (Fig 1B). The homozygous mutants are lethal before LIII stage, preventing synapse counting. In the very few gbb^{1}/gbb^{2} larvae that could be obtained, the number of AZ was 30% reduced (Gbb↓↓) (Fig 1B). The relatively mild reduction of synapses, even in the homozygotes, suggests that Gbb is not the only ligand, or Wit is not the only receptor, for synaptogenesis (see below and Discussion). The up-regulation of PI3K in the motor neuron suppresses these *gbb* phenotypes, including the poor viability of the hetero-allelic combination (Fig 1B). This suppression places PI3K functionally down-stream from Gbb. We also tested a constitutively active form of PI3K, PI3K*, which rescued the viability trait of the homozygous *gbb* mutants (Fig 1B). The synapse reduction trait, however, was not fully rescued, perhaps due to the relatively minor pro-synaptogenesis effect of the PI3K* construct itself. This difference between PI3K and PI3K* constructs could result from their relative levels of expression due to their chromosomal sites of insertion, and/or stability of the proteins, among other reasons. Nevertheless, PI3K* proved more effective in the rescue of the mutant genotype of the canonical Gbb receptor, Wit (see below and Discussion).

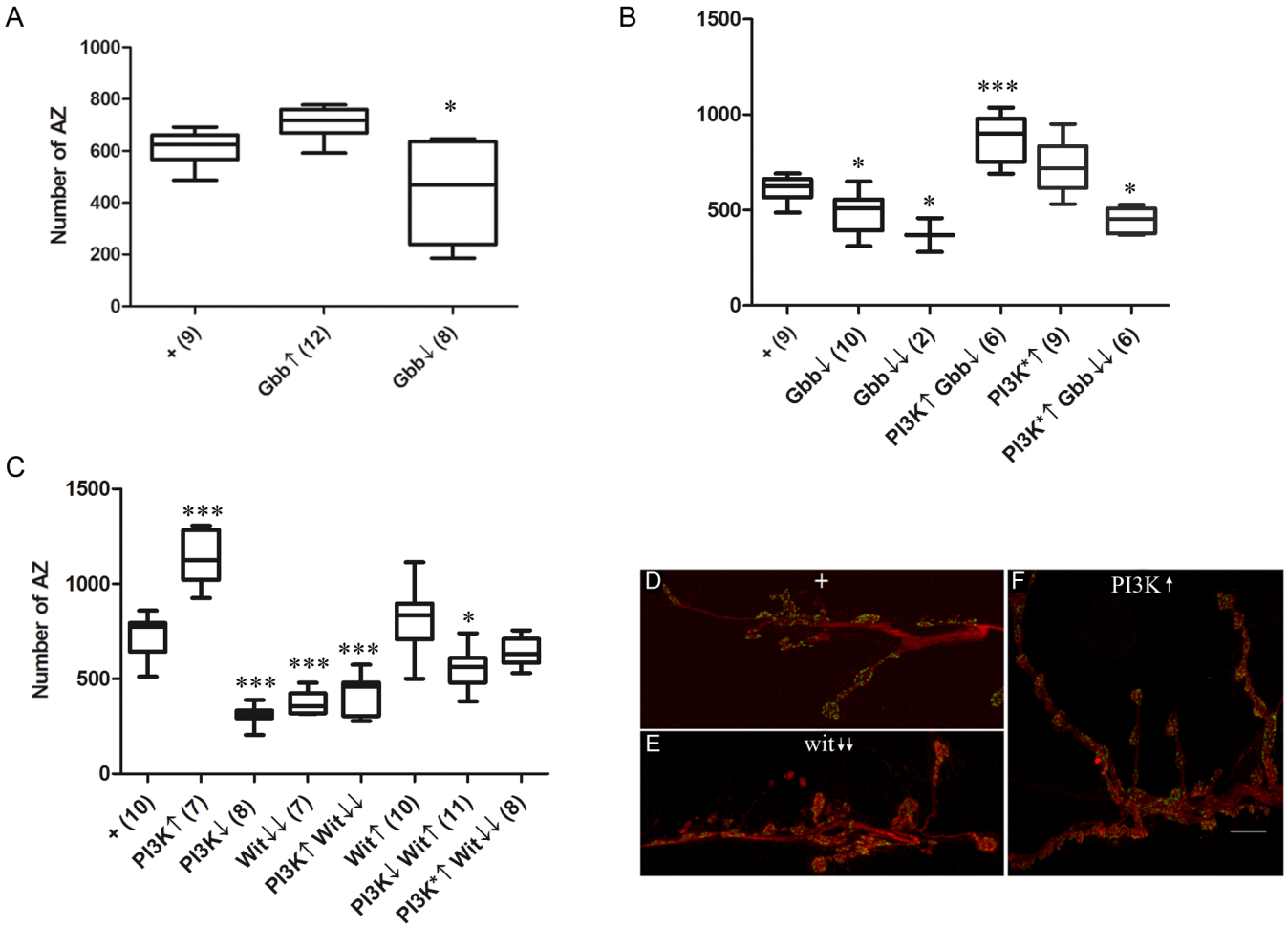

Fig 1. Ligand and receptor of the pro-synaptogenesis pathway. A) The over- (↑) or down-expression (↓) of the ligand Gbb in the muscle elicits mild changes in the number of synapses as indicated by the number of active zones (AZ) viewed as nc82 spots. Genotypes: **+** = *Mhc-Gal4/+*. **Gbb**↑ = *Mhc-Gal4/+;UAS-gbb/+*. **Gbb**↓ = *Mhc-Gal4/+;UAS-gbb^{RNAi}/+*. **B)** The *gbb* mutant larvae, either in heterozygous (Gbb↓) or homozygous (Gbb↓↓) conditions show reduced number of synapses. These data support a role of this ligand in synaptogenesis. Note, however, that synapses have not been eliminated (see main text). The viability of homozygotes is very poor and only two LIII larvae could be obtained. This is evidence that Gbb plays additional developmental roles beyond synaptogenesis. The up-regulation of the native form of PI3K suppresses the synapse effect in the heterozygotes although the effect of PI3K on its own is somewhat reduced (compare with PI3K↑ in panel C). The constitutively active PI3K, PI3K*, improves the viability of the homozygous *gbb* null mutants but the mutant synapse number is only weakly recovered, and it remains clearly below normal (see main text). Genotypes: + = *D42-Gal4/+*. **Gbb**↓ = *gbb^{1}/+; D42-Gal4/+*. **Gbb**↓↓ = *gbb^{1}/gbb^{2}; D42-Gal4/+*. **PI3K**↑**Gbb**↓ = *UAS-PI3K/gbb^{1}; D42-Gal4/+*. **PI3K***↑ = *UAS-PI3K*/+; D42-Gal4/+*. **PI3K***↑ **Gbb**↓↓ **=** *UAS-PI3K*/+; gbb^{1}/gbb^{2}; D42-Gal4/+*. **C)** The up-regulation of the native form of PI3K (PI3K↑) increases the number of synapses while its down-regulation (PI3K↓) yields the opposite effect. The overexpression of the receptor Wit is ineffective for synapse formation while the mutant condition (Wit↓↓**)** strongly reduces synapses. Note, however, that neither Wit nor Gbb depletion can eliminate synapses fully. Combinations of Wit and PI3K show that the mutant condition for Wit prevails over the overexpression of PI3K suggesting that PI3K requires activation by Wit. Consistent with this notion, the downregulation of PI3K still maintains its phenotype of reduced synapse number even though Wit is over-expressed. In the same line, a constitutively active form of PI3K, PI3K*, suppresses the mutant condition for the receptor. These results support the conclusion that PI3K is functionally downstream from the receptor Wit. Genotypes: **+** = *D42-Gal4/+* pooled with *OK6-Gal4/+*. **PI3K**↑ = *UAS-PI3K/+; D42-Gal4/+*. **PI3K**↓ = *UAS-PI3K^{DN}/+; D42-Gal4/+*. **Wit**↓↓ = *OK6-Gal4/+; wit^{A12}/wit^{B11}*. **PI3K**↑**Wit**↓↓ = *OK6-Gal4/UAS-PI3K; wit^{A12}/wit^{B11}*. **Wit**↑ = *D42-Gal4/UAS-Wit*. **PI3K**↓**Wit**↑ = *UAS-PI3K^{DN}/+; D42-Gal4/UAS-Wit*. **PI3K***↑**Wit**↓↓ = *UAS-PI3K*/+; OK6-Gal4/+; wit^{A12}/wit^{B11}*. **D-F)** Representative images of motor neuron 6–7 from larval abdominal segment A3 in normal (+) (**D**), *wit^{A12}/wit^{B11}* (↓) (**E**) and *D42-Gal4>UAS-PI3K* (↑) (**F**) genotypes. Number of NMJ analyzed in independent larvae is indicated in parenthesis adjacent to the genotype. Bar in **F** = 10μm.

https://doi.org/10.1371/journal.pone.0184238.g001

The receptor Wit is a key player for neuromuscular junction (NMJ) development [53, 56]. Eliminating its expression (hetero-allelic combination *wit^{A12}/wit^{B11}*) results in decrease of AZ numbers (Wit↓↓, Fig 1C). This effect supports the role of Wit as a key receptor in synaptogenesis. The co-expression of PI3K↑ yields the phenotype of Wit↓↓ alone, but a constitutive active

form of PI3K, PI3K*, can suppress the Wit↓↓ phenotype (Fig 1C). On the other hand, the over-expression of Wit is ineffective to change AZ numbers and the co-downexpression with PI3K results in the phenotype of PI3K↓ alone (Fig 1C). All these data indicate that PI3K is functionally downstream from Wit and requires its activation by the receptor.

The functional link of PI3K with Wit, considered as a receptor Ser/Thr kinase type (RSTK), appears unusual, since PI3K is more often related to receptors of the Tyr kinase type (RTK) (see Discussion). To further look into this issue, we tested classical RTKs in the context of synaptogenesis (S1 Table). No changes in AZ numbers were observed, underlying the specificity of Wit in neurons. In particular, the lack of effect of Thick veins (Tkv) and Saxophone (Sax), either separately or in combination, indicates that, contrary to NMJ development or growth [72], the role of Wit to signal for synaptogenesis does not rely on Tkv or Sax heterodimers. Among the tested RTKs, we included Torso which is not normally expressed in motor neurons. This ectopic expression was also ineffective to elicit synaptogenesis which further underlies the specificity of PI3K activation by the receptor Wit in the context of synaptogenesis.

Signaling from virtually all RTK pathways debouch in the relive of target gene silencing imposed by the transcriptional repressor Capicua (CIC) which is degraded [77]. We reasoned that, if Wit signals through a RTK pathway, then an increase of CIC levels should mimic the effects of Wit↓. Driving *UAS-cic* to motor neurons (*Gal4-D42*) caused a severe reduction of the number of synapses almost identical to that of Wit↓ (S1B Fig). These results open the possibility that Wit could elicit several modes of signaling depending on binding ligand or oligomerization partner (see Discussion).

Representative images of NMJs showing normal (+), increased (↑) and decreased (↓) AZ numbers illustrate how bouton number, or bouton size, do not correlate with synapse number (Fig 1D–1F, see also S1 Movie to illustrate AZs outside boutons and boutons without AZs). This is one, among several others (see below), argument that justify the need to count synapses directly rather than using bouton number as a surrogate to evaluate synapse number changes (see Materials and methods).

Two other RTKs were also investigated due to their postsynaptic (muscle) localization, Heartless (Htl) and Breathless (Btl) [78–80]. Mutant heterozygotes for each of these two FGFR-like receptors show a significant increase in the number of synapses (S1C Fig), indicating that they play a role in synaptogenesis. Thus, we tested the possible involvement of Htl and Btl on *gbb* expression by qPCR assays. The reduction of Htl (heterozygous htl^{AB42}/+) increased *gbb* transcription while that of Btl (heterozygous btl^{dev1}/+) led to the opposite effect (S2A Fig), suggesting that the two receptors regulate Gbb levels through antagonistic signaling within the muscle. To test if there could be a reverse, neuron-to-muscle, signaling to regulate *gbb*, we carried out additional qPCR assays in larvae with neuronal (*elav-Gal4*) up- or down-expression of PI3K. No transcriptional changes in *gbb* were detected in these larvae (S2A Fig). Thus, the reported activity of Gbb in neurons is not functionally related to PI3K levels. Our data are consistent with the proposal of two distinct pools of Gbb to control synapse structure and function, respectively [76].

In addition, we assayed the transcriptional expression of the known ligands of Htl and Btl; Pyramus (Pyr), Thisbe (Ths) and Branchless (Bnl), respectively [81–84] (S2B–S2D Fig). No effect on the expression of these ligands was observed when PI3K was altered in neurons; which is consistent with the muscular origin of Gbb signaling for synaptogenesis. So far, the data show that, once Gbb is secreted from the muscle and synaptogenesis is triggered in the motor neuron, no feed-back signaling is elicited. That is, once initiated, synaptogenesis proceeds autonomously in the motor neuron. Synapse activity, however, may require Gbb mediated coordination from the postsynaptic side as proposed [76]. Retrograde signaling has been

reported in activity dependent modulation of synapses where it is mediated by BMP [85]. Here, we focus on synapse formation rather than on activity.

Pro-synaptogenesis signaling downstream from the receptor

Since, in addition to tyrosine-kinase, G-protein coupled receptors can activate PI3K, and the small GTPase Ras has been implicated in vertebrate synaptogenesis [86], we tested its *Drosophila* homolog, Ras85D, in the Wit/PI3K signaling context. In the first series of experiments, neither the overexpression of Ras85D nor its downregulation by a dominant negative form, $Ras85D^{DN}$, revealed any effect on synapse number (Fig 2A). Also, co-manipulation of Ras85D and Wit in either direction or combination failed to show synapse number effects. Although these data could be taken as evidence that Ras85D does not play a role in *Drosophila* synaptogenesis, in contrast to vertebrates, the subsequent series of experiments with PI3K proved the opposite.

The simultaneous up-regulation of Ras85D and PI3K suppressed the synapse number increase due to PI3K alone (Fig 2B). This result demonstrates that the *UAS-Ras85D* construct is effective and that both proteins are functionally linked in the context of synaptogenesis. Furthermore, the *UAS-*$Ras85D^{DN}$ construct (Ras85D↓) is also effective because it transforms the synapse increase due to PI3K↑ into a significant decrease (Fig 2B). Thus, consistent with vertebrates, *Drosophila* Ras85D is also involved in synaptogenesis, and we can add that it acts by counteracting the role of PI3K. Since, in certain pathways, PI3K needs Ras binding for maximal activity [45], we considered PI3K as a potential site of convergence with Ras85D in the context of synaptogenesis. To determine if the Ras85D requirement occurs at the PI3K step, we tested a form of PI3K in which the Ras binding site is deleted, $PI3K^{\Delta RBD}$. This myc-tagged $PI3K^{\Delta RBD}$ form elicited a synapse increase equivalent to that of the normal PI3K (myc-PI3K) demonstrating that Ras binding is dispensable for PI3K activity in this context (Fig 2B). Consistent with the functional link between Ras85D and PI3K, the down regulation of Ras85D did suppress the pro-synaptic effect of $PI3K^{\Delta RBD}$ yielding a strong decrease (Fig 2B).

As a further attempt to locate Ras85D in the signaling hierarchy, we tested by Western blot the relative levels of phospho-AKT in flies over-expressing Ras85D [87]. The data show that the mechanism of Ras85D activity does not involve an increase of p-AKT levels (Fig 2C). Therefore, we can conclude that, contrary to other signaling contexts, PI3K-Ras85D binding is not a requirement in synaptogenesis, placing the role of Ras85D in synaptogenesis further down along the pathway.

Intermediate signaling in the pro-synaptogenesis pathway

Highwire (Hiw) has been reported as a negative regulator of NMJ growth in *Drosophila* [50, 59] and *C. elegans* [88]. This interpretation is based on the observation that *Hiw* mutants in both species show overgrown NMJs. Hiw has, at least, two different substrates: Wallenda, the first MAPK of the JNK cascade [50], and the transcriptional factor Medea [44, 89]. We tested the involvement of PI3K in the Hiw-MAPK signaling (Fig 3A).

As expected, the Hiw↑ condition increased significantly the number of synapses. The loss-of-function allele Hiw^{ND8} (Hiw↓) or the overexpression of a form deleted in the E3 ubiquitin ligase domain, $Hiw^{\Delta 3}$, yielded only a trend towards synapse number reduction that failed to reach statistical significance (Fig 3A). However, as in the case of Ras85D above, the phenotypic effects of the loss-of-function condition for Hiw became evident when tested in combinations with PI3K. The co-expression of Hiw↑ and PI3K↓ results in the mutual suppression of the single phenotypes and yields normal number of synapses (Fig 3A). The opposite combination, Hiw↓PI3K↑, transforms the PI3K↑ into a significant reduction of synapse number; thus,

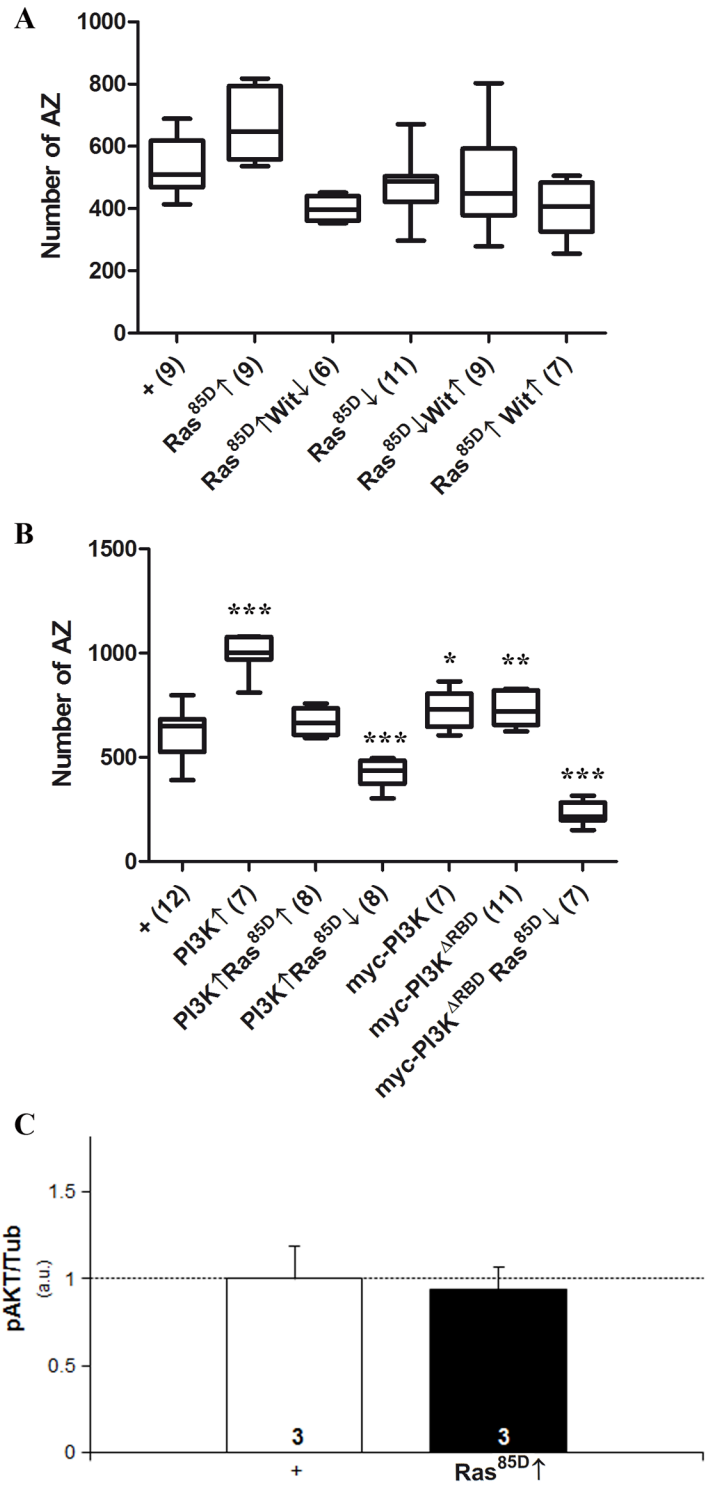

Fig 2. Signaling factors downstream from the receptor Wit. A) The over- or down-expression of Ras85D, either alone or in combination with manipulations of Wit, seem ineffective to change synapse number. Further experiments, however, proved the contrary (see below). Genotypes: **+** = *D42-Gal4/+*. **Ras85D↑** = *UAS-Ras85D/+; D42-Gal4/+*. **Ras85D↑Wit↓** = *UAS-Ras85D/+; D42-Gal4/UAS-Wit^{RNAi}*. **Ras85D↓** = *UAS-Ras85D^{DN}/+; +/+; D42-Gal4/+*. **Ras85D↓Wit↑** = *UAS-Ras85D^{DN}/+; UAS-Wit /+; D42-Gal4/+*. **Ras85D↑Wit↑** = *UAS-Wit/UAS-Ras85D; D42-Gal4/+*. **B**) PI3K-Ras85D interactions. Both, the over- or down-expression of Ras85D, which seemed ineffective on the synapse number, suppress the synapse increase due to PI3K↑

when jointly expressed. In the case of Ras85D↓ the phenotype is converted into synapse decrease. These features demonstrate that Ras85D is functionally related to PI3K in the context of synaptogenesis. The up-regulation of a PI3K form that is deleted in the Ras phosphorylation site, *myc-PI3K*$^{\Delta RBD}$, is still able of increase synapses even though its control, *myc-PI3K*, is somewhat less effective than PI3K. The *PI3K*$^{\Delta RBD}$ form, as the normal PI3K, transforms the Ras85D↓ phenotype into a severe synapse reduction. These data are consistent with Ras85D being functionally located somewhere down stream in the PI3K pathway. Genotypes: **+** = *D42-Gal4/+*. **PI3K↑** = *UAS-PI3K/+; D42-Gal4/+*. **PI3K↑Ras85D↑ =** *UAS-Ras85D/+; UAS-PI3K/+; D42-Gal4/+*. **PI3K↑Ras85D↓** = *UAS-Ras85D*^{DN}*/+; UAS-PI3K/+; D42-Gal4/+*. **myc-PI3K↑** = *D42-Gal4/UAS-myc-Dp110*. **myc-PI3K**$^{\Delta RBD}$**↑** = *D42-Gal4/UAS-myc-Dp110*^{RBD}. **myc-PI3K**$^{\Delta RBD}$**↑Ras85D↓** = *UAS-Ras85D*^{DN}*/+; D42-Gal4/UAS-myc-Dp110*^{RBD}. **C)** Western blot analysis (triplicates) of phospho-AKT relative levels under Ras85D overexpression. No increase of pAKT is detected demonstrating that Ras85D is functionally downstream from AKT. Genotypes: **+** = *D42-Gal4/+*. **Ras85D↑** = *UAS-Ras85D/+*; *D42-Gal4/+*.

https://doi.org/10.1371/journal.pone.0184238.g002

revealing the expected effect of Hiw↓ (Fig 3A). A further evidence of the Hiw-PI3K interaction is reflected in the synergy of the Hiw↓PI3K↓ combination which results in lethality earlier than the third larval instar. This feature prevented synapse counting. Taken together, these results are consistent with the functional location of Hiw downstream from PI3K. Interestingly, the *Hiw*^{ND8} mutant exhibited the reported increase in branch length [55, 60], which contrasts with the lack of effect on synapse number (S3 Table). This is another example illustrating the independence of neuritogenesis with respect to synaptogenesis. The case of Hiw is also in line with a previous report on LIMK1 which binds the Wit receptor to promote synapse stability, but the binding is dispensable for synapse growth or function [90].

The *Drosophila* MAPKs *Wallenda (Wnd)*, *Hemipterous (Hep)* and *Basket (bsk)* are homologues of vertebrate DLK (MAPK), MKK7 (MAPKK) and JNK (MAPKKK), respectively. Their role in synaptogenesis and their relationship with Hiw are relatively well established [50], albeit complex. The context-dependence of the Hiw-MAPKs signaling is illustrated by the recently reported cell autonomous and non-cell autonomous effects of Hiw. Whereas Hiw attenuates Wnd, Bsk and the transcription factor Jun (see below) in the neuron, in glial cells, the transcriptional output of Hiw seems to be through Fos, which acts on adjacent neurons via an unidentified secreted factor [91]. Here, we confirmed most of the expected MAPK effects in the NMJ with increases in synapse number after Wnd and Bsk upregulations (Fig 3B).

In the case of Hep, its upregulation does not seem to produce the expected synapse increase (Fig 3B). The homologue in vertebrates, MKK7, cooperates with MKK4 to activate JNK/Bsk [92]. This cooperative effect is non-redundant and it exhibits a wide repertoire of context-dependent signaling properties [93]. Thus, it is plausible that the fly Hep would require a MKK4 equivalent to display its synaptogenesis effects. On the issue of neuritogenesis *versus* synaptogenesis (see above), it is worth noting that Wnd↑ and Hep↑ yielded the reported branch overgrowth (S3A–S3C Fig) [49, 50], but synapses were increased in Wnd↑ only. Likewise, Hiw↓ increased branching (S3D Fig**),** but not synapses. This suggests that neurito- and synaptogenesis share some signaling steps while they keep others as specific.

Concerning Bsk, the ↑ condition yielded the expected synapse increase but the ↓ condition seemed ineffective (Fig 3B). However, as in previous cases, Bsk↓ revealed its effect on synaptogenesis when combined with other regulatory elements of the pathway. The joint up-regulation of PI3K and Bsk, two factors promoting synapse increase, maintain their single phenotypes without evidences of synergy (Fig 3B). This is consistent with the location of both factors in the same pathway. Further, if Bsk would be down stream of PI3K in a simple functional dependency, one would expect that Bsk↓ would suppress PI3K↑. This double genotype still showed synapse increase, although not as high as PI3K↑ alone (Fig 3B). This result suggests that the actual output from Bsk is subject to the regulation by additional factors beyond PI3K and the tested MAPKs.

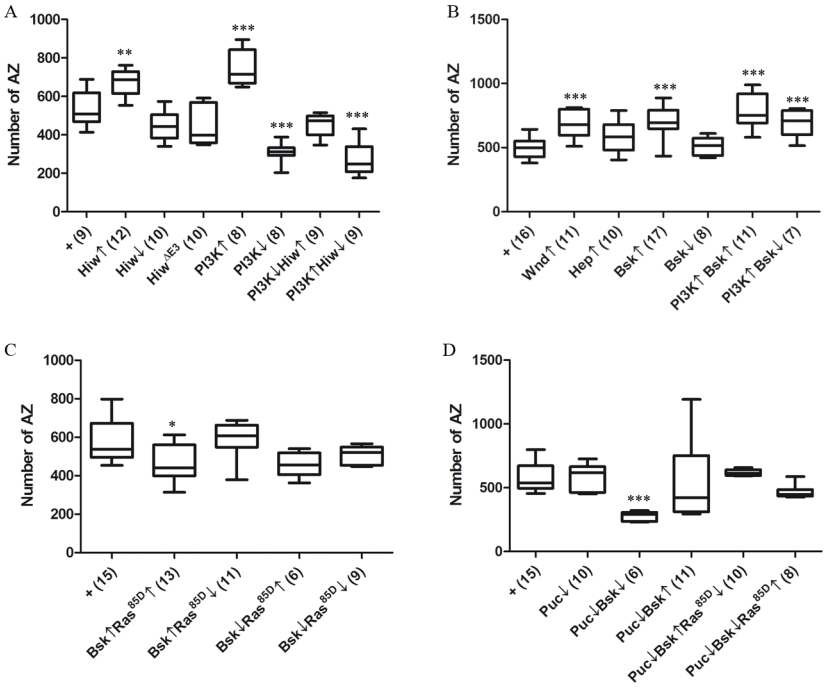

Fig 3. Intermediate signaling in the pro-synaptogenesis pathway. A) Interactions between Hiw and PI3K. The overexpression (Hiw↑) increases the number of synapses, while the mutant *hiw*^{ND8} or a form deleted in the E3 domain, Hiw$^{\Delta E3}$, show a non-significant tendency towards reduction only. However, while the over-expression of PI3K (PI3K↑) increases the number of synapses and its downregulation with a dominant negative form (PI3K↓) reduces it, both effects are suppressed by manipulating Hiw in the opposite directions. These data place Hiw functionally downstream from PI3K in the pathway. Genotypes: **+** = *D42-Gal4/+*. **Hiw↑** = *UAS-Hiw/+; D42-Gal4/+*. **Hiw↓** = males *hiw*^{ND8}*; +/+; D42-Gal4/+*. **Hiw$^{\Delta E3}$↑** = *D42-Gal4/UAS-NT-Hiw*$^{\Delta RING}$. **PI3K↑** = *UAS-PI3K/+; D42-Gal4/+*. **PI3K↓** = *UAS-PI3K*^{DN}*/+; D42-Gal4/+*. **PI3K↓Hiw↑** = *UAS-Hiw/ UAS-PI3K*^{DN}*; D42-Gal4/+*. **PI3K↑Hiw↓** = males *hiw*^{ND8}*; UAS-PI3K/+; D42-Gal4/+*. **B**) The MAPKs of the pathway. Wnd shows the expected pro-synaptogenesis effect while Hep fails to reach statistical significance. However, their target, Bsk/JNK, does show the expected synapse increase. Apparently, the Bsk↓ construct is ineffective and there is no evidence of synergy or antagonism with PI3K in the PI3K↑Bsk↑ or PI3K↑ Bsk↓ conditions (however, see below). Genotypes: **+** = *D42-Gal4/+*. **Wnd↑** = *UAS-Wnd/+; D42-Gal4/+*. **Hep↑** = *UAS-Hep/+; D42-Gal4/+*. **Bsk↑** = *UAS-Bsk/+; D42-Gal4/+*. **Bsk↓** = *D42-Gal4/UAS-Bsk*^{DN}. **PI3K↑Bsk↑** = *UAS-Bsk/UAS-PI3K; D42-Gal4/+*. **PI3K↑Bsk↓** = *UAS-PI3K/+; D42-Gal4/UAS-Bsk*^{DN}. **C)** The possible regulation of Bsk by Ras85D. Although the up-regulation of Bsk had proven pro-synaptogenic, its concomitant over-expression with the seemingly ineffective Ras85D transforms the pro- into an anti-synaptogenesis effect. Also, the apparently ineffective Ras85D↓ suppresses the pro-synaptogenic effect of Bsk↑. These data are indicative of a regulatory interaction between Ras85D and Bsk. The Bsk↓ condition, which proved ineffective, remained unchanged irrespective of the two possible alterations of Ras85D. Genotypes: **+** = *D42-Gal4/+*. **Bsk↑Ras^{85D}↑** = *UAS-Bsk/UAS-Ras85D; D42-Gal4/+*. **Bsk↑Ras^{85D}↓** = *UAS-Ras85D*^{DN}*/+; UAS-Bsk/+; D42-Gal4/+*. **Bsk↓Ras^{85D}↑** = *UAS-Ras85D/+; D42-Gal4/UAS-Bsk*^{DN}. **Bsk↓Ras^{85D}↓** = *UAS-Ras85D*^{DN}*/+; +/+; D42-Gal4/UAS-Bsk*^{DN}. **D)** The Bsk regulator Puc and the convergence with Ras85D in a tripartite interaction. Whereas the downregulation of Puc or Bsk separately yields no effect on synaptogenesis, their joint co-downregulation results in a strong decrease of the number of synapses. Also, the synapse increase elicited by Bsk↑ is rendered non-significant because of the wide dispersion of values elicited by the joint down regulation of Puc. The two triple combinations tested result in a notable reduction of the variability in the number of synapses (see text). Together, the data in **C** and **D** reveal a complex regulatory network at the final step of the MAPK cascade. Genotypes: **+** = *D42-Gal4/+*. **Puc↓** = *UAS-puc*^{RNAi}*/+; D42-Gal4/+*. **Puc↓Bsk↓** = *UAS-puc*^{RNAi}*/+; D42-Gal4/UAS-Bsk*^{DN}. **Puc↓Bsk↑** = *UAS-Bsk/UAS-puc*^{RNAi}*; D42-Gal4/+*. **Puc↓Bsk↑Ras^{85D}↓** = *UAS-Ras85D*^{DN}*/+; UAS-puc*^{RNAi}*/UAS-Bsk; D42-Gal4/+*. **Puc↓Bsk↓Ras^{85D}↑** = *UAS-Ras85D*, *UAS-puc*^{RNAi}*/+; D42-Gal4/ UAS-Bsk*^{DN}.

https://doi.org/10.1371/journal.pone.0184238.g003

Since we had concluded (see above) that Ras85D is functionally located downstream from PI3K, we considered if Ras85D could contribute to the pathway through a regulatory convergence on Bsk. Thus, we tested the joint ↓ and ↑ conditions for Bsk and Ras85D. The synapse number increase caused by Bsk↑ is transformed into reduction by Ras85D↑ which, by itself,

had no effect (Fig 3C). This transformation of phenotype is suggestive of antagonistic regulation between both enzymatic activities or upon a third substrate. Consistent with this interpretation, the Bsk↑ phenotype is cancelled by Ras85D↓ yielding normal synapse number (Fig 3C). The other two combinations possible, whose single components had no synaptic effect, remained ineffective (Fig 3C).

Beyond the novel regulatory role of Ras85D over Bsk proposed here, Bsk has been shown to be regulated also by the phosphatase *puckered* (*puc*) in epithelial cells [94]. We tested if the synaptogenic effects of Bsk could be modified by Puc. Although Puc↓ and Bsk↓ had no effect on synapses separately, the double combinations resulted in strong reduction of synapse number, indicating that Puc is also a Bsk regulator in this context (Fig 3D). As reasoned above, uncovering a phenotype by the combination of two elements which appeared ineffective on their own is an indication that both elements may be part of a binary system of regulation. Furthermore, the seemingly ineffective Puc↓ condition suppresses the effect of Bsk↑ by dispersing the values of synapse number beyond statistical significance (Fig 3D).

To evaluate if the regulatory roles of Ras85D and Puc over Bsk are independent or redundant, we assayed triple combinations of these constructs. Puc↓ does not modify the suppression that Ras85D↓ plays over Bsk↑ already (Fig 3C and 3D). Also, Puc↓ does not modify the lack of effects exhibited by Bsk↓ and Ras85D↑, either separately or in combination. Taken together, these data may indicate that Bsk and Ras85D/Puc antagonize each other in the context of synaptogenesis, perhaps by helping to set the normal activity threshold of Bsk. In this way, Bsk activity level is revealed as a particularly sensitive step in the signaling pathway and subject to the dual, but independent, regulation by Puc and Ras85D.

Effectors of the pro-synaptogenesis pathway

AP-1 is a transcriptional complex that includes the heterodimer Jun/Fos [95]. It is known to play multiple roles in development and, in conjunction with the MAPK cascade, it is involved in neuronal growth [49, 96] and hence, in neural plasticity and memory [97, 98]. Actually, *puc* seems to modulate target gene expression by antagonizing a Rho GTPase pathway that stabilizes AP-1, perhaps through a kinase-dependent mechanism [99].

We tested the relative contributions of Jun and Fos to synaptogenesis. Out of the four genotypes possible, only Jun↑ gave a phenotype, synapse increase, which justifies its qualification as a pro-synaptogenesis element (Fig 4A). As in the case of Ras85D above, the seemingly ineffective constructs revealed their role when in combination with other elements. The joint overexpression of Jun and Fos maintained the synapse increase due to Jun↑ alone. However, the effect of the later becomes transformed into synapse reduction by the co-expression with the apparently ineffective Fos↓ (Fig 4A).

As reasoned for the case of Bsk and Ras85D above, this result with Jun↑Fos↓ suggests a functional antagonism between Jun and Fos in the context of synaptogenesis, as if the two components of the AP-1 complex would counterbalance each other. The role of Fos as transcriptional activator has been shown to be context dependent, in particular the context provided by Jun and Mad [100] (see also below on the synaptic effects of Mad). If the regulation of AP-1 stability by Puc and a Rho GTPase turns out to be effective in the context of synaptogenesis as proposed [99], it is likely that revealing synapse phenotypes would require joint manipulations of several of these components.

Anti- and pro-synaptogenesis pathways and their interactions

The reported inhibition of Medea (Med) by Hiw [59] and the differential activity of Jun prompted us to analyze the effect of Med transcription factor and its partner, Mothers-against-

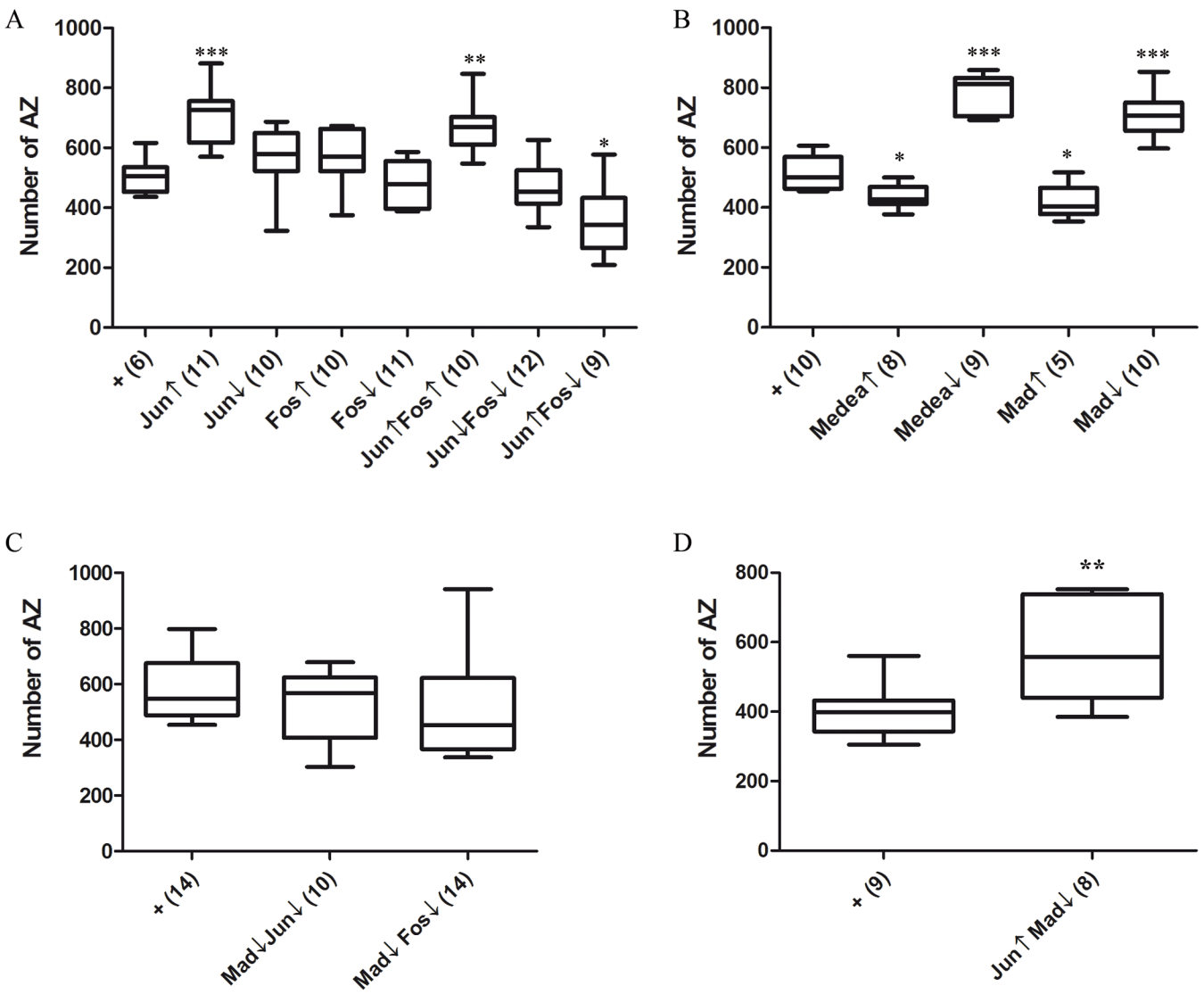

Fig 4. Effectors of the pathway. A) Epistasis analysis of the AP-1 components, Fos and Jun. Single manipulations of these two transcription factors in either direction yields the expected synapse increase in the case of Jun↑ only, which could be interpreted as if the other three constructs were ineffective. However, Fos↓ transforms the Jun↑ synapse increase effect into a decrease. This and other results throughout this study demonstrate that the seemingly ineffective constructs are functional. Likely, Jun and Fos play their role through interactions with other anti-synaptogenesis transcription factors (see below). Genotypes: **+** = *D42-Gal4/+*. **Jun↑** = *D42-Gal4/UAS-Jun*. **Jun↓** = *UAS-Jun^{DN}/+; D42-Gal4/+*. **Fos↑** = *UAS-Fos/+; D42-Gal4/+*. **Fos↓** = *UAS-Fos^{DN}/+; D42-Gal4/+*. **Jun↑Fos↑** = *UAS-Fos/+; D42-Gal4/ UAS-Jun*. **Jun↓Fos↓** = *UAS-Fos^{DN}/ UAS-Jun^{DN}; D42-Gal4/+*. **Jun↑Fos↓** = *UAS-Fos^{DN}/+; D42-Gal4/UAS-Jun*. **B)** The Med-Mad components. The up- or down-regulation of these two transcription factors yield effects consistent with a role as negative regulators of synaptogenesis which implies the existence of an anti-synaptogenesis pathway. Genotypes: **+** = *D42-Gal4/+*. **Medea↑** = *D42-Gal4/UAS-Medea$^{\#5.13A3}$*. **Medea↓** = *D42-Gal4/UAS-TRiP.JF02218attP*. **Mad↑** = *UAS-Mad$^{\#2A2}$/D42-Gal4/+*. **Mad↓** = *UAS-Mad^{RNAi} /+; D42-Gal4/+*. **C)** Mad interactions with AP-1. The apparently ineffective Jun↓ and Fos↓ constructs suppress the Mad↓ phenotype when jointly expressed. This set of data proves that the constructs are effective and that Fos and Jun interact with the anti-synaptogenesis factor Mad. Genotypes: **+** = *D42-Gal4/+*. **Mad↓Jun↓** = *UAS-Mad^{RNAi} /UAS-Jun^{DN}; D42-Gal4/+*. **Mad↓Fos↓** = *UAS-Fos^{DN}/UAS-Mad^{RNAi}; D42-Gal4/+*. **D)** In a separate experiment, hence the reason for a separate panel, two conditions that had shown pro-synaptogenesis effects, Jun↑ and Mad↓, although they still show synapse increase, the magnitude of the effect is lower than each element separately. This is suggestive of an antagonistic interaction between these two transcription factors. Genotypes: **+** = *D42-Gal4/+*. **Jun↑Mad↓** = *UAS-Mad^{RNAi} /+; D42-Gal4/UAS-Jun*.

https://doi.org/10.1371/journal.pone.0184238.g004

dpp (Mad/Mnt), in the context of synaptogenesis. Interestingly, both factors exhibited coherent anti-synaptogenesis phenotypes. That is, decrease of synapse number in the ↑ condition and increase of synapses in the ↓ condition (Fig 4B). Mad and Med are known for their role in preventing cell differentiation to promote proliferation [101]. Here, they seem to reveal an anti-synaptogenesis signaling pathway without proliferation effects, given that axon numbers in the NMJ remained normal in these genotypes. Since transcription factors with putative pro- and anti-synaptogenesis roles had been identified, we explored the joint effects of some of them. The apparently ineffective Jun↓ condition suppressed the Mad↓ phenotype (Fig 4C). This result is relevant because it proves that the Jun↓ construct is functional (see above). Likewise, the Fos↓ condition suppressed the Mad↓ phenotype (Fig 4C). Also, the combination of two factors that yield synapse increase separately, Jun↑ and Mad↓ (Fig 4A and 4B) produced a synapse increase greatly attenuated with respect to the separate factors (Fig 4D). These data represent evidence that AP-1, either as a Jun/Fos heterodimer or as independent components, and Mad functionally interact in the context of synaptogenesis in an antagonistic manner.

The canonical signaling pathway of Mad/Med includes the transcriptional co-regulator Yorkie and the microRNA bantam [102]. Thus, we tested bantam (Ban) in the context of synaptogenesis. The Ban↑ condition elicited a wide dispersion of synapse number values that render the tendency towards reduction as non-statistically significant. However, that condition suppressed the effects of PI3K↑, Hiw↑ and Ras85D↑ when jointly expressed (Fig 5A). In addition, the apparently ineffective Ban↑ transformed the phenotypes of Bsk↑ and Bsk↓ (Fig 3B) into a synapse reduction (Fig 5A). These data justified the allocation of Ban to the anti-synaptogenesis pathway and revealed its downregulation effects upon several elements of the pro-synaptogenesis pathway with the notable exception of Akt↑. The case of Akt is indicative that Ban does not target that gene and, in addition, that Akt has a substrate functionally downstream of Ban (see below). Thus, bantam should be included in the long list of microRNAs which contribute to synapse control [103].

The identification of transcriptional regulators with anti-synaptogenesis effects implies a corresponding signaling pathway that would counteract the pro-synaptogenesis pathway described hereto. Thus, we explored candidate genes that encode proteins akin to those constituting the pro-synaptogenesis signaling, MAPK and GTPases, mainly. The candidate genes were chosen based on previous reports of their functional interactions with *yorkie* (*yki*), a canonical member of the Mad/Medea transcriptional complex [104]. Out of the seven candidates tested, the two small GTPases Ras-like-a (Rala) and Ras64B (Ras64B), along with the two MAPKs Licorne (Lic) and p38a yielded synaptic phenotypes compatible with their adscription to the anti-synaptogenesis pathway (Fig 5B). Testing Licorne and p38a was justified because these two kinases share the same pathway in other cellular contexts [105, 106]. Here, p38 seems to contribute to the anti-synaptogenesis signaling while data on Licorne are too variable to draw a conclusion (Fig 5B). Concerning Rala, this neural GTPase plays a role in the activity-dependent changes at the postsynaptic side [107]. Thus, it seems coherent that, down-regulating it in the presynaptic side would increase synapse number. By contrast, the tyrosine kinase receptor punt (Put), the protein kinases Slipper (Slpr) and the apoptotic signaling-1 (Ask1/Pk92B) caused no effect (Fig 5B). The lack of effect of Ask1 represents another example of a context-dependent specificity for signaling. In human islet cells, Ask1 is functionally related to PI3K and JNK signaling [108], but it does not seems to be the case for synaptogenesis in fly neurons. Remarkably, all these anti-synaptogenesis components belong to the same functional classes (small GTPases, MAPK, etc.) as those of the pro-synaptogenesis pathway (see Discussion). The Yki transcriptional cofactor is known to receive signaling through the Hippo-Salvador-Warts pathway [109]. An alternative Hippo pathway has been reported that does not use

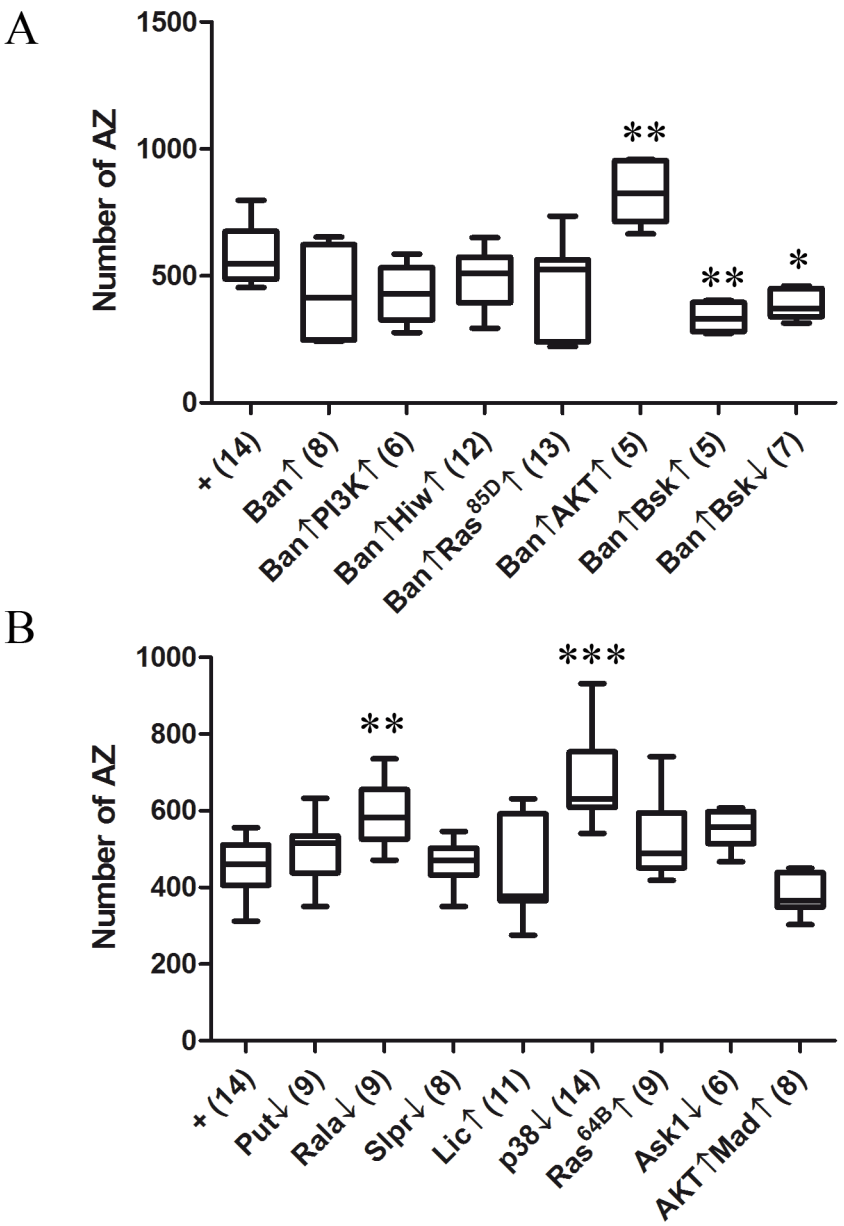

Fig 5. The anti-synaptogenesis pathway. A) The microRNA bantam shows a tendency towards synapse reduction which becomes evident by suppressing the synapse increase of PI3K↑, Hiw↑ and Bsk↑. By contrast, AKT escapes the repression by Ban since it maintains its synapse increase phenotype reported previously. Although below statistical significance, the pro-synaptogenesis tendency exhibited by Ras85D↑ seems also reverted by Ban. Also, the apparently ineffective Bsk↓ or the pro-synaptogenesis Bsk↑, both become anti-synaptogenic by Ban. These data justify the inclusion of Ban in the anti-synaptogenesis pathway and indicate additional targets for this microRNA. Genotypes: **+** = *D42-Gal4/+*. **Ban↑** = *D42-Gal4/UAS-bantam*. **Ban↑PI3K↑** = *UAS-PI3K/+; D42-Gal4/UAS-bantam*. **Ban↑Hiw↑** = *UAS-Hiw/+; D42-Gal4/UAS-bantam*. **Ban↑Ras85D↑** = *UAS-Ras85D/+; D42-Gal4/UAS-bantam*. **Ban↑AKT↑** = *D42-Gal4/UAS-bantam,UAS-Akt*. **Ban↑Bsk↑** = *UAS-Bsk/+; D42-Gal4/UAS-bantam*. **Ban↑Bsk↓** = *UAS-Bsk^{DN}/+; +/+; D42-Gal4/UAS-bantam*. **B)** Assays of selected MAPK and GTPases candidates for the anti-synaptogenesis signaling. Genotypes: **+** = *D42-Gal4/+*. **Put↓** = *UAS-put^{RNAi}/+; D42-Gal4/+*. **Rala↓** = *UAS-Rala^{DN}/+; D42-Gal4/+*. **Slpr↓** = *D42-Gal4/UAS-Slpr^{RNAi}*. **Lic↑** = *UAS-Lic/+; +/+; D42-Gal4/+*. **p38↓** = *UAS-p38a^{RNAi}/+; D42-Gal4/+*. **Ras64B↑** = *UAS-Ras64B^{V14}/+; D42-Gal4/+*. **Ask1↓** = *D42-Gal4/UAS-Ask1^{RNAi}*. **AKT↑Mad↑** = *UAS-Akt/+; +/+; D42-Gal4/UAS-Mad$^{#2A2}$*.

https://doi.org/10.1371/journal.pone.0184238.g005

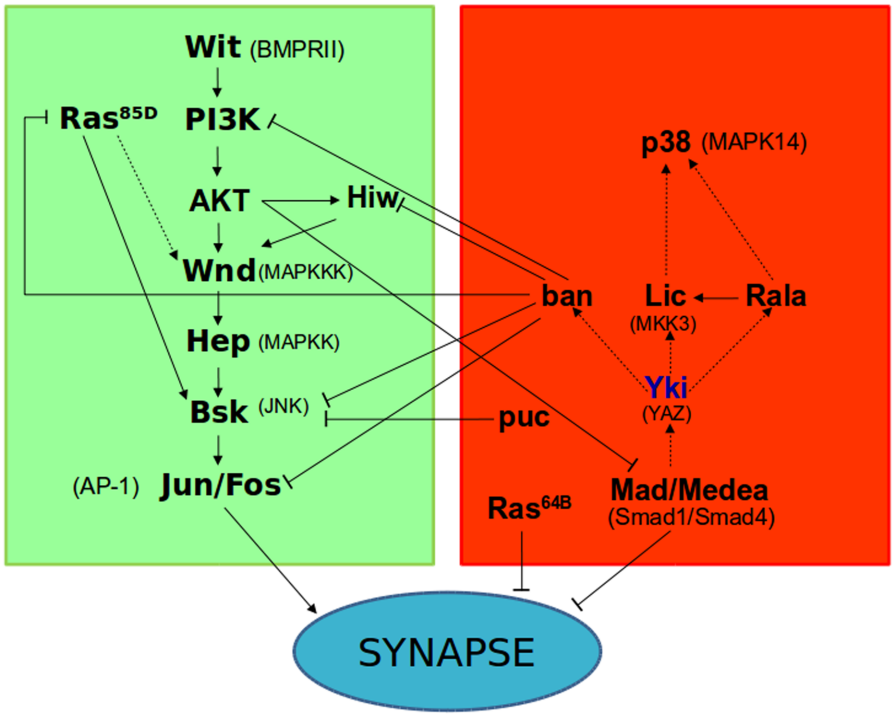

Fig 6. Summary diagram of antagonistic signaling pathways for synaptogenesis and their interactions. The pro-synaptogenesis pathway is shown in green while the anti-synaptogenesis one is shown in red. Arrows indicate activation and blunt lines indicate repression. Full lines correspond to interactions tested in this study and dotted lines refer to studies in other cellular contexts. The factor Yki was not included in this study and it is shown to illustrate interactions reported with the anti-synaptogenesis factors tested here. The vertebrate orthologues are shown between parentheses.

https://doi.org/10.1371/journal.pone.0184238.g006

Yki as a transcriptional effector and that, remarkably, mediates neuronal bouton formation [110]. This is another evidence of the strong context-dependence of signaling pathways.

Finally, the substrate for Akt downstream from Ban that we hypothesized above was tested in the double genotype with Mad, the final effector of the anti-synaptogenesis pathway. Both elements together, Akt↑Mad↑, cancelled each other yielding a normal number of synapses (Fig 5B). This result is consistent with the observed lack of suppression of Akt↑ by Ban (Fig 5A) and suggests that Mad may be targeted by Akt in the context of synaptogenesis. The results in this report compose a scenario in which a delicate signaling balance between two antagonistic pathways determines the number of synapses that a neuron will establish under a particular functional status (Fig 6).

Discussion

The epistasis assays have determined the *in vivo* functional links between PI3K and other previously known pro-synaptogenesis factors. Epistasis assays are based on the combined expression of two or more UAS constructs. Several double combinations in this study have produced a phenotype in spite of the apparent ineffectiveness of the single constructs. This type of results underscores the necessity to use epistasis assays in order to reveal functional interactions in vivo, hence, biologically relevant. In addition to the pro-synaptogenesis signaling, the study has revealed an anti-synaptogenesis pathway that composes a signaling equilibrium to determine the actual number of synapses. The magnitude of the synapse number changes elicited by the factors tested here are mostly within the range of 20–50%. Are these values significant

to cause behavioral changes? Reductions in the order of 30% of excitatory or inhibitory synapses in adult *Drosophila* local olfactory interneurons transform perception of certain odorants from attraction to repulsion and vice versa [10]. In schizophrenia patients, a 16% loss of inhibitory synapses in the brain cortex has been reported [12]. In *Rhesus* monkeys, the pyramidal neurons in layer III of area 46 in dorsolateral prefrontal cortex show a 33% spine loss, and a significant reduction in learning task performance during normal aging [111]. Thus, it seems that behavior is rather sensitive to small changes in synapse number irrespective of the total brain mass.

The signaling interactions analyzed here were chosen because they were reported in other cellular systems and species previously. Some of these interactions have been confirmed (e.g.: Gbb/Wit), while others have proven ineffective in the context of synaptogenesis (e.g.: Ras85D/PI3K binding). Likely, the two signaling pathways, pro- and anti-synaptogenesis, are not the only ones relevant for synapse formation. For example, in spite of the null condition of the *gbb* and *wit* mutant alleles used here, the resulting synaptic phenotypes are far less extreme than expected if these two factors would be the only source of signaling for synaptogenesis. Although it could be argued that the incomplete absence of synapses in the mutant phenotypes could result from maternal perdurance, Wit is not part of the oocyte endowment while Gbb is. Three alternative possibilities may be considered, additional ligands for Wit, additional receptors for Gbb, and a combination of the previous two. Beyond the identity of these putative additional ligands and receptors, the stoichiometry between ligands and receptors may certainly be relevant. Actually, Gbb levels are titrated by Crimpy [68, 71]. An equivalent quantitative regulation could operate on Wit. The reported data on Wit illustrate already the diversity of the functional repertoire of this receptor. Wit can form heteromeric complexes with Thick veins (Tkv) or Saxophone (Sax) receptors to receive Dpp/BMP4 or Gbb/BMP7 as ligands [112, 113]. However, the same study also showed that Wit could dimerize with another receptor, Baboo, upon binding of Myoglianin to activate a different and antagonistic signaling pathway, TGFβ/activin-like [see also [114, 115]].

The Gbb/Wit/PI3K signaling analyzed here is likely not the only pro-synaptogenesis pathway in flies and vertebrates. The ligand wingless (Wg), member of the Wnt family, and the receptors Frizzled have been widely documented as relevant in neuromuscular junction development, albeit data on synapse number are scant [116, 117]. Interestingly, however, the downstream intermediaries can be as diverse as those mentioned above for Wit [118]. Although generally depicted as linear pathways, a more realistic image would be a network of cross-interacting signaling events whose in situ regulation and cellular compartmentalization remains fully unexplored.

The quantitative regulation of receptors is most relevant to understand their biological effects. In that context, is worth noting that Tkv levels are distinctly regulated from those of Wit and Sax through ubiquitination in the context of neurite growth [119]. On the other hand, although the receptor Wit is considered a RSTK type [120], the functional link with PI3K is a feature usually associated to the RTK type instead. The link of Wit with a kinase has a precedent with LIMK1 that binds to, and is functionally downstream from, Wit in the context of synapse stabilization [90]. Thus, Wit should be considered a wide spectrum receptor in terms of its ligands, co-receptor partners and, consequently, signaling pathways elicited. Actually, the Wit amino acid sequence shows both, Tyr and Ser/Thr motifs justifying its initial classification as a "dual" type of receptor (http://flybase.org). In this report we have not determined if Wit heterodimerizes with other receptors, as canonical RSTKs do, or if it forms homodimers, as canonical RTKs do. However, the lack of synaptogenesis effects by the putative co-receptors, Tkv and Sax, and the phenotypic similarity with the manipulation of the standard RTK

signaling effector Cic, leaves open the possibility that Wit could play RTK-like functions, at least in the context of synaptogenesis.

Consistent with the proposal of a dual mechanism for Wit, its activation seems to be a requirement to elicit two independent signaling steps, PI3K and Ras85D, that could reflect RTK and RSTK mechanisms, respectively. Both steps are independent because the mutated form of PI3K unable to bind Ras85D, $PI3K^{\Delta RBD}$, is as effective as the normal PI3K to elicit synaptogenesis. PI3K and Ras85D signaling, however, seem to converge on Bsk revealing a novel feature of this crossroad point. The activity level of Bsk is known to be critical in many signaling processes [121, 122]. The peculiarities of Bsk/JNK activity include its coordinated regulation by p38a and Slpr in the context of stress heat response without interference on the developmental context [123]. Another modulator, Puc, was described as a negative feed-back loop in the context of oxidative stress [124]. The Puc mediated loop is operative also for synaptogenesis, while that of p38a/Slpr is relevant for p38a only, as shown here. Further, Ras85D represents an additional regulator in the neural scenario. The triple regulation of Bsk/JNK by Ras85D, Puc and the MAPKs seems to stablish a narrow range of activity thresholds within which normal number of synapses is determined.

The concept of signaling thresholds is also unveiled in this study by the identification of another signaling pathway that opposes synapse formation. The pro- and anti-synaptogenesis pathways have similar constituents, including small GTPases, MAPKs and transcriptional effectors, Mad/Smad, which are canonical for RSTK receptors. The RSTK type II receptor Put, which can mediate diverse signaling pathways according to the co-receptor bound [125] can be discarded in either the pro- or the anti-synaptogenesis pathways. Thus, the main receptor for the anti-synaptogenesis pathway remains to be identified.

Concerning small GTPases, the pro-synaptogenesis pathway uses Ras85D while its counterpart uses the poorly studied Ras64B. The anti-synaptogenesis pathway includes an additional member of this family of enzymes, Rala. This small GTPase plays a role in the exocyst-mediated growth of the muscle membrane specialization that surrounds the synaptic bouton as a consequence of synapse activity [107]. That is, Rala can influence synapse physiology acting from the postsynaptic side. The experimental expression of a constitutively active form of Rala in the neuron does not seem to affect the overall synaptic terminal branching [107]. However, the null *ral* mutant shows reduced synapse branching and its vertebrate homolog is expressed in the central nervous system [126]. We found here that Rala under-expression in neurons yields an elevated number of synapses. Thus, it is likely that this small GTPase acts as a break to synaptogenesis, hence its inclusion in the antagonistic pathway.

Synaptogenesis and neuritogenesis are distinct processes since each one can be differentially affected by the same mutant (e.g.: Hiw). Both features, however, share some signals (e.g.: Wnd, Hep). This signaling overlap is akin to the case of axon specification versus spine formation for constituents of the apico/basal polarity complex Par3-6/aPKC [127]. These and other examples illustrated in this study underscore the need to discriminate between synapses and boutons. This study is focused on the cell autonomous signaling that takes place in the neuron. Non-cell autonomous signals (e.g.: originated in the glia or hemolymph circulating) have not been considered. The active role of glia in axon pruning and bouton number has been the subject of other studies [128, 129]. Considering the reported role of Hiw through the midline glia in the remodeling of the giant fiber interneuron [91] it is not unlikely that the glia-to-neuron signaling may share components with the neuron autonomous signaling addressed here.

The summary scheme (Fig 6) describes the scenario where two signaling pathways mutually regulate each other. Epistasis assays are the only experimental approach for *in vivo* studies of more than one signaling component, albeit this type of assay is only feasible in *Drosophila*. The

corresponding protein acronyms in humans are shown in parenthesis in Fig 6. Thus, it is plausible that vertebrate synaptogenesis will be regulated by a similar antagonistic signaling.

The regulatory equilibrium as a mechanism to determine a biological parameter is the most relevant feature in this scenario for several reasons. First, because this type of mechanism can respond very fast to changes in the physiological status of the cell, and, second because it provides remarkable precision to the trait to be regulated, synapse number in this case [see [130]]. Although bi-stable regulatory mechanisms are known in other contexts, the case of synapse number may seem unexpected because the highly dynamic nature of synapse number has been recognized only recently [1–3, 70]. Consequently, a molecular signaling mechanism endowed with proper precision and time resolution must sustain this dynamic process. The balanced equilibrium uncovered here, although most likely still incomplete in terms of its components, offers such a mechanism.

Supporting information

S1 Fig. Synapse visualization. A) Co-localization of synapse markers. Active zones are labeled in red with nc82 antibody while postsynaptic densities are shown in green (anti-GluRIID). The motor neuron membrane is shown in blue by the anti-HRP antibody. Note the correspondence of nc82 and GluRIID spots. **B)** The overexpression of the transcriptional repressor *capicua* (Cic) reduces synapses to the same level as the wit^{A12}/wit^{B11} mutant (see also main Fig 1C). The dependence on *capicua* and the signaling through PI3K suggest that Wit may act as a RTK rather than a Ser/Thr kinase receptor. **C)** Postsynaptic FGFR-like receptors. The heterozygous mutant conditions for muscle receptors Htl or Btl increase synapse number. This is consistent with a repressive role in the levels of Gbb and, thus, in the increased pro-synaptogenesis signaling (see also S2 Fig). Genotypes: **Control** = *D42-Gal4/+*. **Cic↑** = *D42-Gal4/UAS-cic*. **Htl↓** = htl^{AB42}/+; *D42-Gal4/+*. **Btl↓** = btl^{dev1}/+; *D42-Gal4/+*. Bar in **A** = 5 μm. Number of independent larvae analyzed is shown in parenthesis. A single NMJ from abdominal segment A3 was analyzed per larvae.
(TIF)

S2 Fig. Transcriptional effects on receptors and ligand-encoding genes in the muscle. A) Based on q-PCR assays, Gbb expression is increased as a result of the haploinsufficiency of Htl receptor. By contrast, the haploinsufficiency of Btl receptor leads to the opposite effect illustrating their antagonistic regulation on Gbb expression. The up- or down-regulation of PI3K in neurons has no effect on Gbb transcription. This result indicates that PI3K does not alter *gbb* transcription in the neuron nor triggers a signaling that could have modified that transcription in the muscle (see main text). **B-D**) The neural manipulation of PI3K has no effect on the Htl ligands, Pyramus (Pyr) (**B**) and Thisbe (Ths) (**C**), or on the Btl ligand Branchless (Bnl) (**D**). Genotypes: **+** = *elav-Gal4/+*. **Htl↓** = htl^{AB42}/+. **Btl↑** = btl^{dev1}/+. **PI3K↑** = *UAS-PI3K/+; elav-Gal4/+*. **PI3K↓** = *UAS-*$PI3K^{DN}$*/+; elav-Gal4/+*.
(TIF)

S3 Fig. Synaptogenesis and neuritogenesis are two different processes. A-D) Representative images of NMJs. The number of active zones and the size of the motor neuron deviate in opposite directions in *Hiw↓*. Motor neuron branches are more extensive than control but have fewer synapses. Also, note the frequent location of synapses, nc82 puncta, outside of boutons, particularly in Hiw↓. See also S3 Table. Genotypes: **A** = *D42-Gal4/+*. **B** = *UAS-Wnd/+; D42-Gal4/+*. **C** = *UAS-Hep/+; D42-Gal4/+*. **D** = males hiw^{ND8}*; +/+; D42-Gal4/+*. Bar in **A** = 20 μm.
(TIF)

S1 Table. Receptors without effect in synaptogenesis.
(DOCX)

S2 Table. Number of synapses (raw data).
(XLS)

S3 Table. Number of boutons versus number of synapses.
(DOC)

S1 Movie. 3D reconstruction of a NMJ.
(AVI)

Acknowledgments

Critical comments by lab members are most appreciated. We would like to thank Mr. Cristian Casablanca-García for his technical support with the figures. Transgenic fly stocks were obtained from the Vienna Drosophila Resource Center (VDRC, www.vdrc.at) and fly strains were from Bloomington Stock Center (NIH P40OD018537) (http://flystocks.bio.indiana.edu/).

Author Contributions

Conceptualization: Alberto Ferrús.

Data curation: Sheila Jordán-Álvarez, Elena Santana, Sergio Casas-Tintó, Ángel Acebes.

Formal analysis: Elena Santana.

Funding acquisition: Alberto Ferrús.

Investigation: Sheila Jordán-Álvarez, Elena Santana.

Methodology: Sergio Casas-Tintó.

Project administration: Alberto Ferrús.

Supervision: Ángel Acebes, Alberto Ferrús.

Validation: Sergio Casas-Tintó.

Visualization: Sheila Jordán-Álvarez, Sergio Casas-Tintó.

Writing – original draft: Alberto Ferrús.

Writing – review & editing: Ángel Acebes, Alberto Ferrús.

References

1. De Roo M, Klauser P, Muller D. LTP promotes a selective long-term stabilization and clustering of dendritic spines. PLoS biology. 2008; 6(9):e219. Epub 2008/09/16. https://doi.org/10.1371/journal.pbio.0060219 PMID: 18788894
2. Martin-Pena A, Acebes A, Rodriguez JR, Sorribes A, de Polavieja GG, Fernandez-Funez P, et al. Age-independent synaptogenesis by phosphoinositide 3 kinase. The Journal of neuroscience: the official journal of the Society for Neuroscience. 2006; 26(40):10199–208. Epub 2006/10/06.
3. Rasse TM, Fouquet W, Schmid A, Kittel RJ, Mertel S, Sigrist CB, et al. Glutamate receptor dynamics organizing synapse formation in vivo. Nature neuroscience. 2005; 8(7):898–905. Epub 2005/09/02. PMID: 16136672
4. Gan WB, Kwon E, Feng G, Sanes JR, Lichtman JW. Synaptic dynamism measured over minutes to months: age-dependent decline in an autonomic ganglion. Nature neuroscience. 2003; 6(9):956–60. Epub 2003/08/20. https://doi.org/10.1038/nn1115 PMID: 12925856

5. Middei S, Ammassari-Teule M, Marie H. Synaptic plasticity under learning challenge. Neurobiology of learning and memory. 2014; 115:108–15. Epub 2014/08/19. https://doi.org/10.1016/j.nlm.2014.08.001 PMID: 25132316
6. Trachtenberg JT, Chen BE, Knott GW, Feng G, Sanes JR, Welker E, et al. Long-term in vivo imaging of experience-dependent synaptic plasticity in adult cortex. Nature. 2002; 420(6917):788–94. Epub 2002/12/20. https://doi.org/10.1038/nature01273 PMID: 12490942
7. Appelbaum L, Wang G, Yokogawa T, Skariah GM, Smith SJ, Mourrain P, et al. Circadian and homeostatic regulation of structural synaptic plasticity in hypocretin neurons. Neuron. 2010; 68(1):87–98. Epub 2010/10/06. https://doi.org/10.1016/j.neuron.2010.09.006 PMID: 20920793
8. Ruiz S, Ferreiro MJ, Menhert KI, Casanova G, Olivera A, Cantera R. Rhythmic changes in synapse numbers in Drosophila melanogaster motor terminals. PloS one. 2013; 8(6):e67161. Epub 2013/07/11. https://doi.org/10.1371/journal.pone.0067161 PMID: 23840613
9. Acebes A, Devaud JM, Arnes M, Ferrus A. Central adaptation to odorants depends on PI3K levels in local interneurons of the antennal lobe. The Journal of neuroscience: the official journal of the Society for Neuroscience. 2012; 32(2):417–22. Epub 2012/01/13.
10. Acebes A, Martin-Pena A, Chevalier V, Ferrus A. Synapse loss in olfactory local interneurons modifies perception. The Journal of neuroscience: the official journal of the Society for Neuroscience. 2011; 31(8):2734–45. Epub 2011/03/19.
11. Bernardinelli Y, Nikonenko I, Muller D. Structural plasticity: mechanisms and contribution to developmental psychiatric disorders. Frontiers in neuroanatomy. 2014; 8:123. Epub 2014/11/19. https://doi.org/10.3389/fnana.2014.00123 PMID: 25404897
12. Benes FM, Berretta S. GABAergic interneurons: implications for understanding schizophrenia and bipolar disorder. Neuropsychopharmacology: official publication of the American College of Neuropsychopharmacology. 2001; 25(1):1–27. Epub 2001/05/30.
13. Scheff SW, Price DA. Synaptic pathology in Alzheimer's disease: a review of ultrastructural studies. Neurobiology of aging. 2003; 24(8):1029–46. Epub 2003/12/04. PMID: 14643375
14. Selkoe DJ. Alzheimer's disease is a synaptic failure. Science. 2002; 298(5594):789–91. Epub 2002/10/26. https://doi.org/10.1126/science.1074069 PMID: 12399581
15. Ballard SL, Miller DL, Ganetzky B. Retrograde neurotrophin signaling through Tollo regulates synaptic growth in Drosophila. The Journal of cell biology. 2014; 204(7):1157–72. Epub 2014/03/26. https://doi.org/10.1083/jcb.201308115 PMID: 24662564
16. Baydyuk M, Wu XS, He L, Wu LG. Brain-derived neurotrophic factor inhibits calcium channel activation, exocytosis, and endocytosis at a central nerve terminal. The Journal of neuroscience: the official journal of the Society for Neuroscience. 2015; 35(11):4676–82. Epub 2015/03/20.
17. Chen X, Ganetzky B. A neuropeptide signaling pathway regulates synaptic growth in Drosophila. The Journal of cell biology. 2012; 196(4):529–43. Epub 2012/02/15. https://doi.org/10.1083/jcb.201109044 PMID: 22331845
18. Chater TE, Goda Y. The role of AMPA receptors in postsynaptic mechanisms of synaptic plasticity. Frontiers in cellular neuroscience. 2014; 8:401. Epub 2014/12/17. https://doi.org/10.3389/fncel.2014.00401 PMID: 25505875
19. Chazeau A, Garcia M, Czondor K, Perrais D, Tessier B, Giannone G, et al. Mechanical coupling between transsynaptic N-cadherin adhesions and actin flow stabilizes dendritic spines. Molecular biology of the cell. 2015; 26(5):859–73. Epub 2015/01/09. https://doi.org/10.1091/mbc.E14-06-1086 PMID: 25568337
20. Bayer KU, LeBel E, McDonald GL, O'Leary H, Schulman H, De Koninck P. Transition from reversible to persistent binding of CaMKII to postsynaptic sites and NR2B. The Journal of neuroscience: the official journal of the Society for Neuroscience. 2006; 26(4):1164–74. Epub 2006/01/27.
21. Gleason MR, Higashijima S, Dallman J, Liu K, Mandel G, Fetcho JR. Translocation of CaM kinase II to synaptic sites in vivo. Nature neuroscience. 2003; 6(3):217–8. Epub 2003/02/04. https://doi.org/10.1038/nn1011 PMID: 12563265
22. Sturgill JF, Steiner P, Czervionke BL, Sabatini BL. Distinct domains within PSD-95 mediate synaptic incorporation, stabilization, and activity-dependent trafficking. The Journal of neuroscience: the official journal of the Society for Neuroscience. 2009; 29(41):12845–54. Epub 2009/10/16.
23. Flores CE, Mendez P. Shaping inhibition: activity dependent structural plasticity of GABAergic synapses. Frontiers in cellular neuroscience. 2014; 8:327. Epub 2014/11/12. https://doi.org/10.3389/fncel.2014.00327 PMID: 25386117
24. Vonhoff F, Kuehn C, Blumenstock S, Sanyal S, Duch C. Temporal coherency between receptor expression, neural activity and AP-1-dependent transcription regulates Drosophila motoneuron

dendrite development. Development. 2013; 140(3):606–16. Epub 2013/01/08. https://doi.org/10.1242/dev.089235 PMID: 23293292

25. Kordylewski L. Morphology of motor end-plate and its size relation to the muscle fibre size in the amphibian submandibular muscle. Zeitschrift fur mikroskopisch-anatomische Forschung. 1979; 93(6):1038–50. Epub 1979/01/01. PMID: 317619

26. Lewis ER, Cotman CW. Factors specifying the development of synapse number in the rat dentate gyrus: effects of partial target loss. Brain research. 1980; 191(1):35–52. Epub 1980/06/02. PMID: 7378759

27. Bailey CH, Kandel ER. Structural changes accompanying memory storage. Annual review of physiology. 1993; 55:397–426. Epub 1993/01/01. https://doi.org/10.1146/annurev.ph.55.030193.002145 PMID: 8466181

28. Ataman B, Ashley J, Gorczyca M, Ramachandran P, Fouquet W, Sigrist SJ, et al. Rapid activity-dependent modifications in synaptic structure and function require bidirectional Wnt signaling. Neuron. 2008; 57(5):705–18. Epub 2008/03/18. https://doi.org/10.1016/j.neuron.2008.01.026 PMID: 18341991

29. Nagaoka T, Ohashi R, Inutsuka A, Sakai S, Fujisawa N, Yokoyama M, et al. The Wnt/planar cell polarity pathway component Vangl2 induces synapse formation through direct control of N-cadherin. Cell reports. 2014; 6(5):916–27. Epub 2014/03/04. https://doi.org/10.1016/j.celrep.2014.01.044 PMID: 24582966

30. Darabid H, Perez-Gonzalez AP, Robitaille R. Neuromuscular synaptogenesis: coordinating partners with multiple functions. Nature reviews Neuroscience. 2014; 15(11):703–18. Epub 2014/12/11. PMID: 25493308

31. Cuesto G, Jordan-Alvarez S, Enriquez-Barreto L, Ferrus A, Morales M, Acebes A. GSK3beta inhibition promotes synaptogenesis in Drosophila and mammalian neurons. PloS one. 2015; 10(3):e0118475. Epub 2015/03/13. https://doi.org/10.1371/journal.pone.0118475 PMID: 25764078

32. Cuesto G, Enriquez-Barreto L, Carames C, Cantarero M, Gasull X, Sandi C, et al. Phosphoinositide-3-kinase activation controls synaptogenesis and spinogenesis in hippocampal neurons. The Journal of neuroscience: the official journal of the Society for Neuroscience. 2011; 31(8):2721–33. Epub 2011/03/19.

33. Wang SH, Celic I, Choi SY, Riccomagno M, Wang Q, Sun LO, et al. Dlg5 regulates dendritic spine formation and synaptogenesis by controlling subcellular N-cadherin localization. The Journal of neuroscience: the official journal of the Society for Neuroscience. 2014; 34(38):12745–61. Epub 2014/09/19.

34. Ng SS, Mahmoudi T, Danenberg E, Bejaoui I, de Lau W, Korswagen HC, et al. Phosphatidylinositol 3-kinase signaling does not activate the wnt cascade. The Journal of biological chemistry. 2009; 284 (51):35308–13. Epub 2009/10/24. https://doi.org/10.1074/jbc.M109.078261 PMID: 19850932

35. Voskas D, Ling LS, Woodgett JR. Does GSK-3 provide a shortcut for PI3K activation of Wnt signalling? F1000 biology reports. 2010; 2:82. Epub 2011/02/02. https://doi.org/10.3410/B2-82 PMID: 21283602

36. Cabodi S, Morello V, Masi A, Cicchi R, Broggio C, Distefano P, et al. Convergence of integrins and EGF receptor signaling via PI3K/Akt/FoxO pathway in early gene Egr-1 expression. Journal of cellular physiology. 2009; 218(2):294–303. Epub 2008/10/11. https://doi.org/10.1002/jcp.21603 PMID: 18844239

37. Vanhaesebroeck B, Guillermet-Guibert J, Graupera M, Bilanges B. The emerging mechanisms of isoform-specific PI3K signalling. Nature reviews Molecular cell biology. 2010; 11(5):329–41. Epub 2010/04/10. https://doi.org/10.1038/nrm2882 PMID: 20379207

38. Markus A, Zhong J, Snider WD. Raf and akt mediate distinct aspects of sensory axon growth. Neuron. 2002; 35(1):65–76. Epub 2002/07/19. PMID: 12123609

39. Navarro AI, Rico B. Focal adhesion kinase function in neuronal development. Current opinion in neurobiology. 2014; 27:89–95. Epub 2014/04/08. https://doi.org/10.1016/j.conb.2014.03.002 PMID: 24705242

40. Spilker C, Kreutz MR. RapGAPs in brain: multipurpose players in neuronal Rap signalling. The European journal of neuroscience. 2010; 32(1):1–9. Epub 2010/06/26. https://doi.org/10.1111/j.1460-9568.2010.07273.x PMID: 20576033

41. Acebes A, Ferrus A. Cellular and molecular features of axon collaterals and dendrites. Trends in neurosciences. 2000; 23(11):557–65. Epub 2000/11/14. PMID: 11074265

42. Gallo G. The cytoskeletal and signaling mechanisms of axon collateral branching. Developmental neurobiology. 2011; 71(3):201–20. Epub 2011/02/11. https://doi.org/10.1002/dneu.20852 PMID: 21308993

43. Luo L, Liao YJ, Jan LY, Jan YN. Distinct morphogenetic functions of similar small GTPases: Drosophila Drac1 is involved in axonal outgrowth and myoblast fusion. Genes & development. 1994; 8 (15):1787–802. Epub 1994/08/01.

44. Parkes TL, Elia AJ, Dickinson D, Hilliker AJ, Phillips JP, Boulianne GL. Extension of Drosophila lifespan by overexpression of human SOD1 in motorneurons. Nature genetics. 1998; 19(2):171–4. Epub 1998/06/10. https://doi.org/10.1038/534 PMID: 9620775

45. Orme MH, Alrubaie S, Bradley GL, Walker CD, Leevers SJ. Input from Ras is required for maximal PI (3)K signalling in Drosophila. Nature cell biology. 2006; 8(11):1298–302. Epub 2006/10/17. https://doi.org/10.1038/ncb1493 PMID: 17041587

46. Riesgo-Escovar JR, Jenni M, Fritz A, Hafen E. The Drosophila Jun-N-terminal kinase is required for cell morphogenesis but not for DJun-dependent cell fate specification in the eye. Genes & development. 1996; 10(21):2759–68. Epub 1996/11/01.

47. Rallis A, Moore C, Ng J. Signal strength and signal duration define two distinct aspects of JNK-regulated axon stability. Developmental biology. 2010; 339(1):65–77. Epub 2009/12/29. https://doi.org/10.1016/j.ydbio.2009.12.016 PMID: 20035736

48. Michelson AM, Gisselbrecht S, Buff E, Skeath JB. Heartbroken is a specific downstream mediator of FGF receptor signalling in Drosophila. Development. 1998; 125(22):4379–89. Epub 1998/10/21. PMID: 9778498

49. Etter PD, Narayanan R, Navratilova Z, Patel C, Bohmann D, Jasper H, et al. Synaptic and genomic responses to JNK and AP-1 signaling in Drosophila neurons. BMC neuroscience. 2005; 6:39. Epub 2005/06/04. https://doi.org/10.1186/1471-2202-6-39 PMID: 15932641

50. Collins CA, Wairkar YP, Johnson SL, DiAntonio A. Highwire restrains synaptic growth by attenuating a MAP kinase signal. Neuron. 2006; 51(1):57–69. Epub 2006/07/04. https://doi.org/10.1016/j.neuron.2006.05.026 PMID: 16815332

51. Asha H, Nagy I, Kovacs G, Stetson D, Ando I, Dearolf CR. Analysis of Ras-induced overproliferation in Drosophila hemocytes. Genetics. 2003; 163(1):203–15. Epub 2003/02/15. PMID: 12586708

52. Baonza A, de Celis JF, Garcia-Bellido A. Relationships between extramacrochaetae and Notch signalling in Drosophila wing development. Development. 2000; 127(11):2383–93. Epub 2000/05/11. PMID: 10804180

53. Aberle H, Haghighi AP, Fetter RD, McCabe BD, Magalhaes TR, Goodman CS. wishful thinking encodes a BMP type II receptor that regulates synaptic growth in Drosophila. Neuron. 2002; 33 (4):545–58. Epub 2002/02/22. PMID: 11856529

54. Leevers SJ, Weinkove D, MacDougall LK, Hafen E, Waterfield MD. The Drosophila phosphoinositide 3-kinase Dp110 promotes cell growth. The EMBO journal. 1996; 15(23):6584–94. Epub 1996/12/02. PMID: 8978685

55. Wu C, Wairkar YP, Collins CA, DiAntonio A. Highwire function at the Drosophila neuromuscular junction: spatial, structural, and temporal requirements. The Journal of neuroscience: the official journal of the Society for Neuroscience. 2005; 25(42):9557–66. Epub 2005/10/21.

56. Marques G, Bao H, Haerry TE, Shimell MJ, Duchek P, Zhang B, et al. The Drosophila BMP type II receptor Wishful Thinking regulates neuromuscular synapse morphology and function. Neuron. 2002; 33(4):529–43. Epub 2002/02/22. PMID: 11856528

57. Khalsa O, Yoon JW, Torres-Schumann S, Wharton KA. TGF-beta/BMP superfamily members, Gbb-60A and Dpp, cooperate to provide pattern information and establish cell identity in the Drosophila wing. Development. 1998; 125(14):2723–34. Epub 1998/06/24. PMID: 9636086

58. Wharton KA, Cook JM, Torres-Schumann S, de Castro K, Borod E, Phillips DA. Genetic analysis of the bone morphogenetic protein-related gene, gbb, identifies multiple requirements during Drosophila development. Genetics. 1999; 152(2):629–40. Epub 1999/06/03. PMID: 10353905

59. McCabe BD, Marques G, Haghighi AP, Fetter RD, Crotty ML, Haerry TE, et al. The BMP homolog Gbb provides a retrograde signal that regulates synaptic growth at the Drosophila neuromuscular junction. Neuron. 2003; 39(2):241–54. Epub 2003/07/23. PMID: 12873382

60. Wan HI, DiAntonio A, Fetter RD, Bergstrom K, Strauss R, Goodman CS. Highwire regulates synaptic growth in Drosophila. Neuron. 2000; 26(2):313–29. Epub 2000/06/06. PMID: 10839352

61. Schuster CM, Davis GW, Fetter RD, Goodman CS. Genetic dissection of structural and functional components of synaptic plasticity. I. Fasciclin II controls synaptic stabilization and growth. Neuron. 1996; 17(4):641–54. Epub 1996/10/01. PMID: 8893022

62. Hipfner DR, Weigmann K, Cohen SM. The bantam gene regulates Drosophila growth. Genetics. 2002; 161(4):1527–37. Epub 2002/08/28. PMID: 12196398

63. Budnik VE, Ruiz-Canada CE. The Fly Neuromuscular Junction: Structure and Function: ACADEMIC PRESS; 2006 October 2006.

64. Brand AH, Perrimon N. Targeted gene expression as a means of altering cell fates and generating dominant phenotypes. Development. 1993; 118(2):401–15. Epub 1993/06/01. PMID: 8223268

65. Wagh DA, Rasse TM, Asan E, Hofbauer A, Schwenkert I, Durrbeck H, et al. Bruchpilot, a protein with homology to ELKS/CAST, is required for structural integrity and function of synaptic active zones in Drosophila. Neuron. 2006; 49(6):833–44. Epub 2006/03/18. https://doi.org/10.1016/j.neuron.2006.02.008 PMID: 16543132

66. Bao H, Daniels RW, MacLeod GT, Charlton MP, Atwood HL, Zhang B. AP180 maintains the distribution of synaptic and vesicle proteins in the nerve terminal and indirectly regulates the efficacy of Ca2+-triggered exocytosis. J Neurophysiol. 2005; 94(3):1888–903. https://doi.org/10.1152/jn.00080.2005 PMID: 15888532

67. Fouquet W, Owald D, Wichmann C, Mertel S, Depner H, Dyba M, et al. Maturation of active zone assembly by Drosophila Bruchpilot. The Journal of cell biology. 2009; 186(1):129–45. Epub 2009/07/15. https://doi.org/10.1083/jcb.200812150 PMID: 19596851

68. Guo X, Macleod GT, Wellington A, Hu F, Panchumarthi S, Schoenfield M, et al. The GTPase dMiro is required for axonal transport of mitochondria to Drosophila synapses. Neuron. 2005; 47(3):379–93. https://doi.org/10.1016/j.neuron.2005.06.027 PMID: 16055062

69. Hamanaka Y, Meinertzhagen IA. Immunocytochemical localization of synaptic proteins to photoreceptor synapses of Drosophila melanogaster. The Journal of comparative neurology. 2010; 518(7):1133–55. Epub 2010/02/04. https://doi.org/10.1002/cne.22268 PMID: 20127822

70. Jordan-Alvarez S, Fouquet W, Sigrist SJ, Acebes A. Presynaptic PI3K activity triggers the formation of glutamate receptors at neuromuscular terminals of Drosophila. Journal of cell science. 2012; 125(Pt 15):3621–9. Epub 2012/04/17. https://doi.org/10.1242/jcs.102806 PMID: 22505608

71. Peled ES, Newman ZL, Isacoff EY. Evoked and spontaneous transmission favored by distinct sets of synapses. Current biology: CB. 2014; 24(5):484–93. Epub 2014/02/25. https://doi.org/10.1016/j.cub.2014.01.022 PMID: 24560571

72. Marques G. Morphogens and synaptogenesis in Drosophila. Journal of neurobiology. 2005; 64(4):417–34. Epub 2005/07/26. https://doi.org/10.1002/neu.20165 PMID: 16041756

73. James RE, Broihier HT. Crimpy inhibits the BMP homolog Gbb in motoneurons to enable proper growth control at the Drosophila neuromuscular junction. Development. 2011; 138(15):3273–86. Epub 2011/07/14. https://doi.org/10.1242/dev.066142 PMID: 21750037

74. Banerjee S, Venkatesan A, Bhat MA. Neurexin, Neuroligin and Wishful Thinking coordinate synaptic cytoarchitecture and growth at neuromuscular junctions. Molecular and cellular neurosciences. 2016; 78:9–24. Epub 2016/11/14. https://doi.org/10.1016/j.mcn.2016.11.004 PMID: 27838296

75. Kim NC, Marques G. Identification of downstream targets of the bone morphogenetic protein pathway in the Drosophila nervous system. Developmental dynamics: an official publication of the American Association of Anatomists. 2010; 239(9):2413–25. Epub 2010/07/24.

76. James RE, Hoover KM, Bulgari D, McLaughlin CN, Wilson CG, Wharton KA, et al. Crimpy enables discrimination of presynaptic and postsynaptic pools of a BMP at the Drosophila neuromuscular junction. Developmental cell. 2014; 31(5):586–98. Epub 2014/12/03. https://doi.org/10.1016/j.devcel.2014.10.006 PMID: 25453556

77. Jimenez G, Shvartsman SY, Paroush Z. The Capicua repressor—a general sensor of RTK signaling in development and disease. Journal of cell science. 2012; 125(Pt 6):1383–91. Epub 2012/04/25. https://doi.org/10.1242/jcs.092965 PMID: 22526417

78. Reichman-Fried M, Shilo BZ. Breathless, a Drosophila FGF receptor homolog, is required for the onset of tracheal cell migration and tracheole formation. Mechanisms of development. 1995; 52(2–3):265–73. Epub 1995/08/01. PMID: 8541215

79. Shishido E, Higashijima S, Emori Y, Saigo K. Two FGF-receptor homologues of Drosophila: one is expressed in mesodermal primordium in early embryos. Development. 1993; 117(2):751–61. Epub 1993/02/01. PMID: 8330538

80. Emori Y, Saigo K. Distinct expression of two Drosophila homologs of fibroblast growth factor receptors in imaginal discs. FEBS letters. 1993; 332(1–2):111–4. Epub 1993/10/11. PMID: 8405423

81. Gryzik T, Muller HA. FGF8-like1 and FGF8-like2 encode putative ligands of the FGF receptor Htl and are required for mesoderm migration in the Drosophila gastrula. Current biology: CB. 2004; 14(8):659–67. Epub 2004/04/16. https://doi.org/10.1016/j.cub.2004.03.058 PMID: 15084280

82. Reichman-Fried M, Dickson B, Hafen E, Shilo BZ. Elucidation of the role of breathless, a Drosophila FGF receptor homolog, in tracheal cell migration. Genes & development. 1994; 8(4):428–39. Epub 1994/02/15.

83. Stathopoulos A, Tam B, Ronshaugen M, Frasch M, Levine M. pyramus and thisbe: FGF genes that pattern the mesoderm of Drosophila embryos. Genes & development. 2004; 18(6):687–99. Epub 2004/04/13.

84. Kadam S, McMahon A, Tzou P, Stathopoulos A. FGF ligands in Drosophila have distinct activities required to support cell migration and differentiation. Development. 2009; 136(5):739–47. Epub 2009/01/23. https://doi.org/10.1242/dev.027904 PMID: 19158183

85. Berke B, Wittnam J, McNeill E, Van Vactor DL, Keshishian H. Retrograde BMP signaling at the synapse: a permissive signal for synapse maturation and activity-dependent plasticity. The Journal of neuroscience: the official journal of the Society for Neuroscience. 2013; 33(45):17937–50. Epub 2013/11/08.

86. Seeger G, Gartner U, Arendt T. Transgenic activation of Ras in neurons increases synapse formation in mouse neocortex. J Neural Transm. 2005; 112(6):751–61. Epub 2004/10/14. https://doi.org/10.1007/s00702-004-0226-8 PMID: 15480849

87. Castellano E, Downward J. RAS Interaction with PI3K: More Than Just Another Effector Pathway. Genes & cancer. 2011; 2(3):261–74. Epub 2011/07/23.

88. Schaefer AM, Hadwiger GD, Nonet ML. rpm-1, a conserved neuronal gene that regulates targeting and synaptogenesis in C. elegans. Neuron. 2000; 26(2):345–56. Epub 2000/06/06. PMID: 10839354

89. Raftery LA, Sutherland DJ. TGF-beta family signal transduction in Drosophila development: from Mad to Smads. Developmental biology. 1999; 210(2):251–68. Epub 1999/06/08. https://doi.org/10.1006/dbio.1999.9282 PMID: 10357889

90. Eaton BA, Davis GW. LIM Kinase1 controls synaptic stability downstream of the type II BMP receptor. Neuron. 2005; 47(5):695–708. Epub 2005/09/01. https://doi.org/10.1016/j.neuron.2005.08.010 PMID: 16129399

91. Borgen M, Rowland K, Boerner J, Lloyd B, Khan A, Murphey R. Axon Termination, Pruning, and Synaptogenesis in the Giant Fiber System of Drosophila melanogaster Is Promoted by Highwire. Genetics. 2017; 205(3):1229–45. Epub 2017/01/20. https://doi.org/10.1534/genetics.116.197343 PMID: 28100586

92. Haeusgen W, Herdegen T, Waetzig V. The bottleneck of JNK signaling: molecular and functional characteristics of MKK4 and MKK7. European journal of cell biology. 2011; 90(6–7):536–44. Epub 2011/02/22. https://doi.org/10.1016/j.ejcb.2010.11.008 PMID: 21333379

93. Geuking P, Narasimamurthy R, Lemaitre B, Basler K, Leulier F. A non-redundant role for Drosophila Mkk4 and hemipterous/Mkk7 in TAK1-mediated activation of JNK. PloS one. 2009; 4(11):e7709. Epub 2009/11/06. https://doi.org/10.1371/journal.pone.0007709 PMID: 19888449

94. Martin-Blanco E, Gampel A, Ring J, Virdee K, Kirov N, Tolkovsky AM, et al. puckered encodes a phosphatase that mediates a feedback loop regulating JNK activity during dorsal closure in Drosophila. Genes & development. 1998; 12(4):557–70. Epub 1998/03/21.

95. Ciapponi L, Bohmann D. An essential function of AP-1 heterodimers in Drosophila development. Mechanisms of development. 2002; 115(1–2):35–40. Epub 2002/06/07. PMID: 12049765

96. Collins CA, DiAntonio A. Coordinating synaptic growth without being a nervous wreck. Neuron. 2004; 41(4):489–91. Epub 2004/02/26. PMID: 14980197

97. Gass P, Fleischmann A, Hvalby O, Jensen V, Zacher C, Strekalova T, et al. Mice with a fra-1 knock-in into the c-fos locus show impaired spatial but regular contextual learning and normal LTP. Brain research Molecular brain research. 2004; 130(1–2):16–22. Epub 2004/11/03. https://doi.org/10.1016/j.molbrainres.2004.07.004 PMID: 15519672

98. Sanyal S, Sandstrom DJ, Hoeffer CA, Ramaswami M. AP-1 functions upstream of CREB to control synaptic plasticity in Drosophila. Nature. 2002; 416(6883):870–4. Epub 2002/04/27. https://doi.org/10.1038/416870a PMID: 11976688

99. Dobens LL, Martin-Blanco E, Martinez-Arias A, Kafatos FC, Raftery LA. Drosophila puckered regulates Fos/Jun levels during follicle cell morphogenesis. Development. 2001; 128(10):1845–56. Epub 2001/04/20. PMID: 11311164

100. Szuts D, Bienz M. LexA chimeras reveal the function of Drosophila Fos as a context-dependent transcriptional activator. Proceedings of the National Academy of Sciences of the United States of America. 2000; 97(10):5351–6. Epub 2000/05/11. PMID: 10805795

101. Brummel T, Abdollah S, Haerry TE, Shimell MJ, Merriam J, Raftery L, et al. The Drosophila activin receptor baboon signals through dSmad2 and controls cell proliferation but not patterning during larval development. Genes & development. 1999; 13(1):98–111. Epub 1999/01/14.

102. Oh H, Irvine KD. Cooperative regulation of growth by Yorkie and Mad through bantam. Developmental cell. 2011; 20(1):109–22. Epub 2011/01/18. https://doi.org/10.1016/j.devcel.2010.12.002 PMID: 21238929

103. McNeill E, Van Vactor D. MicroRNAs shape the neuronal landscape. Neuron. 2012; 75(3):363–79. Epub 2012/08/14. https://doi.org/10.1016/j.neuron.2012.07.005 PMID: 22884321

104. Kwon Y, Vinayagam A, Sun X, Dephoure N, Gygi SP, Hong P, et al. The Hippo signaling pathway interactome. Science. 2013; 342(6159):737–40. Epub 2013/10/12. https://doi.org/10.1126/science.1243971 PMID: 24114784

105. Sekine Y, Takagahara S, Hatanaka R, Watanabe T, Oguchi H, Noguchi T, et al. p38 MAPKs regulate the expression of genes in the dopamine synthesis pathway through phosphorylation of NR4A nuclear receptors. Journal of cell science. 2011; 124(Pt 17):3006–16. Epub 2011/09/01. https://doi.org/10.1242/jcs.085902 PMID: 21878507

106. Han ZS, Enslen H, Hu X, Meng X, Wu IH, Barrett T, et al. A conserved p38 mitogen-activated protein kinase pathway regulates Drosophila immunity gene expression. Molecular and cellular biology. 1998; 18(6):3527–39. Epub 1998/06/20. PMID: 9584193

107. Teodoro RO, Pekkurnaz G, Nasser A, Higashi-Kovtun ME, Balakireva M, McLachlan IG, et al. Ral mediates activity-dependent growth of postsynaptic membranes via recruitment of the exocyst. The EMBO journal. 2013; 32(14):2039–55. Epub 2013/07/03. https://doi.org/10.1038/emboj.2013.147 PMID: 23812009

108. Aikin R, Maysinger D, Rosenberg L. Cross-talk between phosphatidylinositol 3-kinase/AKT and c-jun NH2-terminal kinase mediates survival of isolated human islets. Endocrinology. 2004; 145(10):4522–31. Epub 2004/07/10. https://doi.org/10.1210/en.2004-0488 PMID: 15242986

109. Pfleger CM. The Hippo Pathway: A Master Regulatory Network Important in Development and Dysregulated in Disease. Current topics in developmental biology. 2017; 123:181–228. Epub 2017/02/27. https://doi.org/10.1016/bs.ctdb.2016.12.001 PMID: 28236967

110. Sakuma C, Saito Y, Umehara T, Kamimura K, Maeda N, Mosca TJ, et al. The Strip-Hippo Pathway Regulates Synaptic Terminal Formation by Modulating Actin Organization at the Drosophila Neuromuscular Synapses. Cell reports. 2016; 16(9):2289–97. Epub 2016/08/23. https://doi.org/10.1016/j.celrep.2016.07.066 PMID: 27545887

111. Dumitriu D, Hao J, Hara Y, Kaufmann J, Janssen WG, Lou W, et al. Selective changes in thin spine density and morphology in monkey prefrontal cortex correlate with aging-related cognitive impairment. The Journal of neuroscience: the official journal of the Society for Neuroscience. 2010; 30(22):7507–15. Epub 2010/06/04.

112. Lee-Hoeflich ST, Zhao X, Mehra A, Attisano L. The Drosophila type II receptor, Wishful thinking, binds BMP and myoglianin to activate multiple TGFbeta family signaling pathways. FEBS letters. 2005; 579(21):4615–21. Epub 2005/08/16. https://doi.org/10.1016/j.febslet.2005.06.088 PMID: 16098524

113. Bangi E, Wharton K. Dual function of the Drosophila Alk1/Alk2 ortholog Saxophone shapes the Bmp activity gradient in the wing imaginal disc. Development. 2006; 133(17):3295–303. Epub 2006/08/05. https://doi.org/10.1242/dev.02513 PMID: 16887821

114. Demontis F, Patel VK, Swindell WR, Perrimon N. Intertissue control of the nucleolus via a myokine-dependent longevity pathway. Cell reports. 2014; 7(5):1481–94. Epub 2014/06/03. https://doi.org/10.1016/j.celrep.2014.05.001 PMID: 24882005

115. Ghosh AC, O'Connor MB. Systemic Activin signaling independently regulates sugar homeostasis, cellular metabolism, and pH balance in Drosophila melanogaster. Proceedings of the National Academy of Sciences of the United States of America. 2014; 111(15):5729–34. Epub 2014/04/08. https://doi.org/10.1073/pnas.1319116111 PMID: 24706779

116. Koles K, Nunnari J, Korkut C, Barria R, Brewer C, Li Y, et al. Mechanism of evenness interrupted (Evi)-exosome release at synaptic boutons. The Journal of biological chemistry. 2012; 287(20):16820–34. Epub 2012/03/23. https://doi.org/10.1074/jbc.M112.342667 PMID: 22437826

117. Korkut C, Ataman B, Ramachandran P, Ashley J, Barria R, Gherbesi N, et al. Trans-synaptic transmission of vesicular Wnt signals through Evi/Wntless. Cell. 2009; 139(2):393–404. Epub 2009/10/20. https://doi.org/10.1016/j.cell.2009.07.051 PMID: 19837038

118. Messeant J, Ezan J, Delers P, Glebov K, Marchiol C, Lager F, et al. Wnts contribute to neuromuscular junction formation through distinct signaling pathways. Development. 2017. Epub 2017/03/30.

119. Li W, Yao A, Zhi H, Kaur K, Zhu YC, Jia M, et al. Angelman Syndrome Protein Ube3a Regulates Synaptic Growth and Endocytosis by Inhibiting BMP Signaling in Drosophila. PLoS genetics. 2016; 12(5):e1006062. Epub 2016/05/28. https://doi.org/10.1371/journal.pgen.1006062 PMID: 27232889

120. Alexander PB, Wang XF. Resistance to receptor tyrosine kinase inhibition in cancer: molecular mechanisms and therapeutic strategies. Frontiers of medicine. 2015; 9(2):134–8. Epub 2015/05/10. https://doi.org/10.1007/s11684-015-0396-9 PMID: 25957263

121. Zhou YY, Li Y, Jiang WQ, Zhou LF. MAPK/JNK signalling: a potential autophagy regulation pathway. Bioscience reports. 2015; 35(3). Epub 2015/07/17.

122. Zhao HF, Wang J, Tony To SS. The phosphatidylinositol 3-kinase/Akt and c-Jun N-terminal kinase signaling in cancer: Alliance or contradiction? (Review). International journal of oncology. 2015; 47(2):429–36. Epub 2015/06/18. https://doi.org/10.3892/ijo.2015.3052 PMID: 26082006

123. Gonda RL, Garlena RA, Stronach B. Drosophila heat shock response requires the JNK pathway and phosphorylation of mixed lineage kinase at a conserved serine-proline motif. PloS one. 2012; 7(7): e42369. Epub 2012/08/01. https://doi.org/10.1371/journal.pone.0042369 PMID: 22848763

124. Karkali K, Panayotou G. The Drosophila DUSP puckered is phosphorylated by JNK and p38 in response to arsenite-induced oxidative stress. Biochemical and biophysical research communications. 2012; 418(2):301–6. Epub 2012/01/24. https://doi.org/10.1016/j.bbrc.2012.01.015 PMID: 22266315

125. Parker L, Ellis JE, Nguyen MQ, Arora K. The divergent TGF-beta ligand Dawdle utilizes an activin pathway to influence axon guidance in Drosophila. Development. 2006; 133(24):4981–91. Epub 2006/11/23. https://doi.org/10.1242/dev.02673 PMID: 17119022

126. Lalli G. RalA and the exocyst complex influence neuronal polarity through PAR-3 and aPKC. Journal of cell science. 2009; 122(Pt 10):1499–506. Epub 2009/04/23. https://doi.org/10.1242/jcs.044339 PMID: 19383721

127. Zhang H, Macara IG. The PAR-6 polarity protein regulates dendritic spine morphogenesis through p190 RhoGAP and the Rho GTPase. Developmental cell. 2008; 14(2):216–26. Epub 2008/02/13. https://doi.org/10.1016/j.devcel.2007.11.020 PMID: 18267090

128. Awasaki T, Ito K. Engulfing action of glial cells is required for programmed axon pruning during Drosophila metamorphosis. Current biology: CB. 2004; 14(8):668–77. Epub 2004/04/16. https://doi.org/10.1016/j.cub.2004.04.001 PMID: 15084281

129. Fuentes-Medel Y, Logan MA, Ashley J, Ataman B, Budnik V, Freeman MR. Glia and muscle sculpt neuromuscular arbors by engulfing destabilized synaptic boutons and shed presynaptic debris. PLoS biology. 2009; 7(8):e1000184. Epub 2009/08/27. https://doi.org/10.1371/journal.pbio.1000184 PMID: 19707574

130. Marucci L, Barton DA, Cantone I, Ricci MA, Cosma MP, Santini S, et al. How to turn a genetic circuit into a synthetic tunable oscillator, or a bistable switch. PloS one. 2009; 4(12):e8083. Epub 2009/12/10. https://doi.org/10.1371/journal.pone.0008083 PMID: 19997611

6. Chapter II: *The guanine-exchange factor Ric8 binds to the Ca^{+2} sensor NCS-1 to regulate synapse number and neurotransmitter release*.

6.2. Introduction

Este capítulo está compuesto por el manuscrito:

-*The guanine-exchange factor Ric8 binds to the Ca+2 sensor NCS-1 to regulate synapse number and neurotransmitter release*. Jesús Romero-Pozuelo*, Jeffrey S. Dason*, Alicia Mansilla, Soledad Baños-Mateos, José L. Sardina, Antonio Chaves-Sanjuán, Jaime Jurado-Gómez, **Elena Santana**, Harold L. Atwood, Ángel Hernández-Hernández, María José Sánchez-Barrena, Alberto Ferrús. **J Cell Sci. 2014 Oct 1;127(Pt 19):4246-59. doi: 10.1242/jcs.152603**

Este trabajo fue desarrollado en colaboración con el grupo de María-José Sánchez-Barrena del departamento de Cristalografía y Biología Estructural en el Instituto de Física-Química Rocasolano y el grupo de Harold L. Atwood del Departamento de Fisiología de la Universidad de Toronto.

Elena Santana Martín participó en este estudio realizando parte de los experimentos, adquisición de imágenes, posterior procesamiento, parte de análisis estadístico y elaboración de parte del material gráfico. La redacción, elaboración del material gráfico y discusión del trabajo se realizó en colaboración con todos los autores.

La estabilidad de la función neuronal se basa en dos procesos independientes pero íntimamente relacionados: establecimiento del número de sinapsis y liberación de neurotransmisores.
Estos mecanismos tienen vías independientes de señalización pero algunos elementos están implicados en ambos procesos. Tanto en formación de sinapsis como en transmisión sináptica el Ca^{+2} juega un papel esencial. Ciertas proteínas son capaces de unirse a Ca^{+2} con distinta afinidad dando lugar a respuestas celulares diferentes.

Es el caso del sensor de Ca^{+2} Frequenina cuya sobreexpresión en motoneuronas aumenta el número de sinapsis pero disminuye la probabilidad de liberación de neurotransmisor.

El homólogo de Frq en mamíferos es NCS-1. A diferencia de en mamíferos donde solo hay un NCS-1 en *Drosophila* hay dos Frecueninas, Frq1 y Frq2. Actualmente no conocemos por qué ambas frecueninas están conservadas en *Drosophila.* Ambas proteínas comparten un 95% de homología. Nuestros estudios sobre la estructura de ambas frecueninas han demostrado que ciertos aminoácidos de la secuencia de Frq2 que son diferentes en Frq1 permiten la unión específica a la proteína GEF Ric8.

A continuación estudiamos cual es la relación funcional entre Frq2 y Ric8 además de su implicación en el establecimiento del número de sinapsis y la liberación de neurotransmisor.

Dado que Frq es un sensor de Ca^{+2} nuestra hipótesis baraja dos posibilidades, que estos dos eventos estén controlados por un mismo mecanismo mediado por Frq o que liberación de neurotransmisor y formación de sinapsis tengan mecanismos independientes.

En este último caso Frq tendría diferente afinidad por Ca^{+2} o Ric8 desencadenando un proceso u otro. Esta hipótesis se ha investigado mediante análisis de epistasia entre Frq, Ric8 y proteínas G asociadas a Ric8 para determinar sus efectos en el número de sinapsis.

Para establecer el papel de Frq y Ric8 en la transmisión sináptica se realizaron registros electrofisiológicos de botones de forma individual. Nuestros resultados muestran que el control sobre el número de sinapsis y el que regula la probabilidad de activación de la sinapsis, comparten una señalización común, la unión de Ric8a con Frq2, pero siguen vías diferentes tras la activación de proteínas G.

© 2014. Published by The Company of Biologists Ltd | Journal of Cell Science (2014) 127, 4246–4259 doi:10.1242/jcs.152603

RESEARCH ARTICLE

The guanine-exchange factor Ric8a binds to the Ca^{2+} sensor NCS-1 to regulate synapse number and neurotransmitter release

Jesús Romero-Pozuelo[1,*], Jeffrey S. Dason[2], Alicia Mansilla[1], Soledad Baños-Mateos[3,‡], José L. Sardina[4], Antonio Chaves-Sanjuán[3], Jaime Jurado-Gómez[1], Elena Santana[1], Harold L. Atwood[2], Ángel Hernández-Hernández[1,4,5], María-José Sánchez-Barrena[3] and Alberto Ferrús[1,§]

ABSTRACT

The conserved Ca^{2+}-binding protein Frequenin (homolog of the mammalian NCS-1, neural calcium sensor) is involved in pathologies that result from abnormal synapse number and probability of neurotransmitter release per synapse. Both synaptic features are likely to be co-regulated but the intervening mechanisms remain poorly understood. We show here that *Drosophila* Ric8a (a homolog of mammalian synembryn, which is also known as Ric8a), a receptor-independent activator of G protein complexes, binds to Frq2 but not to the virtually identical homolog Frq1. Based on crystallographic data on Frq2 and site-directed mutagenesis on Frq1, the differential amino acids R94 and T138 account for this specificity. Human NCS-1 and Ric8a reproduce the binding and maintain the structural requirements at these key positions. *Drosophila* Ric8a and Gαs regulate synapse number and neurotransmitter release, and both are functionally linked to Frq2. Frq2 negatively regulates Ric8a to control synapse number. However, the regulation of neurotransmitter release by Ric8a is independent of Frq2 binding. Thus, the antagonistic regulation of these two synaptic properties shares a common pathway, Frq2–Ric8a–Gαs, which diverges downstream. These mechanisms expose the Frq2–Ric8a interacting surface as a potential pharmacological target for NCS-1-related diseases and provide key data towards the corresponding drug design.

KEY WORDS: *Drosophila*, Synapse, X-ray crystallography, Ca^{2+}-binding proteins

INTRODUCTION

Neuronal function is largely dependent on the number of established synapses and the release probability per synapse. In many neuron types – motor neurons in particular – these two features appear to be regulated in an antagonistic manner; cells with more synapses exhibit lower probability of release per synapse, whereas cells with fewer synapses show a higher probability of release. Although Ca^{2+} is the major signal regulating both of these neuronal features (Augustine and Charlton, 1986; Komuro and Rakic, 1996; Zheng, 2000; for reviews see Pang and Südhof, 2010; Meriney and Dittrich, 2013; Frank, 2014), and heterotrimeric G protein complexes have been implicated as mediators (Renden and Broadie, 2003; Wolfgang et al., 2004; Klose et al., 2010; reviewed by Ross, 2008; Schmitz, 2014), a mechanistic link between Ca^{2+} surge and G protein signaling is still unknown. Shedding light on this issue is relevant and urgent, because many cognitive diseases, most of which are without an effective treatment, result from the abnormal regulation of synapses.

Frequenin (Frq) is a high-affinity Ca^{2+}-binding protein conserved from yeast to humans [where it is named neuronal calcium sensor 1 (NCS-1)]. Frq was first identified in *Drosophila* (Pongs et al., 1993), in which the gene is duplicated, *frq1* and *frq2*. In this insect and in the zebrafish *Danio rerio*, the two proteins, Frq1 and Frq2, are 95% identical, which represents an unusual case of non-divergent duplicates. In addition, neither of the two proteins has acquired any amino acid changes throughout the 12 sequenced *Drosophila* genomes, which span >40 million years of evolution. Conserved gene/protein duplications are hypothesized to result from the functional subspecialization of one of the components within the context of a more general function for which both duplicates would be required, thus explaining the maintenance of the two virtually identical genes throughout such a long period of time (Rastogi and Liberles, 2005; Sánchez-Gracia et al., 2010). We have tested this hypothesis here.

In *Drosophila*, over- or under- expression of the two Frq proteins yields similar antagonistic effects on synapse number and neurotransmitter release. Overexpressing either Frq1 or Frq2 increases the release of neurotransmitters and decreases the number of synapses, whereas the loss of function of Frq proteins reduces transmitter release and increases the number of synapses (Romero-Pozuelo et al., 2007; Dason et al., 2009). We previously found that Frq proteins control Ca^{2+} levels through the α1 voltage-gated Ca^{2+}-channel subunit encoded by the gene *cacophony* (*cac*) (Dason et al., 2009). The mammalian and snail NCS-1 also controls Ca^{2+}-channel activity (Weiss et al., 2000; Wang et al., 2001; Tsujimoto et al., 2002). NCS-1 interacts with several targets (reviewed by Dason et al., 2012), including calcineurin (Schaad et al., 1996), PI4Kβ (Hendricks et al., 1999), TRPC5 (Hui et al., 2006), D2R (Kabbani et al., 2002; Saab et al., 2009) and PICK1 (Jo et al., 2008). Human interleukin-1 receptor accessory protein-like (IL1RAPL1) interacts with NCS-1, and both proteins are involved in X-linked mental retardation and

[1]Department of Molecular, Cellular and Developmental Neurobiology, Institute Cajal, CSIC, Avenida Dr. Arce 37, Madrid 28002, Spain. [2]Department of Physiology, University of Toronto, Toronto, ON M5S 1A8, Canada. [3]Department of Crystallography and Structural Biology, Institute of Physical-Chemistry 'Rocasolano', CSIC, Serrano 119, Madrid 28006, Spain. [4]Department of Biochemistry and Molecular Biology, University of Salamanca, Salamanca 37007, Spain. [5]Institute for Biomedical Research (IBSAL), Salamanca 37007, Spain. *Present address: German Cancer Research Centre (DKFZ), Signal Transduction in Cancer and Metabolism, Im Neuenheimer Feld 580, 69120 Heidelberg, Germany. ‡Present address: MRC Laboratory of Molecular Biology, Cambridge CB2 0QH, UK.

§Author for correspondence (aferrus@cajal.csic.es)

Received 24 March 2014; Accepted 10 July 2014

Journal of Cell Science

Journal of Cell Science (2014) 127, 4246–4259 doi:10.1242/jcs.152603

autism (Bahi et al., 2003; Pavlowsky et al., 2010). Furthermore, a missense (R102Q) mutation in NCS-1 has been reported in one case of autism (Piton et al., 2008), and schizophrenic and bipolar disorder patients show an excess of NCS-1 in their dorsolateral prefrontal cortex (Koh et al., 2003) and a decrease of the protein in leukocytes (Torres et al., 2009). In view of the large repertoire of functional interactions reported so far, the search for unifying mechanisms that could account for the biology of this Ca^{2+} sensor is justified. A long-debated issue in neurobiology, which could underlie the pathologies mentioned above, is whether the two synaptic features – the probability of release and the number of synapses – are regulated by a single mechanism or result from independent processes that sustain neuron homeostasis. With regard to the Frq proteins, the question is: does Ca^{2+} binding to these proteins trigger a single pathway or, alternatively, two separate pathways? This question has been addressed here, taking advantage of the duplicated *frq* genes in *Drosophila*, in contrast to the single homologous mammalian gene, NCS-1.

RESULTS

Ric8a interacts with Frq2, but not with Frq1

Following a yeast-two hybrid (YTH) screen performed using a *Drosophila* embryonic library and full-length *Frq1* and *Frq2* cDNAs as baits, we isolated Ric8a, a guanine exchange factor (GEF) (i.e. an activator of G protein signaling; AGS), as a binding candidate for Frq2. Screening with Frq1 as bait yielded no candidate for a true positive interaction among 1×10^6 clones tested. With Frq2, however, out of 3.74×10^6 clones, a total of 20 verified cases were isolated. All of them contained the same sequence matching CG15797, which corresponds to nucleotides 326–971 of Ric8a cDNA, and to amino acids 73–288 of Ric8a protein (Fig. 1A). Because Frq1 is 95% identical to Frq2, we tested whether Frq1 could bind to Ric8a in a direct YTH assay. The result was negative. The specificity was further validated by *in vitro* GST pull-down assays. The fusion constructs poly-His–Myc–Frq1 and poly-His–Frq2–HA were expressed in bacteria, purified by affinity chromatography and loaded into GST–Ric8a pre-charged columns, followed by analysis of the corresponding eluates by western blotting. The data showed positive binding for Frq2 but not for Frq1 (Fig. 1B). An *in vivo* validation was obtained from co-immunoprecipitation (co-IP) assays using HEK293 cell extracts co-transfected with Myc–Ric8a and Frq2–HA (Fig. 1C). Although genomic and cDNA sequences were obtained from the same wild-type strain, Canton-S, we noticed that Frq1 and Frq2 RNAs must undergo adenosine-to-inosine editing to yield an I178M amino acid change in both proteins (Fig. 1D). The change, however, proved to be irrelevant to the Ric8a-binding specificity (Fig. 1E). Also, the binding specificity of Ric8a for Frq2 versus Frq1 was confirmed, this time using V5 tags. Based on these *in vitro* and *in vivo* assays, we conclude that the interaction between Frq2 and Ric8a is biologically relevant. However, because Frq1 and Frq2 differ at only 10 amino acids, the issue of binding specificity needs to be addressed.

The crystal structure explains the Frq2–Ric8a binding specificity

To understand the molecular basis of the binding, we solved the Frq2 structure by X-ray crystallography. The hydrophobic and ionic character of the Ca^{2+}-saturated protein allowed its purification to homogeneity. We obtained two types of crystals that were of space groups $P2_1$ and $P2_12_12_1$ (supplementary material Table S1). The structure of the unmyristoylated Ca^{2+}-bound Frq2 was solved by molecular replacement at 2.2 Å ($P2_1$ data) and 2.3 Å ($P2_12_12_1$ data) (Fig. 2A,B,D; supplementary material Movie 1). The globular structure of Frq2 displays two faces – one with the three Ca^{2+}-binding sites exposed to the solvent (EF face) and, opposite to this, another face with a very hydrophobic and elongated solvent-exposed crevice (crevice face) (Fig. 2B,C; supplementary material Movie 1). The overall *Drosophila* Frq2 structure is similar to the following four cases: human NCS-1 [PDB codes 1g8i (Bourne et al., 2001) and 2lcp (Heidarsson et al., 2012)] and yeast (*Saccharomyces cerevisiae*) Frq [PDB codes 1fpw (Ames et al., 2000) and 2ju0 (Strahl et al., 2007], and the root mean square deviation of Ca atoms from the EF-hand regions are 2.1 Å, 3.9 Å (lowest-energy model), 3.2 Å (lowest-energy model) and 2.6 Å, respectively. Among them, the most dissimilar is the human NCS-1 structure 2lcp, solved by nuclear magnetic resonance (NMR; PDB code 1lcp), where helices E from EF-hands 1 and 4 acquire different orientations and the loop between EF-hands 3 and 4 is in a closed conformation, due to interactions with the unstructured C-terminus that is inserted into the hydrophobic crevice.

To understand why Frq2, but not Frq1, interacts with Ric8a, we analyzed the position of the ten differential amino acids to identify candidates for target recognition and binding (Fig. 2A). Amino acids N5, A79, I91, H102, D161 and R162 are solvent exposed and located on the EF face (Fig. 2B, right). By contrast, amino acids D58, T138, G187 and R94 are also solvent exposed but are located on the crevice face (Fig. 2B, left; Fig. 2C). We reasoned that amino acids located near the crevice are more likely to be relevant in target recognition, as is the case with other Ca^{2+}-binding proteins (Ames and Lim, 2012). Amino acid D161, although not in the crevice, is located in the Ca^{2+}-binding loop of the EF4 motif, between positions Z and –Y. This position is occupied by an invariant G in EF hands (Marsden et al., 1990), and it confers flexibility to the Ca^{2+} loop; thus, it should be included among the candidates. D58, R94 and T138 are placed at the edges of the hydrophobic crevice, whereas G187 is disordered and, consequently, not present in the model. D58 in Frq2 is represented by Q58 in Frq1. Because both amino acids exhibit similar side chains, which contain a carboxyl and an amide group, respectively, it is unlikely that the side chain could account for the binding specificity. T138 is located in a loop between EF-3 and EF-4 that is highly motile, a feature that renders it relevant for target binding.

Thus, based on these structural considerations, out of the ten differential amino acids between Frq2 and Frq1, R94, T138 and D161 seem to be the best candidates to account for the binding specificity. To experimentally probe their relevance, we performed co-IP assays in HEK cells, to investigate the interaction between Ric8a and mutated versions of Frq1 that mimic Frq2 at these candidate amino acids. The data show that K94R, S138T and the double mutant pull down Ric8a as effectively as native Frq2. By contrast, the mutated candidate G161D pulls down Ric8a far less effectively than native Frq2 (Fig. 3A). In addition to these key amino acids, the comparison of the structure of the six independent molecules modeled in the asymmetric units of the two crystal forms indicate that the amphipathic C-terminal helix H10 is highly motile and acquires different positions depending on the physicochemical environment. In molecules B and C of the $P2_1$ crystal, H10 is inserted into the hydrophobic crevice, where it makes multiple hydrophobic contacts (Fig. 2B–D; supplementary material Movie

Journal of Cell Science (2014) 127, 4246–4259 doi:10.1242/jcs.152603

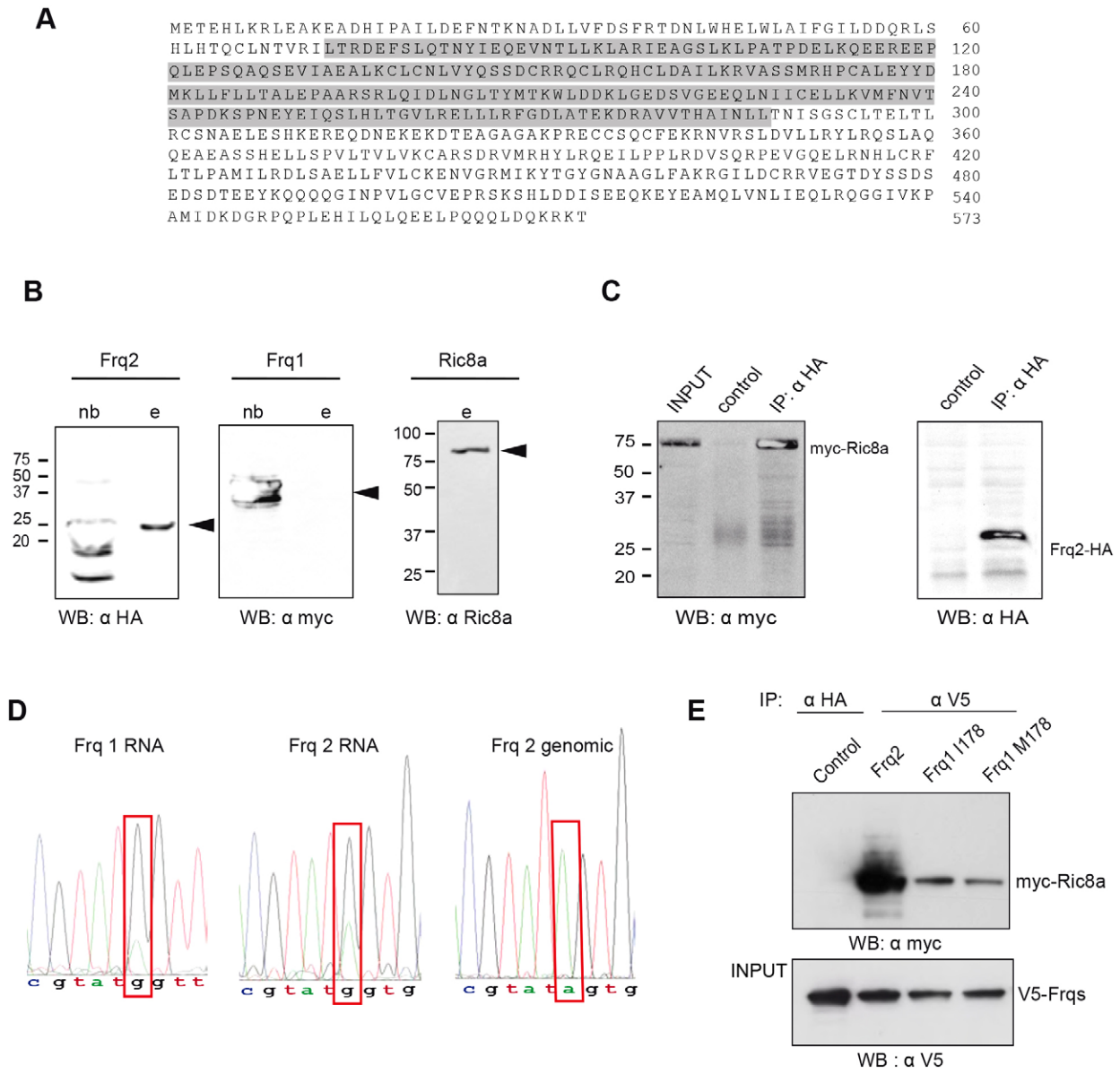

Fig. 1. Direct binding of Frq2 to Ric8a. (A) YTH screenings yielded Ric8a as a specific binding partner for Frq2. All true positive clones corresponded to the Ric8a sequence marked in gray. (B) GST-pulldown assays. HA-tagged Frq2 or Myc-tagged Frq1 were passed through GST–Ric8a-loaded columns. The not-bound (nb) and eluted (e) materials were assayed with antibody against HA (left), Myc (middle) or Ric8a (right). Note that, contrary to HA–Frq2, Myc–Frq1 is not detected (arrowheads indicate target protein size). Blots were mildly overexposed to maximize the detection of binding activity between Ric8a and Frq1. WB, western blot. (C) Co-IP assays of HEK293 cells co-transfected with Myc–Ric8a and Frq2–HA. Cell extracts were incubated with rabbit anti-HA and probed with mouse antibody against Myc (left) or HA (right). Myc–Ric8a co-purifies with Frq2–HA. As unrelated antibody in the two control lanes, we used Mab 22C10. IP, immunoprecipitation. (D) Editing of Frq1 and Frq2 RNAs. During experiments, Frq1 and Frq2 containing either A or G at nucleotide position 534 were cloned even though genomic and cDNA sequences originated from the same wild-type strain, Canton-S. Chromatograms from the sequencing reaction revealed that the genomic nucleotide in that position was A, whereas larval or adult RNAs from both Frq1 and Frq2 contained mainly G and, to a minor extent, A. This unexpected variability results, most likely, from RNA editing of adenosine to inosine by adenosine deaminases (ADARs). This editing in Frq1 and Frq2 changes isoleucine 178 to methionine. (E) Co-IP assays with the edited (Frq1 M178) or the wild-type (Frq1 I178) forms showed no effect on their binding to Ric8a. Gels were overexposed to reveal the minimal binding activity of Frq1 as compared to that of Frq2. In these experiments, Ric8a is tagged with Myc and Frqs are tagged with V5. As unrelated antibody in the control lane, we used anti-HA.

2). However, in molecules A and D of this crystal and in the two molecules of the $P2_12_12_1$ crystal, H10 is solvent exposed (Fig. 2D; supplementary material Table S1). This argues that helix H10 could be important for target interaction because it could contact Ric8a. To test this hypothesis, we generated a Frq2ΔH10 mutant by deleting the last 12 amino acids of the C-terminus, and we performed co-IP assays with Ric8a (Fig. 3A). Binding was found to be 30% stronger in the absence of H10 than with the native Frq2, suggesting that the helix does not interact with Ric8a and functions as a built-in competitive inhibitor that blocks the Ric8a binding site. This is consistent with a recent study on *Caenorhabditis elegans*, which reported that the deletion of the C-terminal tail of NCS-1 did not impair its ability to rescue behavioral defects (Martin et al., 2013). Taken together, R94 and

Journal of Cell Science

Journal of Cell Science (2014) 127, 4246–4259 doi:10.1242/jcs.152603

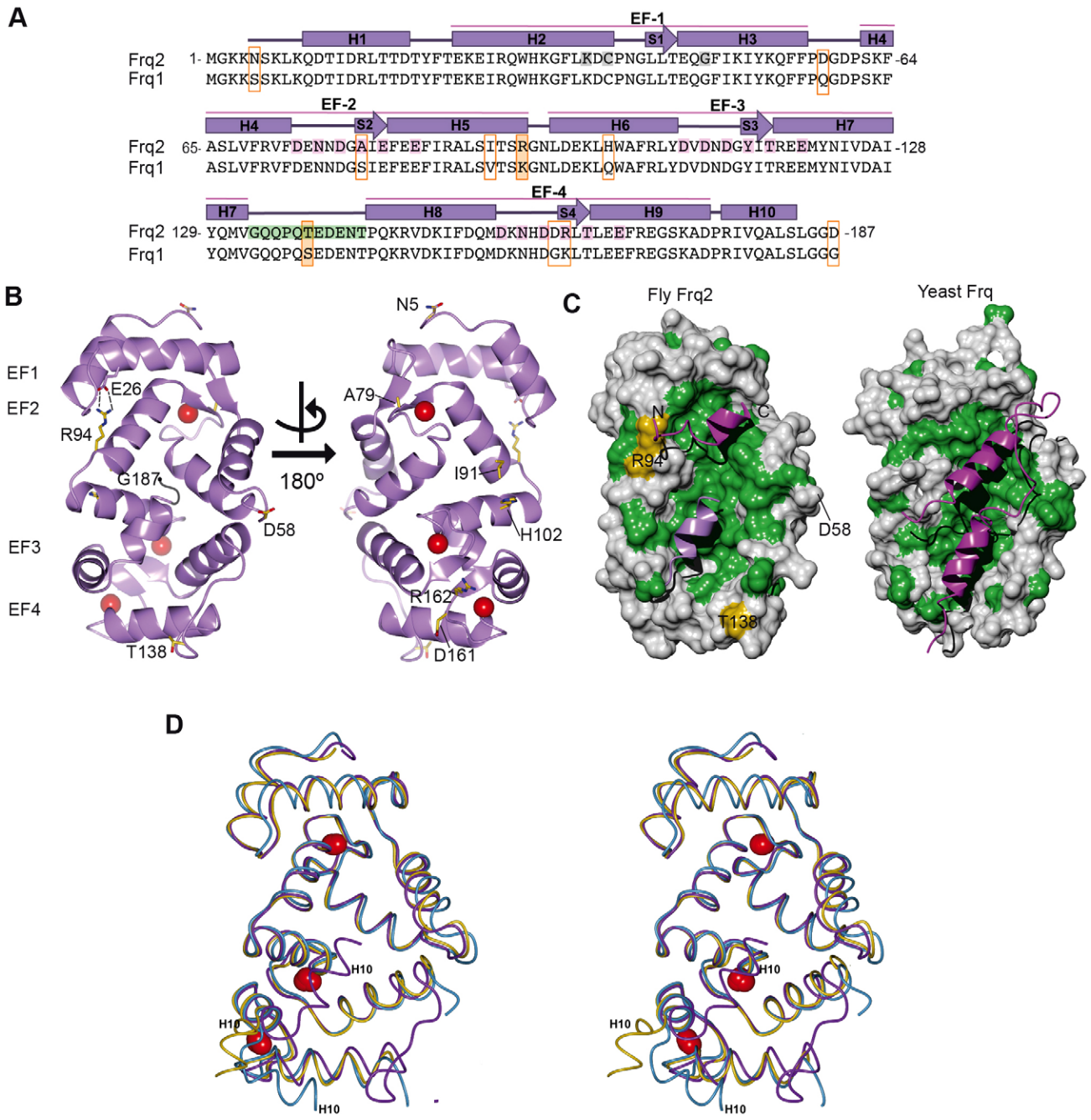

Fig. 2. Structural basis of Frq2–Ric8a binding. (A) *Drosophila* Frq2 and Frq1 alignment with sequence differences indicated (orange squares). The proteins contain four EF motifs (EF), ten α-helices (H) and four short β strands (S). Frq2 binds to three Ca^{2+} ions (pink) at EF-2, EF-3 and EF-4 motifs. Mutations at EF-1 (gray) impede Ca^{2+} binding. R94K and T138S differences are highlighted in orange, and the motile loop between EF-3 and EF-4 is in green. (B) Ribbon representation of Frq2 structure (molecule B, space group $P2_1$) with bound Ca^{2+} (red spheres). Differential Frq1 amino acids are displayed in stick mode. H-bonds between R94 and D26 are indicated with black dashed lines. Left and right panels show the crevice and the EF faces, respectively. The C-terminus that is disordered in the crystal structure (amino acids 184–187) is depicted in gray trace. (C) Surface representation of fly Frq2 (left; molecule B, space group $P2_1$) and yeast Frq (right; PDB code 2ju0). Surface exposed hydrophobic amino acids are in green. In the fly Frq2 (left), note that one H10 helix (lilac ribbon) belongs to the same molecule, whereas the other belongs to molecule D (magenta ribbon). R94 and T138 are depicted in orange. In yeast Frq (right), note the PICK-1 fragment in complex (magenta ribbons). (D) Stereo diagram superposing independent fly Frq2 molecules found in the two crystal forms. Molecules B and D (space group $P2_1$) and molecule A (space group $P2_12_12_1$) are in lilac, yellow and blue, respectively. Helices (H10) and Ca^{2+} ions (red spheres) are indicated.

T138 appear to be key amino acids to explain the selective binding, whereas the motile C-terminal H10 helix regulates site accessibility to Ric8a, the targeted substrate.

The binding is conserved in the human homologs

Although Frq is represented by two genes in *Drosophila*, its human homolog, NCS-1, is encoded by a single gene. Thus, the

Journal of Cell Science (2014) 127, 4246–4259 doi:10.1242/jcs.152603

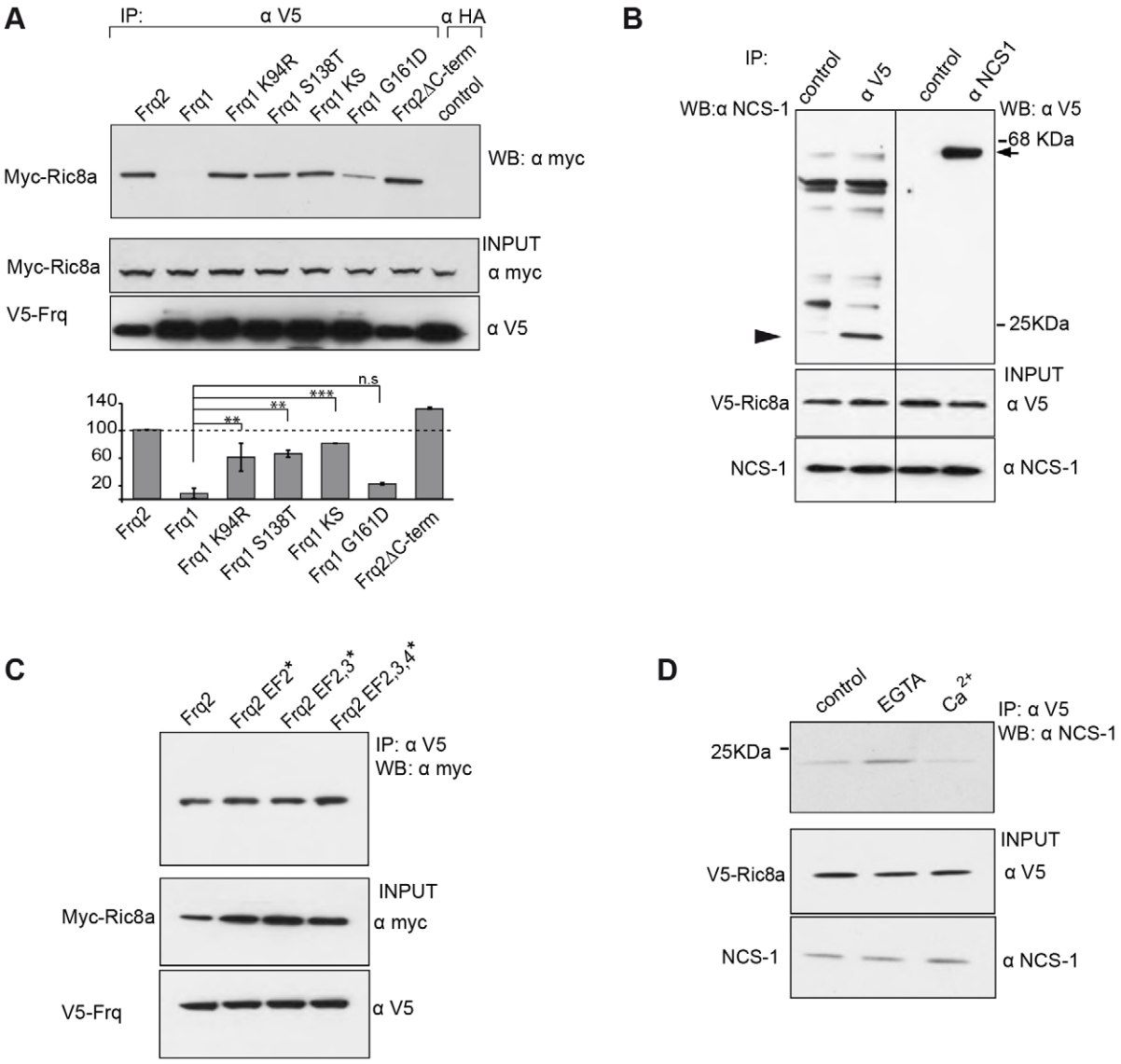

Fig. 3. Validation of key amino acids and Ca^{2+} dependence of Frq2–Ric8a binding. (A) Co-IP assays between Ric8a and mutated versions of Frq1 that mimic Frq2. HEK293 cells were co-transfected with Myc–Ric8a and V5–Frqs. The constructs included wild-type Frq2, wild-type Frq1, Frq1 K94R, Frq1 S138T, double mutant Frq1 K94R plus S138T (Frq1 KS), Frq1 G161D and Frq2 with a 12-amino-acid deletion of its C-terminus (Frq2 ΔC-term). Immunoprecipitation (IP) was performed with antibody against V5 and western blots (WB) were probed with anti-Myc antibodies. Quantifications of each lane from several experiments (mean±s.e.m.) are shown below the blots. Note the minimal binding of Frq1 versus Frq2 and the strong binding of Frq1 K94R, Frq1 S138T and the double mutant. Also note the lack of effect of deleting the C-terminus in Frq2. ***$P<0.001$; **$P<0.01$; ns, non-significant. (B) Co-IP assay from HEK293 cells co-transfected with human NCS-1 and humanV5–Ric8a. The immunoprecipitation of Ric8a (left) pulls down NCS-1 (arrowhead), whereas the immunoprecipitation of NCS-1 (right) pulls down Ric8a (arrow). Input gels show protein levels prior to co-IP. An anti-HA antibody was used as a negative control in both sets of experiments. (C) Co-IP assay between Ric8a and Frq2 forms with mutations in key amino acids of the Ca^{2+}-binding EF-hands. Frq2 EF2*, E84A; Frq2 EF2,3*, E84A+E120A; Frq2 EF2,3,4*, E84A+E120A+E167A. Ric8a binding is not abolished by any of these mutations. (D) Co-IP assay from HEK293 cells co-transfected with human NCS-1 and human V5–Ric8a in the presence of EGTA (20 mM) or Ca^{2+} (5 mM). Ric8a binding is favored in the absence of Ca^{2+}.

Frq2-specific interaction with Ric8a identified in *Drosophila* might not necessarily be conserved between the human counterparts. We addressed this issue by co-IP assays performed in HEK cells transfected with human NCS-1 and human Ric8a (Fig. 3B). The data show a strong interaction between the two proteins. Human NCS-1 contains an arginine at position 94, as does fly Frq2. Also, the fact that *Drosophila* S138T Frq1 binds to Ric8a means that hydrophobic contacts might occur between Ric8a and the extra methyl group that is provided by T138, but not S138. Human NCS-1 contains a L at position 138, and thus the necessary hydrophobic contact could be maintained. Finally, R94 is hidden in the two solved human NCS-1 structures (Bourne et al., 2001; Heidarsson et al., 2012). The C-terminal end shows a helical fold in the crystal structure (Bourne et al., 2001), as we observe in our structure, and it is unstructured in the NMR model (Heidarsson et al., 2012). Our data indicate that the C-terminal helix H10 would need to destabilize and leave the crevice in order to interact with Ric8a,

Journal of Cell Science

Journal of Cell Science (2014) 127, 4246–4259 doi:10.1242/jcs.152603

as demonstrated here for *Drosophila* Frq2. Thus, we can conclude that the interaction identified in *Drosophila* is functionally and structurally conserved in humans.

Ric8a binds to Frq2 in the absence of Ca^{2+}

Because Frq2 is a Ca^{2+}-binding protein, and the solved crystal structure corresponds to that observed under Ca^{2+}-saturated conditions, we questioned whether the binding to Ric8a is Ca^{2+}-dependent. To this end, we carried out co-IP assays in HEK cells co-transfected with *Drosophila* Ric8a and normal and mutated forms of Frq2 (Fig. 3C). In comparison to the wild-type Frq2, versions with mutations in the functional EF hand motifs showed equivalent binding activity, suggesting that Ca^{2+} is not a requirement for Ric8a–Frq2 binding. Furthermore, we assayed the binding of the human homologs in the presence of EGTA (20 mM) or Ca^{2+} (5 mM) (Fig. 3D) and found that the binding is favored in the absence of Ca^{2+}. Thus, we interpret that, under normal cellular physiological conditions and conditions of very low Ca^{2+} concentration, Ric8a and Frq2 will be mostly in the bound state (see Discussion).

Ric8a and Frq2 colocalize in the nervous system

Drosophila Frq2 is expressed in the larval and adult central nervous system (CNS) (Pongs et al., 1993; Romero-Pozuelo et al., 2007). Ric8a/synembryn is also expressed in the CNS of *C. elegans* (Miller et al., 2000) and mammals (Tõnissoo et al., 2003). In *Drosophila*, Ric8a has been found to localize in mitotic neuroblasts, where it regulates G protein complexes, at early stages of embryonic development (Hampoelz et al., 2005; Wang et al., 2005). However, it is not known whether this is also the case for differentiated neurons, where Frq2 is expressed. To clarify this, we performed *in situ* hybridization for Ric8a in whole fly embryos. The data show a broad expression during late stages (st.14–16) in the ventral ganglion and the brain (Fig. 4A,B). Similar to Frq proteins (Pongs et al., 1993), Ric8a was also detected in both type Is and Ib boutons, in close proximity to synaptic active zones (Fig. 4C,D). This signal is specific, because it was lost by driving UAS-$Ric8a^{RNAi}$ expression (Fig. 4E,F). Furthermore, we investigated the subcellular localization of the two proteins by co-transfecting Myc–Ric8a and Frq2–HA into S2 cells. Both proteins were present in the cytoplasm but they only overlapped close to the plasma membrane (Fig. 4G–J). Thus, Ric8a and Frq2 fulfil the localization criteria to undergo a functional interaction at the presynaptic cell membrane.

Ric8a regulates the number of synapses

We previously found that Frq restrains synaptic growth. An increase in the amount of Frq produces a decrease in branching, bouton number and total synapses, whereas a decrease in Frq levels yields the opposite effect (Romero-Pozuelo et al., 2007; Dason et al., 2009). Because Ric8a interacts with Frq2, we applied the same experimental strategy to analyze the possible role of Ric8a in synapses. For this *in vivo* study, in addition to the standard overexpression and knockdown conditions, we analyzed double combinations of Frq2 and Ric8a constructs in order to identify the functional hierarchy of both proteins.

The data show that RNAi-mediated knockdown of Ric8a decreases the number of presynaptic active zones, whereas the same effect requires the overexpression of Frq2 (Fig. 5A; Table 1). This suggests that Frq2 might negatively modulate Ric8a. Ric8a overexpression does not yield a significant effect. However, in conjunction with Frq2 knockdown, a strong increase in synapse number results. This observation further supports a negative regulation of Ric8a by Frq2. Also, combinations of two

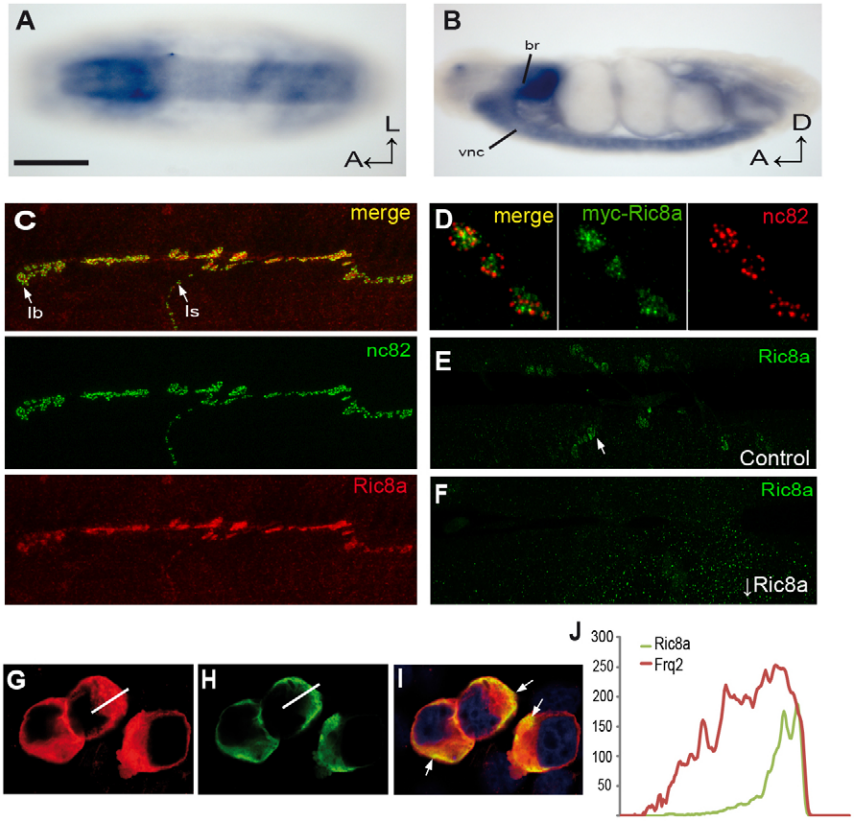

Fig. 4. Ric8a expression. (A,B) Dorsal (A) and lateral (B) views of *in situ* hybridization of a Ric8a RNA probe to the early embryo, revealing that the expression is primarily neural. Anterior is to the left. A, anterior; L, lateral; D, dorsal; br, brain; vnc, ventral nerve cord. (C) The anti-Ric8a serum shows that the protein is localized at larval motor neuron terminals (*D42-Gal4*) of Is and Ib bouton types. (D) The signal is abundant in boutons, particularly close to nc82-marked synaptic active zones. (E,F) The signal is abolished by the expression of a Ric8a RNAi, which validates the antibody. (G–I) Transfected S2 cells showing the localization of Myc–Ric8a (green) and Frq2–HA (red). Images are single confocal planes. The colocalization is noticeable at the cell periphery underlying the plasma membrane (arrows in I). Nuclei are revealed with DAPI. (J) Signal quantification along the white lines marked in G and H. The single scale bar represents 100 μm (A,B), 20 μm (C,E,F), 8 μm (D) and 6 μm (G–I).

Journal of Cell Science (2014) 127, 4246–4259 doi:10.1242/jcs.152603

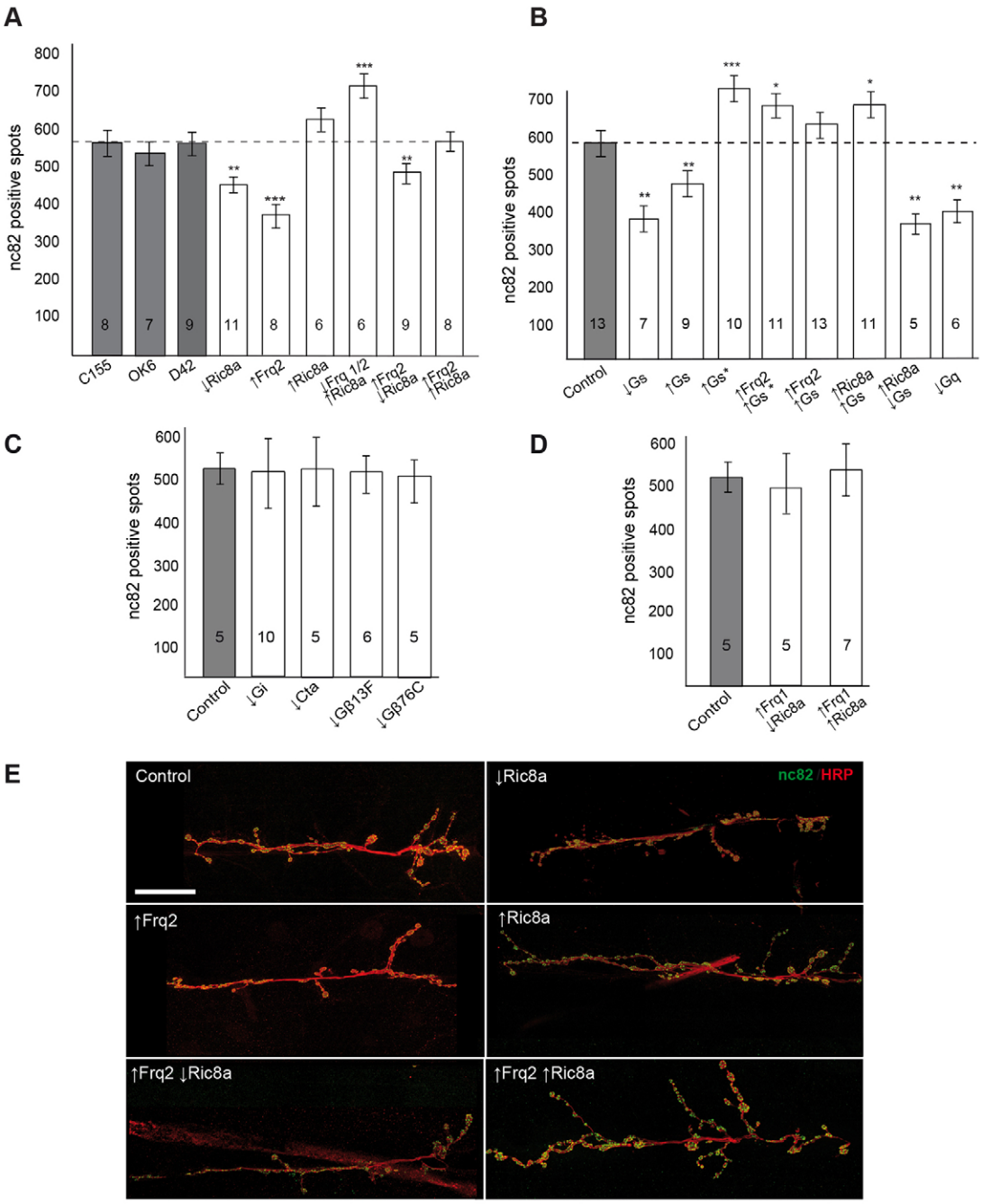

Fig. 5. Regulation of the number of synapses by Ric8a, Frq2 and Gα proteins. (A) The three Gal4 drivers (*C155, OK6, D42*) used throughout this study show equivalent synapse numbers. Reduction in the number of synapses occurs both in Ric8a underexpressers and in Frq2 overexpressers. Although overexpression of Ric8a (↑ Ric8a) does not yield significant effects, in combination with Frq2 knockdown (↓ Frq2) it results in a strong increase in the number of synapses. Consistent with this, the combination of Frq2 overexpression and Ric8a knockdown (↑ Frq2 ↓ Ric8a) shows a significant decrease in synapse number, and overexpression of both Frq2 and Ric8a (↑ Frq2 ↑ Ric8a) suppresses this effect. These data indicate that Frq2 acts as a negative regulator of Ric8a in the control of synapse number. (B) Both knockdown (↓ Gs) and overexpression (↑ Gs) of Gs reduce the number of synapses, but a constitutively active form (↑ Gs*), yields the opposite effect. Consistent with the proposed negative regulation of Ric8a by Frq2, the constitutive effects of Gs* bypass the opposing ones from Frq2 overexpression. This effect is not observed with the non-activated Gs (↑ Frq2 ↑ Gs). However, consistent with the required activation of Gs by Ric8a, the double combination of Gs and Ric8a overexpression (↑ Gs ↑ Ric8a) yields a significant increase in synapse number, and the mild effect of Ric8a overexpression is counteracted by the simultaneous knockdown of Gs. Synapse number seems to be also regulated by Gq. (C) Changes in other Gα (Gi, Cta) or Gβ (Gβ13F, Gβ76C) subtypes yielded no effect, indicating that synapse number is regulated specifically by Gs and Gq. (D) Frq1 overexpression does not show the same effects in combination with manipulation of Ric8a as are observed with Frq2. Numbers inside bars indicate the number of independent female larvae analyzed. Data show the mean±s.e.m.; ***$P<0.001$; **$P<0.01$; *$P<0.05$. (E) Representative NMJs of relevant genotypes. Each image is a composite of a single NMJ. Synaptic active zones are identified as nc82-immunopositive spots (green) and the motor neuron axonal membrane is labeled with anti-HRP (red). Recordings were obtained in larvae from several vials in each cross. Scale bars: 20 μm. Genotypes are listed in supplementary material Table S2.

Journal of Cell Science (2014) 127, 4246–4259 doi:10.1242/jcs.152603

Table 1. Summary of phenotypes caused by the overexpression or knockdown of the corresponding proteins

Protein	Synapse number*	Release**	Source of data
Frq2 ↑	Decrease	Increase	Figs 5,6; Dason et al., 2009; Romero-Pozuelo et al., 2007
Frq2 ↓	Increase	Decrease	Dason et al., 2009; Romero-Pozuelo et al., 2007
Ric8a ↑	No change	Increase	Figs 5,6
Ric8a ↓	Decrease	Decrease	Figs 5,6
Gs ↓	Decrease	Increase	Figs 5,6
Gq ↓	Decrease	nd	Fig. 5
Gi ↓	No change	nd	Fig. 5
Cta ↓	No change	nd	Fig. 5
Gβ13F ↓	No change	nd	Fig. 5
Gβ76C ↓	No change	nd	Fig. 5

*Number of nc82-positive spots; **Amplitude of evoked EJP (in 1 mM Ca^{2+}); ↑, overexpression; ↓, knockdown; nd, not determined.

conditions that, individually, showed identical phenotypes (e.g. synapse number decrease due to Frq2 overexpression or Ric8a knockdown) yielded the same effect as the two independent manipulations (Fig. 5A). This is indicative that the two proteins work in the same pathway. By contrast, the synapse number decrease that results from Frq2 overexpression is suppressed by the simultaneous overexpression of Ric8a (Fig. 5A). These data further suggest that normalcy results from the balanced activities of Ric8a and Frq2, and that Ric8a is downstream of Frq2.

Ric8a regulates synapse number through Gα protein activity

As a guanine-exchange factor (GEF), Ric8a interacts *in vitro* with several Gα proteins (Tall et al., 2003), for which it serves as a scaffolding protein, thus facilitating further interactions with specific signaling pathways (Andreeva et al., 2007). However, the *in vivo* relevance of these Ric8a–G-protein interactions is mostly unknown. We tested the four *Drosophila* Gα proteins, Gαs, Gαq, Gαi (referred to here as Gs, Gq and Gi) and Concertina (Cta) on synapse number. Gs regulates neuron morphology in *Drosophila* (Wolfgang et al., 2004) and binds to Ric8a in humans (Klattenhoff et al., 2003). Here, we analyzed the putative involvement of Gs in the Frq2–Ric8a interaction output. In agreement with previous reports, attenuated Gs expression reduced synapse number. However, the same effect was observed when Gs expression was increased (Fig. 5B). This property – the same phenotype under conditions of either overexpression or knockdown – suggests that the protein needs to be activated and performs its normal function within a range of activity levels. Most likely, the overexpression of a non-activated form out-competes the endogenously activated Gs (an excess of the non-activated form of Gs would behave as a dominant negative), whereas the under-expression would have resulted in an activity level below the normal threshold. To test this possibility, we used a constitutively active form of Gs, Gs* (Connolly et al., 1996), which yielded a phenotype opposite to that of the under-expression, resulting in synapse number increase (Fig. 5B). The phenotype observed following overexpression of non-activated Gs – a decrease in synapse number – was transformed into the expected synapse number increase when combined with the overexpression of Ric8a, the Gs activator. In addition, the Gs-knockdown phenotype prevailed over that of Ric8a overexpression, demonstrating that Gs is functionally downstream of Ric8a (Fig. 5B). Taken together, the data indicate that Gs is required *in vivo* for synaptogenesis, but it requires activation by Ric8a, which, in turn, is downregulated by Frq2.

With respect to other Gα types, Gq appears to regulate synaptogenesis, because the Gq-knockdown condition showed a reduction in synapse number (Fig. 5B). This is consistent with the functional similarity that the two Gα subtypes show in many physiological contexts (Wolfgang et al., 2004). The Gi-knockdown condition showed no effect on synapse number (Fig. 5C) and Cta, whose sequence is rather divergent from the rest of Gα subtypes (Boto et al., 2010), also yielded no effect (Fig. 5C). With respect to non-Gα proteins, we assayed Gβ13F and Gβ76C, and found that these also had no effect on synapse number (Fig. 5C). Thus, we can conclude that both Gs and Gq regulate synapse number.

Although the structural analysis demonstrated the binding specificity of Ric8a for Frq2, rather than Frq1, we tested this specificity *in vivo*. As shown above (Fig. 5A), Ric8a knockdown elicited a reduction in the number of synapses either by itself or in conjunction with Frq2 overexpression, consistent with Frq2 being a negative regulator of Ric8a. By contrast, the equivalent genetic combination with Frq1 yielded a normal phenotype in terms of synapse number (Fig. 5D). A normal phenotype was also obtained under conditions of Ric8a overexpression (Fig. 5D). Representative examples of neuromuscular junctions (NMJs) are shown in Fig. 5E. These results rule out the possibility that Frq1 could be a negative regulator of Ric8a. Nevertheless, because Frq1 and Frq2 have been shown to regulate synapse number (Dason et al., 2009) (Table 1), it is still plausible that Frq1 could participate in this regulation without directly binding to Ric8a.

Ric8a regulates neurotransmitter release

Given that the over- or underexpression of Frq increases or decreases quantal content per synapse, respectively (Romero-Pozuelo et al., 2007; Dason et al., 2009), we performed intracellular recordings to determine whether Ric8a also modulates synaptic transmission. Ric8a overexpression increased evoked excitatory junction potentials (EJPs), whereas Ric8a knockdown decreased them (Fig. 6A). In both cases, there was no change in the frequency of spontaneously occurring miniature (m)EJPs, but a mild increase in amplitude (Fig. 6B). We further characterized the effects of Ric8a on synaptic transmission by performing macropatch focal recordings on individual type Ib boutons. Ric8a overexpression increased the amplitude of excitatory junction currents (EJCs) and the number of quanta released per bouton, whereas Ric8a knockdown reduced it (Fig. 6B,C). To further analyze whether the effects on synaptic transmission could result from changes in the number of synapses per bouton, we counted the number of synapses in boutons of the same size (5 µm diameter) and position (the end of a branch) as those used for recordings. The over- or

Journal of Cell Science (2014) 127, 4246–4259 doi:10.1242/jcs.152603

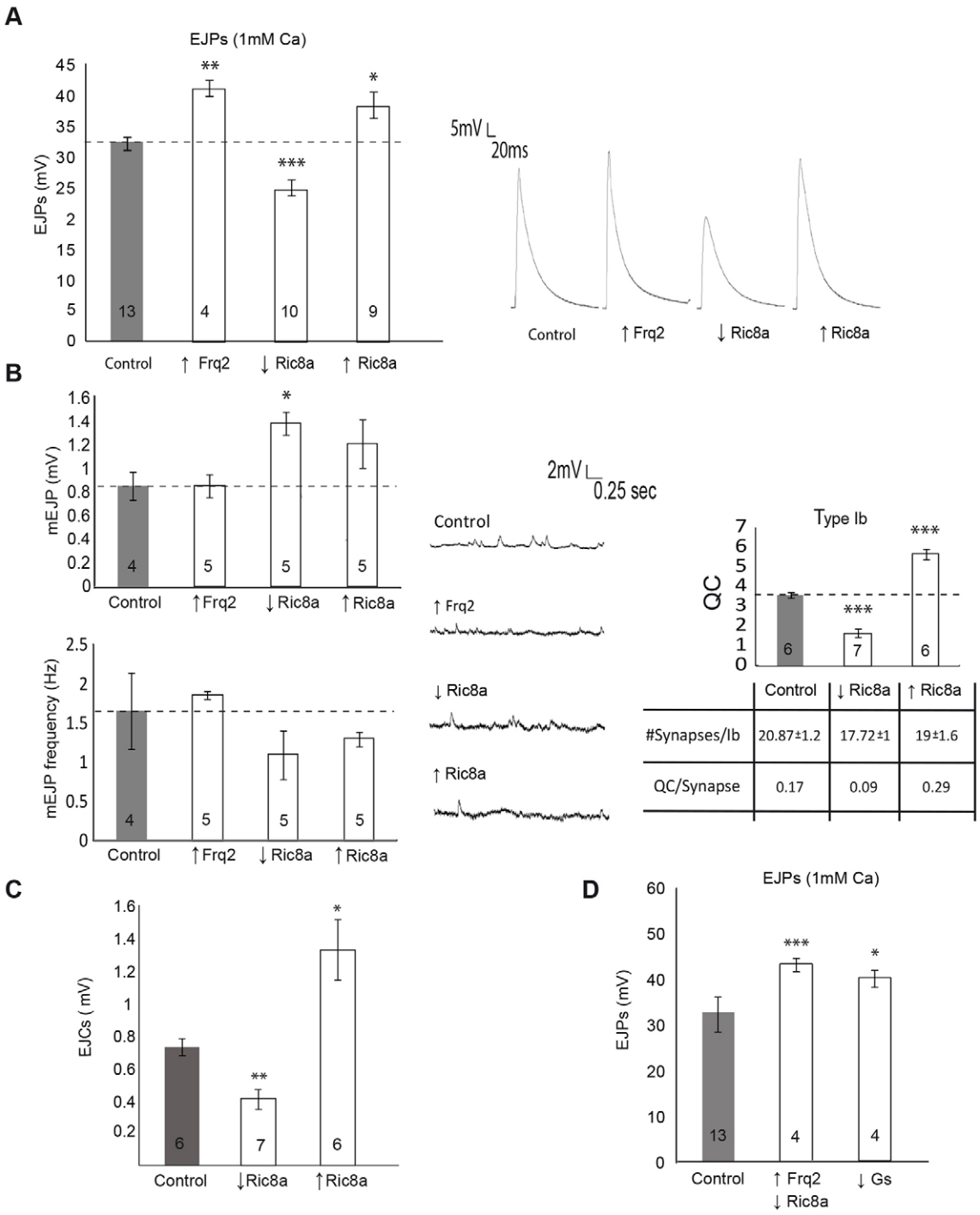

Fig. 6. Regulation of neurotransmitter release by Ric8a and Gs. (A) Evoked EJP amplitudes of muscle from larvae with Ric8a knockdown (↓ Ric8a) were decreased in comparison to those of controls, whereas they were increased following overexpression of Ric8a (↑ Ric8a) or Frq2 (↑ Frq2). Sample traces of EJPs obtained in 1 mM Ca^{2+} are shown on the right for the corresponding samples. (B) Spontaneous mEJP amplitudes in several genotypes. No significant differences were found except in Ric8a-knockdown animals. Also, no significant differences were found in the frequency of mEJPs. Sample traces of mEJPs are shown on the right. The quantal content (QC) of release from type Ib boutons is affected by the levels of Ric8a. The table below the graph indicates the average number of synapses per Ib bouton and the release per synapse. (C) EJC values from the same terminals used to calculate QC. (D) Evoked EJP amplitudes of larvae with a combination of Frq2 overexpression and Ric8a knockdown (↑ Frq2 ↓ Ric8a) are larger than those of controls. Given that the individual genotypes showed opposite effects on release (A), the result indicates that each protein regulates neurotransmission through independent mechanisms. Gs is also required for normal release. Numbers inside histograms indicate the number of NMJs and female larvae analyzed. Data show the mean±s.e.m.; ***$P<0.001$; **$P<0.01$; *$P<0.05$. Genotypes are listed in supplementary material Table S2.

underexpression of Ric8a does not change the average number of synapses per Ib bouton (20.8±1.2 in controls versus 19±1.6 following Ric8a overexpression and 17.7±1 following Ric8a knockdown) (Fig. 6B). Thus, we conclude that Ric8a modulates the quantal content per synapse as we have previously found for Frq2 (Dason et al., 2009).

Journal of Cell Science

Journal of Cell Science (2014) 127, 4246–4259 doi:10.1242/jcs.152603

Intriguingly, the changes elicited by manipulating Ric8a on the probability of release are in the same direction as those elicited by manipulating Frq2, whereas, in terms of the regulation of synapse number, Frq2 and Ric8a yield opposite effects (Fig. 5A; Fig. 6A; Table 1). These observations indicate that the Frq2–Ric8a interaction could trigger differential mechanisms responsible for the regulation of synapse number or neurotransmitter release. To clarify this, we studied how the Frq2–Ric8a interaction affects synaptic release. Because in the independent genotypes (Fig. 6A) both proteins caused the same effects on release, a negative modulation of Ric8a by Frq2 seems unlikely. In the double mutant experiments, we combined two conditions that exhibit opposing phenotypes – Frq2 overexpression, which increases release, and Ric8a knockdown, which reduces it. We reasoned that if Ric8a is negatively regulated by Frq2, this double mutant combination should show the same, or stronger, phenotype than Ric8a knockdown alone. However, the data show that it is the Frq2-overexpression phenotype that dominates, suppressing that of Ric8a knockdown (Fig. 6D). Alternatively, if Ric8a is positively regulated by Frq2, their combination should show mutual suppression of the single phenotypes, and this is not observed. Thus, we must conclude that Ric8a and Frq2 regulate release through different mechanisms.

Attending to the role of Ric8a as a GEF, and given the evidence that Gα proteins are involved in neurotransmitter release, we tested their single and combined effects. In agreement with previous reports (Renden and Broadie, 2003), we found that the knockdown of Gs increased release (Fig. 6D). Thus, the GEF Ric8a might regulate synaptic release through at least the Gs subtype of Gα proteins. Concerning other Gα subtypes, in *C. elegans* the interaction of Ric8a with Gq has been demonstrated in the context of neurotransmitter release (Miller et al., 1999; Miller et al., 2000). Taken together, these data show that Ric8a is a GEF that functionally interacts with Gs, and likely Gq, in the context of regulating the probability of neurotransmitter release.

DISCUSSION

Here, we describe a novel interaction between Frq2 and Ric8a. In addition, we show that Ric8a regulates both synapse number and neurotransmitter release. Contrary to most other GEFs, Ric8a is not coupled to a membrane receptor but it traffics from the cytoplasm instead. This strategic positioning and trafficking renders Ric8a as a suitable link between the Ca^{2+} surge and G protein signaling in the context of synapse regulation. The effects on synapse number imply cytoskeletal changes, possibly mediated by tubulin (Roychowdhury and Rasenick, 2008; Davé et al., 2011). The Gs-binding site in tubulin is also used to bind to adenylyl cyclase, eliciting further cyclic nucleotide signaling (Afshar et al., 2004). Consistent with the cytoplasm-to-membrane translocation of Frq/NCS-1, Ric8a and Gα, the cAMP-dependent signaling also requires compartmentalization (Willoughby and Cooper, 2007; Baillie, 2009), suggesting that these proteins assemble in membrane micro-domains at an early step of synaptogenesis. Gs also activates voltage-dependent Ca^{2+} channels (Mattera et al., 1989) in a reinforcing feed-back loop following the initial Ca^{2+} inflow due to membrane depolarization. Concerning Gq, in addition to binding to tubulin, it also activates PLCβ, which mobilizes Ca^{2+} from internal stores (Mizuno and Itoh, 2009), further augmenting the Ca^{2+} surge. These Gs- and Gq-mediated events sustain the Ca^{2+} dynamics in Frq mutants that we have described previously (Dason et al., 2009), and reveal Ric8a as a convergence point of both Ca^{2+} sources.

It is worth noting that, like Frqs but contrary to Ric8a, Gs also causes opposite effects on synapse number and release probability (Table 1). This observation argues in favor of a common mechanism that co-regulates these two neuronal properties in an antagonistic manner. A largely debated issue is whether this coordination results from independent mechanisms of cell homeostasis, or from a single mechanism with two separate outputs. Ric8a and Frq2 regulate both synaptic features. However, they yield similar effects on release while also mediating opposing effects on synapse number (Table 1), which rules out the possibility that release and synapse number could result from one single Frq2–Ric8a-dependent mechanism. Double mutant experiments show that Frq2 acts as a negative regulator of Ric8a in the control of synapse number. By contrast, in the context of transmitter release, the two proteins seem to operate through independent mechanisms. We hypothesize that Ric8a could be part of a switch mechanism for the control of release versus synaptogenesis, which would explain the antagonistic regulation of the two neuronal features (Fig. 7). Based on the *in vivo* study provided by the genetic analysis, and because Frq2 can bind to Ric8a in the absence of Ca^{2+}, we envision that the expected conformational change that Ca^{2+} binding will cause in Frq2 structure will lead to the release of Ric8a (that, as a GEF, will activate G proteins), triggering the signaling cascade to regulate synapse number and the probability of neurotransmitter release. In this context, the motile H10-helix-based mechanism (see below) could titrate the amount of Ric8a that binds to Frq2 and, hence, regulate the levels or type of G-protein signaling. Concerning Frq1, its involvement in synapse regulation is clear (Romero-Pozuelo et al., 2007; Dason et al., 2009) but, in light of the data reported here, its mechanism of activity must be independent of Ric8a and remains to be identified.

The Frq2 versus Frq1 specificity of the Ric8a interaction validates the functional specialization hypothesis for the maintenance of conserved gene duplications (Rastogi and Liberles, 2005; Sánchez-Gracia et al., 2010). Benefiting from the duplicated Frq in *Drosophila* and through the crystallography-inspired site-directed mutagenesis of candidate amino acids in Frq1, residues R94 and T138 are found to determine the binding specificity. At position 94, the presence of an arginine and not a lysine seems to be crucial. The guanidinium group instead of an amine would permit additional H-bond interactions through nitrogen Nε (Fig. 2B). At position 138, the methyl group of the Thr side chain seems to be interacting with hydrophobic contacts. To our knowledge, there is no precedent of two structurally almost identical Ca^{2+} sensors whose binding specificity is determined by only two amino acid differences.

The dynamics of the binding process deserves some comment. The monoclinic structure shows that molecules B and C display an occluded crevice due to the insertion of two H10 helices – their own helix H10 and a second one from another molecule (Fig. 2C). This situation resembles the interaction between yeast Frq and PICK-1, where PICK-1 uses two α-helical segments, and suggests that, in molecules B and C, these H10 helices mimic the interaction with Ric8a. From the crystal structures presented here, we can infer that in cells, under high Ca^{2+} concentrations, the motile H10 must be inserted into the crevice, occluding it to impede promiscuity of this site. In the presence of Ric8, the target will displace the H10 helix and proper insertion will occur (supplementary material Movie 2). A similar mechanism has been proposed for yeast and human Frq and KChIP1 interacting with their corresponding targets, PI4K3β (Ames et al., 2000; Strahl

Journal of Cell Science (2014) 127, 4246–4259 doi:10.1242/jcs.152603

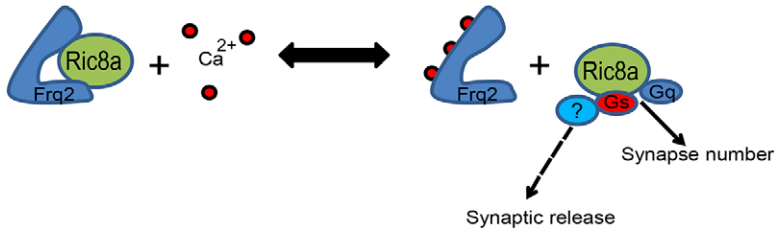

Fig. 7. Summary diagram with the functional roles of the analyzed proteins. Under normal conditions, Frq2 is bound to Ric8a, preventing the signaling through G proteins. Following the Ca^{2+} surge, Frq2 binds to Ca^{2+}, changing its conformation. This change liberates Ric8a, which triggers the signaling cascade through Gs and Gq to regulate synapse number. Likely additional intermediate interactions might involve adenyl cyclase, tubulin, etc. A faster process would regulate synaptic release through a still unknown element. This hypothetical mechanism would be reversible upon Ca^{2+} clearance from the cytoplasm. Also, the process likely includes trafficking of Frq2–Ric8a between the plasma membrane and the cytosolic compartments.

et al., 2007), dopamine D2/D3 receptors (Lian et al., 2011) and the Kv4.3 channel (Pioletti et al., 2006; Wang et al., 2007). It is plausible that the transient occlusion of the crevice by H10 will serve as a mechanism to quantitatively regulate the probability of binding to Ric8a, as suggested for human Frq (Heidarsson et al., 2012) and similar to the chain-and-ball model of voltage-dependent K^+ channels for its open-closed status (Fan et al., 2012).

In humans, the interaction is conserved, suggesting a potential role in pathology. IL1RAPL1 and NCS-1 are implicated in X-linked mental retardation and autism (Handley et al., 2010; Pavlowsky et al., 2010). The autism-related missense (R102Q) mutation in NCS-1 abolishes Ca^{2+} dependence, owing to a weakened conformational stability of its C-terminus that affects the cytosolic-to-membrane cycling of NCS-1 (Heidarsson et al., 2012). Because Frq2–NCS-1 is a negative regulator of Ric8, it is plausible that modifying the equivalent cycling of Ric8a and Gs or disrupting the protein–protein interactions with small compounds could modulate the pathological processes.

MATERIALS AND METHODS

Experimental system

We used the glutamatergic neuromuscular junction (NMJ) of the female third larval instar as our experimental system. Synapses were visualized using confocal microscopy with the monoclonal antibody nc82, which identifies the Bruchpilot protein, a constituent of the presynaptic active zone (Wagh et al., 2006; Owald et al., 2010), located at the edge of the characteristic T bar specialization of fly synapses (Hamanaka and Meinertzhagen, 2010). Also, presynaptic nc82 spots correlate with postsynaptic GluRII clusters (Wagh et al., 2006; Jordán-Álvarez et al., 2012). Throughout the text, we refer to nc82-positive spots as mature synapses. All counts were obtained from muscle fibre 6/7 of the abdominal segment 3, along with the electrophysiological recordings. One NMJ was studied per female larva and 8–12 larvae were examined per genotype, collected from different crosses and vials to prevent rearing artifacts. Synapse counts were obtained from multiple vials and crosses spanning over 2 years. Recordings were obtained from larvae collected from different vials (3–5) of each cross, and crosses were set at various times throughout a year. In all cases, each cross involved ~10–15 males and 20–30 females.

Fly stocks and genetics

The Gal4/UAS system was used to over- or underexpress selected gene constructs (Brand and Perrimon, 1993). RNAi transgenes for *Frq2*, *Ric8a*, *Gαs60A*, *Gαq49B*, *Gαi65A*, *Gαconcertina*, *Gβ76C* and *Gβ13F* were from the Vienna *Drosophila* RNAi center or the Bloomington collection. Lines for the overexpression of normal or constitutively active forms of *Gαs*, *P{UAS-Gαs60A.C}9* and *P{UAS-Gαs60A.Q215L}16*, respectively, were from the Bloomington stock center. As neural drivers, we used routinely *OK6-Gal4*, *D42-Gal4* and *elav-Gal4^{C155}* http://flybase.org/reports/FBst0008760.htmlhttp://flybase.org/reports/FBst0008760.html. All crosses were raised at 27℃ to maximize the Gal4 expression (Matsumoto et al., 1978). Control values from the Gal4 lines correspond to siblings from experimental crosses or to *Gal4-x/UAS-LacZ* outcrosses.

Yeast two-hybrid assays

Frq1 and *Frq2* cDNAs, cloned into pAS2-1, were used as baits. Y190 yeast colonies expressing the Gal4 DNA-binding domain fused to Frq1 or Frq2 were identified by immunoblotting with anti-Frq antibody (Gomez et al., 2001). The Gal4 activation domain was supplied as an embryo cDNA library in pGAD10 (Clontech). The subsequent transformation followed standard procedures, using a concentration of 25 mM 3-AT. A total of 1×10^6 and 3.74×10^6 library transformants were screened with the Frq1 and Frq2 baits, respectively. Validation of YTH results followed standard procedures.

GST-pulldown assays

Six copies of the c-Myc epitope were fused to the N-terminus of Frq1 cDNA and cloned into pRSET(A) (Invitrogen) vector in phase with a poly-His epitope. Similarly, a HA epitope was C-terminally fused to Frq2 by PCR and cloned into the pRSET(C) vector (Invitrogen) in phase with a poly-His epitope. Both constructs were used for standard expression in bacteria and purified under native conditions using His-GraviTrap columns (GE Healthcare). Eluted proteins were desalted in PD-10 columns (GE Healthcare). Ric8a cDNA was PCR amplified from the LD22866 clone (DBGP) and cloned in phase with GST into the pGEX-3X vector (GE Healthcare). The GST–Ric8a fusion protein was expressed in bacteria and attached to GST-Trap columns (GE Healthcare). An aliquot of the flow-through was kept for the subsequent gels as the unbound protein, serving as positive control. The previously purified Myc–Frq1, Frq1–HA or Frq2–HA were rinsed six times with washing buffer (50 mM Tris-HCl pH 7.5, 200 mM NaCl) and passed through one of the GST–Ric8a pre-charged columns. The two columns were rinsed six times with washing buffer and eluted with 200 mM glycine pH 2.5. The eluted volumes were neutralized by the addition of Tris-HCl pH 7.5 and concentrated with Amicom Ultra (10 K) filters (Millipore).

Co-immunoprecipitation and western blotting

The Myc-Ric8a and the Frq2-HA tagged cDNAs (see above) were cloned into pCDNA3.1 vector (Invitrogen). In the co-IP assays, to test the amino acid relevance in the Ric8a interaction, and due to the possible role of the C-terminus in stabilizing the interaction, a V5 epitope was tagged to the N-terminus of Frq2 and Frq1 by subcloning them into the nV5-pCDNA3.1 plasmid. Point mutations in Frq2 were performed with the Change-IT Directed Mutagenesis Kit (Affymetrix USB) following the manufacturer's instructions. The human Ric8a cDNA (a gift from Gregory G. Tall, University of Rochester Medical Center, Rochester, NY) was subcloned in nV5pCDNA3.1. The NCS-1 construct (provided by Robert D. Burgoyne; Institute of Translational Medicine, Liverpool, UK) was subcloned in pCDNA3.1. Co-transfections into HEK293 cells

Journal of Cell Science

were performed using Superfect reagent (Qiagen), and the cells were lysed 48 h thereafter. Pre-cleared lysates were incubated overnight at 4℃ with or without rabbit anti-HA, anti-V5 (Invitrogen), anti-c-Myc or anti-NCS-1 (Cell Signaling Technology) antibodies as indicated in each experiment. For negative controls, inmunoprecipitations were performed with an unrelated antibody (see figure legends). Samples were incubated with Protein-G–Sepharose (Sigma). Standard procedures for SDS-PAGE and protein transfer onto membranes were used. 10% of the lysate prior to immunoprecipitation was run as the input. The following antibodies and dilutions were used for western blotting; rabbit anti-NCS-1 (1:1000), mouse anti-V5 (1:2000), mouse anti-c-Myc (1:1000; Sigma, M4439), rabbit anti-HA (1:1000; Sigma, H6908), rabbit anti-Ric8a (1:1000; provided by Juergen A. Knoblich; Institute of Molecular Biotechnology of the Austrian Academy of Sciences, Vienna, Austria). In order to avoid heavy/light chain antibody interference, blots were incubated with mouse or rabbit TrueBlot (Rockland).

Protein expression, purification and crystallization

Details on the expression, purification and crystallization of Frq2 have been published previously (Baños-Mateos et al., 2014). To summarize, the *Frq2* cDNA was obtained by RT-PCR from whole *Drosophila* purified RNA extracts and was sequenced. A full-length cDNA was cloned into the pET-Duet plasmid (Novagen) for protein expression in *Escherichia coli*. The Ca^{2+}-loaded protein was purified in two chromatographic steps using hydrophobic and ion-exchange columns (GE Healthcare). The final sample was dialyzed against water and concentrated to 15 mg/ml for protein crystallization. Two different types of plate-like crystals were obtained in the presence of 0.1 M $CaCl_2$ using PEG4K as the precipitant. Crystal form I (CF-I) was obtained at 4℃ and belonged to the monoclinic system. Crystal form II (CF-II) was obtained at 20℃ using the detergent Triton X-114 as an additive and corresponded to the orthorhombic system. The crystal structures and structure factors were deposited in the Protein Data Bank [PDB codes: 4by5 (CF-I) and 4by4 (CF-II)].

Diffraction data collection and structure solution

X-ray diffraction data were collected at 100 K using the ESRF Grenoble Synchrotron radiation source. The diffraction data were processed using Mosflm (Leslie, 2006) and scaled with Scala (Evans, 2006). Data collection statistics are summarized in supplementary material Table S1. Crystals from CF-I and CF-II belonged to space groups $P2_1$ and $P2_12_12_1$ respectively. The structure of the human Frequenin/NCS-1 (PDB code 1g8i) was used to solve the structure of *Drosophila* Frq2 by molecular replacement with Phaser (McCoy et al., 2007). The structures were refined at 2.2 Å (CF-I) and 2.3 (CF-II) Å using NCS restraints and jelly body refinement with Refmac (Murshudov et al., 1997). The models were updated with Coot (Emsley and Cowtan, 2004). The stereochemistry of the models was checked with MolProbity (Chen et al., 2010). Analysis of the structure was done with CCP4i programs (Winn et al., 2011), and images were created with CCP4mg (McNicholas et al., 2011). The crystal structures and structure factors were deposited in the Protein Data Bank [PDB codes: 4by5 (CF-I) and 4by4 (CF-II)].

Electrophysiology

Whole-cell intracellular recordings and extracellular focal recordings were obtained from the ventral longitudinal muscle fiber 6–7 (abdominal segment 3) in HL6 saline (Macleod et al., 2002) as described previously (Romero-Pozuelo et al., 2007). Briefly, sharp glass electrodes filled with 3 M KCl (~40 MΩ) were used to impale the muscle to measure spontaneously occurring miniature excitatory junction potentials (mEJPs) and stimulus-evoked excitatory junction potentials (EJPs). Extracellular focal recordings on single type Ib boutons (identified using Nomarski optics) were made using focal electrodes with tips having an inner diameter of 5 µm. Quantal content was calculated for individual boutons by measuring the amplitude of stimulus-evoked excitatory junction currents (EJCs) and dividing it by the mean amplitude of the spontaneous miniature excitatory junction currents (mEJCs). Cut segmental nerves were stimulated at 2 Hz using a suction electrode.

Statistics

All numerical data are presented as the mean±s.e.m. Statistical significance was calculated using Student's two-tailed *t*-test (unpaired two samples for means) after application of the Kolmogorov-Smirnov method to verify the normality of data distribution. ***$P<0.001$; **$P<0.01$; *$P<0.05$.

Acknowledgements

We thank the European Synchrotron Radiation Facility (ID14-1 and ID23 beam line) and Javier Garzón and Pilar Sánchez (Cajal Institute, Madrid, Spain) for advice on G-proteins. We are also grateful to Milton P. Charlton (funded by the Canadian Institutes of Health, grant number MOP-82827) and Ernesto Sánchez for use of laboratory equipment and space.

Competing interests

The authors declare no competing interests.

Author contributions

J.R.-P., J.S.D., A.M. and M.-J.S.-B. performed experiments, evaluated results and wrote the manuscript. S.B.-M., J.L.S, A.C.-S., J.J.-G. and E.S. performed experiments. A.H.-H. designed experiments and interpreted data. H.L.A. evaluated data and edited the manuscript. A.F. conceived of the research, evaluated results and wrote the manuscript.

Funding

Research was funded by grants from the Ministerio de Economía y Competitividad, Spain [grant numbers BFU2009-12410/BMC to A.F. and BIO2011-28184-C02-02 to M.J.S-B.]; and the Canadian Institutes of Health Research [grant number MOP-37774 to H.L.A.]. M.J.S-B. was supported by a Ramón y Cajal contract [grant number RYC-2008-03449].

Supplementary material

Supplementary material available online at
http://jcs.biologists.org/lookup/suppl/doi:10.1242/jcs.152603/-/DC1

References

Afshar, K., Willard, F. S., Colombo, K., Johnston, C. A., McCudden, C. R., Siderovski, D. P. and Gönczy, P. (2004). RIC-8 is required for GPR-1/2-dependent Galpha function during asymmetric division of C. elegans embryos. *Cell* **119**, 219-230.

Ames, J. B. and Lim, S. (2012). Molecular structure and target recognition of neuronal calcium sensor proteins. *Biochim. Biophys. Acta* **1820**, 1205-1213.

Ames, J. B., Hendricks, K. B., Strahl, T., Huttner, I. G., Hamasaki, N. and Thorner, J. (2000). Structure and calcium-binding properties of Frq1, a novel calcium sensor in the yeast Saccharomyces cerevisiae. *Biochemistry* **39**, 12149-12161.

Andreeva, A. V., Kutuzov, M. A. and Voyno-Yasenetskaya, T. A. (2007). Scaffolding proteins in G-protein signaling. *J. Mol. Signal.* **2**, 13.

Augustine, G. J. and Charlton, M. P. (1986). Calcium dependence of presynaptic calcium current and post-synaptic response at the squid giant synapse. *J. Physiol.* **381**, 619-640.

Bahi, N., Friocourt, G., Carrié, A., Graham, M. E., Weiss, J. L., Chafey, P., Fauchereau, F., Burgoyne, R. D. and Chelly, J. (2003). IL1 receptor accessory protein like, a protein involved in X-linked mental retardation, interacts with Neuronal Calcium Sensor-1 and regulates exocytosis. *Hum. Mol. Genet.* **12**, 1415-1425.

Baillie, G. S. (2009). Compartmentalized signalling: spatial regulation of cAMP by the action of compartmentalized phosphodiesterases. *FEBS J.* **276**, 1790-1799.

Banos-Mateos, S., Chaves-Sanjuan, A., Mansilla, A., Ferrus, A. and Sanchez-Barrena, M. J. (2014). Frq2 from Drosophila melanogaster: cloning, expression, purification, crystallization and preliminary X-ray analysis. *Acta crystallographica. Section F, Structural biology communications* **70**, 530-534.

Boto, T., Gomez-Diaz, C. and Alcorta, E. (2010). Expression analysis of the 3 G-protein subunits, Galpha, Gbeta, and Ggamma, in the olfactory receptor organs of adult Drosophila melanogaster. *Chem. Senses* **35**, 183-193.

Bourne, Y., Dannenberg, J., Pollmann, V., Marchot, P. and Pongs, O. (2001). Immunocytochemical localization and crystal structure of human frequenin (neuronal calcium sensor 1). *J. Biol. Chem.* **276**, 11949-11955.

Brand, A. H. and Perrimon, N. (1993). Targeted gene expression as a means of altering cell fates and generating dominant phenotypes. *Development* **118**, 401-415.

Chen, V. B., Arendall, W. B., 3rd, Headd, J. J., Keedy, D. A., Immormino, R. M., Kapral, G. J., Murray, L. W., Richardson, J. S. and Richardson, D. C. (2010). MolProbity: all-atom structure validation for macromolecular crystallography. *Acta Crystallogr. D Biol. Crystallogr.* **66**, 12-21.

Connolly, J. B., Roberts, I. J., Armstrong, J. D., Kaiser, K., Forte, M., Tully, T. and O'Kane, C. J. (1996). Associative learning disrupted by impaired Gs signaling in Drosophila mushroom bodies. *Science* **274**, 2104-2107.

Dason, J. S., Romero-Pozuelo, J., Marin, L., Iyengar, B. G., Klose, M. K., Ferrús, A. and Atwood, H. L. (2009). Frequenin/NCS-1 and the Ca2+-channel alpha1-subunit co-regulate synaptic transmission and nerve-terminal growth. *J. Cell Sci.* **122**, 4109-4121.

Dason, J. S., Romero-Pozuelo, J., Atwood, H. L. and Ferrús, A. (2012). Multiple roles for frequenin/NCS-1 in synaptic function and development. *Mol. Neurobiol.* **45**, 388-402.

Davé, R. H., Saengsawang, W., Lopus, M., Davé, S., Wilson, L. and Rasenick, M. M. (2011). A molecular and structural mechanism for G protein-mediated microtubule destabilization. *J. Biol. Chem.* **286**, 4319-4328.

Emsley, P. and Cowtan, K. (2004). Coot: model-building tools for molecular graphics. *Acta Crystallogr. D Biol. Crystallogr.* **60**, 2126-2132.

Evans, P. (2006). Scaling and assessment of data quality. *Acta Crystallogr. D Biol. Crystallogr.* **62**, 72-82.

Fan, Z., Ji, X., Fu, M., Zhang, W., Zhang, D. and Xiao, Z. (2012). Electrostatic interaction between inactivation ball and T1-S1 linker region of Kv1.4 channel. *Biochim. Biophys. Acta* **1818**, 55-63.

Frank, C. A. (2014). How voltage-gated calcium channels gate forms of homeostatic synaptic plasticity. *Front. Cell. Neurosci.* **8**, 40.

Gomez, M., De Castro, E., Guarin, E., Sasakura, H., Kuhara, A., Mori, I., Bartfai, T., Bargmann, C. I. and Nef, P. (2001). Ca2+ signaling via the neuronal calcium sensor-1 regulates associative learning and memory in C. elegans. *Neuron* **30**, 241-248.

Hamanaka, Y. and Meinertzhagen, I. A. (2010). Immunocytochemical localization of synaptic proteins to photoreceptor synapses of Drosophila melanogaster. *J. Comp. Neurol.* **518**, 1133-1155.

Hampoelz, B., Hoeller, O., Bowman, S. K., Dunican, D. and Knoblich, J. A. (2005). Drosophila Ric-8 is essential for plasma-membrane localization of heterotrimeric G proteins. *Nat. Cell Biol.* **7**, 1099-1105.

Handley, M. T., Lian, L. Y., Haynes, L. P. and Burgoyne, R. D. (2010). Structural and functional deficits in a neuronal calcium sensor-1 mutant identified in a case of autistic spectrum disorder. *PLoS ONE* **5**, e10534.

Heidarsson, P. O., Bjerrum-Bohr, I. J., Jensen, G. A., Pongs, O., Finn, B. E., Poulsen, F. M. and Kragelund, B. B. (2012). The C-terminal tail of human neuronal calcium sensor 1 regulates the conformational stability of the Ca^{2+}- activated state. *J. Mol. Biol.* **417**, 51-64.

Hendricks, K. B., Wang, B. Q., Schnieders, E. A. and Thorner, J. (1999). Yeast homologue of neuronal frequenin is a regulator of phosphatidylinositol-4-OH kinase. *Nat. Cell Biol.* **1**, 234-241.

Hui, H., McHugh, D., Hannan, M., Zeng, F., Xu, S. Z., Khan, S. U., Levenson, R., Beech, D. J. and Weiss, J. L. (2006). Calcium-sensing mechanism in TRPC5 channels contributing to retardation of neurite outgrowth. *J. Physiol.* **572**, 165-172.

Jo, J., Heon, S., Kim, M. J., Son, G. H., Park, Y., Henley, J. M., Weiss, J. L., Sheng, M., Collingridge, G. L. and Cho, K. (2008). Metabotropic glutamate receptor-mediated LTD involves two interacting Ca(2+) sensors, NCS-1 and PICK1. *Neuron* **60**, 1095-1111.

Jordán-Álvarez, S., Fouquet, W., Sigrist, S. J. and Acebes, A. (2012). Presynaptic PI3K activity triggers the formation of glutamate receptors at neuromuscular terminals of Drosophila. *J. Cell Sci.* **125**, 3621-3629.

Kabbani, N., Negyessy, L., Lin, R., Goldman-Rakic, P. and Levenson, R. (2002). Interaction with neuronal calcium sensor NCS-1 mediates desensitization of the D2 dopamine receptor. *J. Neurosci.* **22**, 8476-8486.

Klattenhoff, C., Montecino, M., Soto, X., Guzmán, L., Romo, X., García, M. A., Mellstrom, B., Naranjo, J. R., Hinrichs, M. V. and Olate, J. (2003). Human brain synembryn interacts with Gsalpha and Gqalpha and is translocated to the plasma membrane in response to isoproterenol and carbachol. *J. Cell. Physiol.* **195**, 151-157.

Klose, M. K., Dason, J. S., Atwood, H. L., Boulianne, G. L. and Mercier, A. J. (2010). Peptide-induced modulation of synaptic transmission and escape response in Drosophila requires two G-protein-coupled receptors. *J. Neurosci.* **30**, 14724-14734.

Koh, P. O., Undie, A. S., Kabbani, N., Levenson, R., Goldman-Rakic, P. S. and Lidow, M. S. (2003). Up-regulation of neuronal calcium sensor-1 (NCS-1) in the prefrontal cortex of schizophrenic and bipolar patients. *Proc. Natl. Acad. Sci. USA* **100**, 313-317.

Komuro, H. and Rakic, P. (1996). Intracellular Ca2+ fluctuations modulate the rate of neuronal migration. *Neuron* **17**, 275-285.

Leslie, A. G. (2006). The integration of macromolecular diffraction data. *Acta Crystallogr. D Biol. Crystallogr.* **62**, 48-57.

Lian, L. Y., Pandalaneni, S. R., Patel, P., McCue, H. V., Haynes, L. P. and Burgoyne, R. D. (2011). Characterisation of the interaction of the C-terminus of the dopamine D2 receptor with neuronal calcium sensor-1. *PLoS ONE* **6**, e27779.

Macleod, G. T., Hegström-Wojtowicz, M., Charlton, M. P. and Atwood, H. L. (2002). Fast calcium signals in Drosophila motor neuron terminals. *J. Neurophysiol.* **88**, 2659-2663.

Marsden, B. J., Shaw, G. S. and Sykes, B. D. (1990). Calcium binding proteins. Elucidating the contributions to calcium affinity from an analysis of species variants and peptide fragments. *Biochem. Cell Biol.* **68**, 587-601.

Martin, V. M., Johnson, J. R., Haynes, L. P., Barclay, J. W. and Burgoyne, R. D. (2013). Identification of key structural elements for neuronal calcium sensor-1 function in the regulation of the temperature-dependency of locomotion in C. elegans. *Mol. Brain* **6**, 39.

Matsumoto, K., Toh-e, A. and Oshima, Y. (1978). Genetic control of galactokinase synthesis in Saccharomyces cerevisiae: evidence for constitutive expression of the positive regulatory gene gal4. *J. Bacteriol.* **134**, 446-457.

Mattera, R., Graziano, M. P., Yatani, A., Zhou, Z., Graf, R., Codina, J., Birnbaumer, L., Gilman, A. G. and Brown, A. M. (1989). Splice variants of the alpha subunit of the G protein Gs activate both adenylyl cyclase and calcium channels. *Science* **243**, 804-807.

McCoy, A. J., Grosse-Kunstleve, R. W., Adams, P. D., Winn, M. D., Storoni, L. C. and Read, R. J. (2007). Phaser crystallographic software. *J. Appl. Crystallogr.* **40**, 658-674.

McNicholas, S., Potterton, E., Wilson, K. S. and Noble, M. E. (2011). Presenting your structures: the CCP4mg molecular-graphics software. *Acta Crystallogr. D Biol. Crystallogr.* **67**, 386-394.

Meriney, S. D. and Dittrich, M. (2013). Organization and function of transmitter release sites at the neuromuscular junction. *J. Physiol.* **591**, 3159-3165.

Miller, K. G., Emerson, M. D. and Rand, J. B. (1999). Goalpha and diacylglycerol kinase negatively regulate the Gqalpha pathway in C. elegans. *Neuron* **24**, 323-333.

Miller, K. G., Emerson, M. D., McManus, J. R. and Rand, J. B. (2000). RIC-8 (Synembryn): a novel conserved protein that is required for G(q)alpha signaling in the C. elegans nervous system. *Neuron* **27**, 289-299.

Mizuno, N. and Itoh, H. (2009). Functions and regulatory mechanisms of Gq-signaling pathways. *Neurosignals* **17**, 42-54.

Murshudov, G. N., Vagin, A. A. and Dodson, E. J. (1997). Refinement of macromolecular structures by the maximum-likelihood method. *Acta Crystallogr. D Biol. Crystallogr.* **53**, 240-255.

Owald, D., Fouquet, W., Schmidt, M., Wichmann, C., Mertel, S., Depner, H., Christiansen, F., Zube, C., Quentin, C., Körner, J. et al. (2010). A Syd-1 homologue regulates pre- and postsynaptic maturation in Drosophila. *J. Cell Biol.* **188**, 565-579.

Pang, Z. P. and Südhof, T. C. (2010). Cell biology of Ca2+-triggered exocytosis. *Curr. Opin. Cell Biol.* **22**, 496-505.

Pavlowsky, A., Gianfelice, A., Pallotto, M., Zanchi, A., Vara, H., Khelfaoui, M., Valnegri, P., Rezai, X., Bassani, S., Brambilla, D. et al. (2010). A postsynaptic signaling pathway that may account for the cognitive defect due to IL1RAPL1 mutation. *Curr. Biol.* **20**, 103-115.

Pioletti, M., Findeisen, F., Hura, G. L. and Minor, D. L., Jr (2006). Three-dimensional structure of the KChIP1-Kv4.3 T1 complex reveals a cross-shaped octamer. *Nat. Struct. Mol. Biol.* **13**, 987-995.

Piton, A., Michaud, J. L., Peng, H., Aradhya, S., Gauthier, J., Mottron, L., Champagne, N., Lafrenière, R. G., Hamdan, F. F., Joober, R. et al.; S2D team (2008). Mutations in the calcium-related gene IL1RAPL1 are associated with autism. *Hum. Mol. Genet.* **17**, 3965-3974.

Pongs, O., Lindemeier, J., Zhu, X. R., Theil, T., Engelkamp, D., Krah-Jentgens, I., Lambrecht, H. G., Koch, K. W., Schwemer, J., Rivosecchi, R. et al. (1993). Frequenin—a novel calcium-binding protein that modulates synaptic efficacy in the Drosophila nervous system. *Neuron* **11**, 15-28.

Rastogi, S. and Liberles, D. A. (2005). Subfunctionalization of duplicated genes as a transition state to neofunctionalization. *BMC Evol. Biol.* **5**, 28.

Renden, R. B. and Broadie, K. (2003). Mutation and activation of Galpha s similarly alters pre- and postsynaptic mechanisms modulating neurotransmission. *J. Neurophysiol.* **89**, 2620-2638.

Romero-Pozuelo, J., Dason, J. S., Atwood, H. L. and Ferrús, A. (2007). Chronic and acute alterations in the functional levels of Frequenins 1 and 2 reveal their roles in synaptic transmission and axon terminal morphology. *Eur. J. Neurosci.* **26**, 2428-2443.

Ross, E. M. (2008). Coordinating speed and amplitude in G-protein signaling. *Curr. Biol.* **18**, R777-R783.

Roychowdhury, S. and Rasenick, M. M. (2008). Submembraneous microtubule cytoskeleton: regulation of microtubule assembly by heterotrimeric Gproteins. *FEBS J.* **275**, 4654-4663.

Saab, B. J., Georgiou, J., Nath, A., Lee, F. J., Wang, M., Michalon, A., Liu, F., Mansuy, I. M. and Roder, J. C. (2009). NCS-1 in the dentate gyrus promotes exploration, synaptic plasticity, and rapid acquisition of spatial memory. *Neuron* **63**, 643-656.

Sánchez-Gracia, A., Romero-Pozuelo, J. and Ferrús, A. (2010). Two frequenins in Drosophila: unveiling the evolutionary history of an unusual neuronal calcium sensor (NCS) duplication. *BMC Evol. Biol.* **10**, 54.

Schaad, N. C., De Castro, E., Nef, S., Hegi, S., Hinrichsen, R., Martone, M. E., Ellisman, M. H., Sikkink, R., Rusnak, F., Sygush, J. et al. (1996). Direct modulation of calmodulin targets by the neuronal calcium sensor NCS-1. *Proc. Natl. Acad. Sci. USA* **93**, 9253-9258.

Schmitz, F. (2014). Presynaptic [Ca(2+)] and GCAPs: aspects on the structure and function of photoreceptor ribbon synapses. *Front. Mol. Neurosci.* **7**, 3.

Strahl, T., Huttner, I. G., Lusin, J. D., Osawa, M., King, D., Thorner, J. and Ames, J. B. (2007). Structural insights into activation of phosphatidylinositol 4-kinase (Pik1) by yeast frequenin (Frq1). *J. Biol. Chem.* **282**, 30949-30959.

Tall, G. G., Krumins, A. M. and Gilman, A. G. (2003). Mammalian Ric-8A (synembryn) is a heterotrimeric Galpha protein guanine nucleotide exchange factor. *J. Biol. Chem.* **278**, 8356-8362.

Tõnissoo, T., Meier, R., Talts, K., Plaas, M. and Karis, A. (2003). Expression of ric-8 (synembryn) gene in the nervous system of developing and adult mouse. *Gene Expr. Patterns* **3**, 591-594.

Torres, K. C., Souza, B. R., Miranda, D. M., Sampaio, A. M., Nicolato, R., Neves, F. S., Barros, A. G., Dutra, W. O., Gollob, K. J., Correa, H. et al. (2009). Expression of neuronal calcium sensor-1 (NCS-1) is decreased in

leukocytes of schizophrenia and bipolar disorder patients. *Prog. Neuropsychopharmacol. Biol. Psychiatry* **33**, 229-234.

Tsujimoto, T., Jeromin, A., Saitoh, N., Roder, J. C. and Takahashi, T. (2002). Neuronal calcium sensor 1 and activity-dependent facilitation of P/Q-type calcium currents at presynaptic nerve terminals. *Science* **295**, 2276-2279.

Wagh, D. A., Rasse, T. M., Asan, E., Hofbauer, A., Schwenkert, I., Dürrbeck, H., Buchner, S., Dabauvalle, M. C., Schmidt, M., Qin, G. et al. (2006). Bruchpilot, a protein with homology to ELKS/CAST, is required for structural integrity and function of synaptic active zones in Drosophila. *Neuron* **49**, 833-844.

Wang, C. Y., Yang, F., He, X., Chow, A., Du, J., Russell, J. T. and Lu, B. (2001). Ca(2+) binding protein frequenin mediates GDNF-induced potentiation of Ca(2+) channels and transmitter release. *Neuron* **32**, 99-112.

Wang, H., Ng, K. H., Qian, H., Siderovski, D. P., Chia, W. and Yu, F. (2005). Ric-8 controls Drosophila neural progenitor asymmetric division by regulating heterotrimeric G proteins. *Nat. Cell Biol.* **7**, 1091-1098.

Wang, H., Yan, Y., Liu, Q., Huang, Y., Shen, Y., Chen, L., Chen, Y., Yang, Q., Hao, Q., Wang, K. et al. (2007). Structural basis for modulation of Kv4 K+ channels by auxiliary KChIP subunits. *Nat. Neurosci.* **10**, 32-39.

Weiss, J. L., Archer, D. A. and Burgoyne, R. D. (2000). Neuronal Ca2+ sensor-1/frequenin functions in an autocrine pathway regulating Ca2+ channels in bovine adrenal chromaffin cells. *J. Biol. Chem.* **275**, 40082-40087.

Willoughby, D. and Cooper, D. M. (2007). Organization and Ca2+ regulation of adenylyl cyclases in cAMP microdomains. *Physiol. Rev.* **87**, 965-1010.

Winn, M. D., Ballard, C. C., Cowtan, K. D., Dodson, E. J., Emsley, P., Evans, P. R., Keegan, R. M., Krissinel, E. B., Leslie, A. G., McCoy, A. et al. (2011). Overview of the CCP4 suite and current developments. *Acta Crystallogr. D Biol. Crystallogr.* **67**, 235-242.

Wolfgang, W. J., Clay, C., Parker, J., Delgado, R., Labarca, P., Kidokoro, Y. and Forte, M. (2004). Signaling through Gs alpha is required for the growth and function of neuromuscular synapses in Drosophila. *Dev. Biol.* **268**, 295-311.

Zheng, J. Q. (2000). Turning of nerve growth cones induced by localized increases in intracellular calcium ions. *Nature* **403**, 89-93.

7. **Chapter III**: *Orb2 as modulator of Brat and their role at the Neuromuscular Junction*

7.1. Introduction

Este capítulo está compuesto por el manuscrito:
-*Orb2 as modulator of Brat and their role at the Neuromuscular Junction.* Elena Santana and Sergio Casas-Tintó.
J Neurogenet. 2017 Dec;31(4):181-188. doi: 10.1080/01677063.2017.1393539

Elena Santana Martín participó en este estudio desarrollando el diseño experimental, planificando y realizando los experimentos, adquiriendo y procesando los datos, interpretación y análisis de los resultados, la redacción del texto y elaboración del material gráfico. Parte de la redacción y la discusión se realizó en colaboración entre los autores.

Orb2 es una proteína con características priónicas. El cambio conformacional de monómero a oligómero induce traducción a nivel local del mRNA de sus proteínas diana. El papel de Orb2 se ha estudiado principalmente en cerebro adulto, donde está implicado en aprendizaje y memoria.
En este trabajo exploramos el papel que tiene Orb2 durante el desarrollo del sistema nervioso a nivel de la terminación neuromuscular.
La reducción de la proteína Orb2 produce un descenso del número de sinapsis mientras que la sobreexpresión no induce ningún efecto visible.
Además, demostramos la relevancia del cambio conformacional de Orb2 de represor (monómero) a activador (oligómero) de la traducción de RNA mensajeros de sus proteínas diana.
El mecanismo queda ilustrado en la relación de Orb2 con Brat, ya que, en mutantes para Orb2 incapaces de oligomerizar, se reduce la cantidad de proteína Brat en células de cerebro de *Drosophila.*

Debido a la relación entre Orb2 y Brat, también se inducen experimentalmente cambios en la expresión de Brat para analizar su papel en la formación de sinapsis.

El RNA de interferencia de Brat aumenta el número de sinapsis, avalando la hipótesis de Brat como elemento anti- sinaptogénico, demostrado previamente en trabajos anteriores.

Dado que Brat es la proteína diana de Orb2 realizamos experimentos de epistasia para establecer la relación jerárquica entre ambos elementos. La combinación del RNA de interferencia de ambas proteínas produce un número de sinapsis similar al control, sugiriendo que Orb2 efectivamente regula a Brat.

Nuestros resultados muestran que cambios en los niveles de Brat y Orb2 pueden modular el número de sinapsis. Dado que estos cambios inducen un cambio en sinapsis, pero no en volumen neuronal, podemos concluir que ambas proteínas están relacionadas con diferenciación pero no proliferación ni crecimiento.

Además analizamos los niveles de transcripción de proteínas presentes en la terminación neuromuscular de larva de *Drosophila.* Nuestros resultados demuestran que efectivamente Orb2 es un regulador de la traducción, no de la transcripción. Por otro lado demostramos que la modulación de Brat, conocido regulador de la transcripción, reduce los niveles de transcripción de proteínas presentes en la sinapsis.

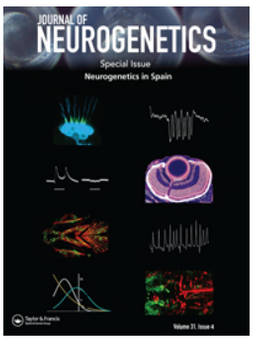

Journal of Neurogenetics

ISSN: 0167-7063 (Print) 1563-5260 (Online) Journal homepage: http://www.tandfonline.com/loi/ineg20

Orb2 as modulator of Brat and their role at the neuromuscular junction

Elena Santana & Sergio Casas-Tintó

To cite this article: Elena Santana & Sergio Casas-Tintó (2017) Orb2 as modulator of Brat and their role at the neuromuscular junction, Journal of Neurogenetics, 31:4, 181-188, DOI: 10.1080/01677063.2017.1393539

To link to this article: https://doi.org/10.1080/01677063.2017.1393539

View supplementary material

Published online: 06 Nov 2017.

Submit your article to this journal

Article views: 77

View related articles

View Crossmark data

Citing articles: 1 View citing articles

Full Terms & Conditions of access and use can be found at
http://www.tandfonline.com/action/journalInformation?journalCode=ineg20

JOURNAL OF NEUROGENETICS, 2017
VOL. 31, NO. 4, 181–188
https://doi.org/10.1080/01677063.2017.1393539

Taylor & Francis
Taylor & Francis Group

ORIGINAL RESEARCH ARTICLE

Check for updates

Orb2 as modulator of Brat and their role at the neuromuscular junction

Elena Santana and Sergio Casas-Tintó

Instituto Cajal, CSIC, Madrid, Spain

ABSTRACT

How synapses are built and dismantled is a central question in neurobiology. A wide range of proteins and processes from gene transcription to protein degradation are involved. Orb2 regulates mRNA translation depending on its monomeric or oligomeric state to modulate nervous system development and memory. Orb2 is expressed in *Drosophila* larval brain and neuromuscular junction (NMJ), Orb2 knockdown causes a reduction of synapse number and defects in neuronal morphology. Brain tumor (Brat) is an Orb2 target; it is expressed in larval brain related with cell growth and proliferation. Brat downregulation induces an increase in synapse number and abnormal growth of buttons and branches in neurons. In absence of Orb2, Brat is overexpressed suggesting that Orb2 is negatively regulating Brat mRNA translation. Orb2 or Brat control the expression of specific genes related to neuronal function. Orb2 is required for *Liprin* and *Synaptobrevin* transcription meanwhile Brat is required for *Synaptobrevin* and *Synaptotagmin* transcription. We present here evidences of a novel genetic mechanism to regulate synapse fine tuning during development and propose an equilibrium between Orb2 conformational state and nervous system formation.

Abbreviations: aPKC: atypical protein kinase C; Brat: Brain Tumor; Brp: Bruchpilot; Capt: Capulet; Nlg: Neuroligin; NMJ: Neuromuscular Junction; Syb: Synaptobrevin

ARTICLE HISTORY
Received 30 June 2017
Accepted 13 October 2017

KEYWORDS
NMJ; conformational change; synapse; gene expression; central nervous system; drosophila

Introduction

Orb2 has been postulated as a major player in the study of long-term memory. The protein belongs to the CPEB2 subfamily and is characterized for binding to specific mRNAs to regulate their translation at the presynaptic side. It has two isoforms with different physical properties, Orb2A and Orb2B. Upon synaptic stimulation Orb2A undergoes conformational changes toward an oligomeric form (active), and then Orb2A recruits Orb2B to bind and activate translation of certain mRNAs such as *Brat, aPKC, Nlg and Capt*. In the adult brain, Orb2 regulates protein translation involved in memory persistence (Keleman, Kruttner, Alenius, & Dickson, 2007; Kimura *et al.*, 2015; Majumdar *et al.*, 2012). The main Orb2 targets in the nervous system are brain tumor (Brat), Neuroligin and Branchless (Mastushita-Sakai, White-Grindley, Samuelson, Seidel, & Si, 2010). However, Orb2 is not only active in the brain, it plays a key role in asymmetric cell division, establishment of polarity axis in the developing egg and early embryo (Hafer, Xu, Bhat, & Schedl, 2011). We have analyzed the role of Orb2 in the establishment of neuronal active zones at the neuromuscular junction (NMJ) during development. NMJ is a stereotypic structure which exhibits a consistent arborization pattern through the abdominal segments (Cantera, Kozlova, Barillas-Mury, & Kafatos, 1999). Changes in the activity of specific signaling pathways such as Phosphatidylinositol-4,5-bisphosphate 3-kinase (PI3K) or Decapentaplegic (Dpp) (Aberle *et al.*, 2002; Fulga & Van Vactor, 2008; Mozer & Sandstrom, 2012) lead to alterations in morphology, number of branches or buttons and changes in the number of active zones (Marques *et al.*, 2002). Our aim is to decipher the role of Orb2 in NMJ and evaluate the consequences of Orb2 misexpression in synaptogenesis.

In addition, we have studied *Brat* regulation by Orb2 and the effect on cell growth. Brat is a negative regulator of mRNA synthesis expressed during larval brain development. Loss of Brat in neuroblasts leads to cell growth and volume increase (Bello, Reichert, & Hirth, 2006). *Brat* mutants exhibit supernumerary satellite buttons in NMJs together with an increase in volume and number of larval brain cells (Shi *et al.*, 2013). Orb2 binds to specific mRNAs to regulate its translation in activated synapses (Mastushita-Sakai *et al.*, 2010). Given Brat and Orb2 localization and function, we investigate Orb2 and Brat input to NMJ formation.

We assessed the expression of three genes which are essential for nervous system development: *Synaptobrevin* (*Syb*) and *Bruchpilot* (*Brp*). These proteins are involved in NMJs development and function, neurotransmitter release and vesicle trafficking. Brp is a cytoskeletal protein critical for structural integrity of dense bodies (T-bars) at pre-synaptic zones (Fouquet *et al.*, 2009; Wagh *et al.*, 2006). Syb is involved in neurotransmitter secretion (T. E. Lloyd *et al.*, 2000) and synaptic vesicle docking (V. Lloyd, 2000). In this

CONTACT Sergio Casas Tintó scasas@cajal.csic.es Instituto Cajal, CSIC, Avda. Doctor Arce, 37., Madrid 28002, Spain
Supplemental data for this article can be accessed here.
© 2017 Informa UK Limited, trading as Taylor & Francis Group

study we analyze the interaction between Orb2 and its target mRNA Brat, and we establish how this interaction can regulate NMJ development and integrity through the regulation of synaptic proteins.

Materials and methods

Drosophila strains

D42-Gal4 (w; Pw[+mW.hs]=GawBD42)* (Sanyal, 2009) Orb2 GFP and Orb2$^{\Delta AGFP}$ developed and kindly gifted from Keleman Lab (Kruttner *et al.*, 2012). UAS-Brat (y^{1} w*; P[Mae-UAS.6.11]brat^{LA00213}) was from Bloomington Stock Center (NIH P40OD018537) (http://flystocks.bio.indiana.edu/). UAS-Orb2^{RNAi} (KK 101114) and UAS-Brat^{RNAi} (KK 113206) were provided by VDRC (http://stockcenter.vdrc.at/control/main).

Drosophila dissection and immunostaining

The total number of mature active zones per NMJ was quantified in NMJs of third instar larvae. All genetic manipulations are driven to selected motor neurons by using the binary Gal4/UAS system (Brand & Perrimon, 1993) using the motoneuron *D42-Gal4* driver. Active zones were visualized using a mouse monoclonal antibody nc82 (1:20, DSHB, IA) which identifies the protein Bruchpilot. Neuronal membranes were labeled with rabbit anti-HRP (1:300, Jackson ImmunoResearch, West Grove, PA). Fluorescent secondary antibodies were Alexa 488 (goat anti-mouse, 1:500, Molecular Probes, Eugene, OR) and Alexa 568 (goat anti-rabbit, 1:500, Molecular Probes). Larvae were mounted in Vectashield (Vector Labs, Burlingame, CA).

To localize Orb2 or Brat proteins, third instar larval brain or NMJ were dissected. Orb2 protein was visualized using an anti-GFP (mouse,1:200 Invitrogen, Carlsbad, CA) or orb4H8-s (mouse, undiluted, Hybridoma Bank) and Brat was visualized using Brat antibodies (1:200) kindly gifted from Knoblich Lab and Sonenberg Lab (Montreal, Canada).

Image acquisition

Synapse quantifications were obtained from the NMJ in muscle fiber 6/7 of the third abdominal segment. Confocal Images were acquired with a Leica Confocal Microscope TCS SP5 II (Mannheim, Germany). Serial optical sections at 1024×256 were obtained every 1 µm with a 63× objective. IMARIS software (Bitplane, Belfast, UK) was used to determine the number of synapses with the 'spot counter' module.

For larval brain sections, images were acquired at 1024×1024 resolution and images were taken every 2 µm with a 20× objective. For cell area measurement and GFP pixel intensity sections of larva brain ventral nerve cord were taken at 1024×1024 resolution every 1 µm with an 63× objective and 3.5× zoom. Measurements were done by using the measurement log tool from Adobe Photoshop CS5.1.

Statistics

Data are shown as mean ± SD. Statistical significance was calculated using a Student's two-tailed *t*-test with mean, SD and N for synapse number counting $^{*}p < .05$.

RNA extraction and RT-qPCR

Total RNA was extracted from 10 wandering larvae of the selected genotypes. RNA was extracted with Trizol and phenol chloroform. Total RNA concentration was measured by using NanoDrop ND-1000. cDNA was synthetized from 1 µg of total RNA using M-MLV RT (Invitrogen). cDNA samples from 1:5 dilutions were used for real-time PCR reactions. Transcription levels were determined in a 14 µL volume in triplicate using SYBR Green (Applied Biosystem, Foster City, CA) and 7500qPCR (Thermo Fisher, Waltham, MA). We analyzed transcription levels of *Synaptobrevin* and *Brp* and *Rp49* as housekeeping gene reference.

Data analyses

After completing each real-time PCR run, outlier data were analyzed using 7500 software (Applied Biosystems). Ct values of triplicates from at least two independent qPCR experiments were analyzed calculating $2^{-\Delta\Delta Ct}$ and comparing the results using a *t*-test with GraphPad (GraphPad Software, La Jolla, CA).

Results

Orb2 localizes in NMJ

Orb2 is broadly expressed in *Drosophila* adult brain, including the mushroom bodies, structures implicated in memory formation (Keleman *et al.*, 2007). However, its expression during NMJ development has not been described yet. To visualize Orb2 protein and determine its expression and localization we used a green fluorescent tagged form of Orb2 (Orb2GFP) (see materials and methods).

Brp is present in synaptic boutons at the NMJ visualized with nc82 antibody (1 A-A'). Orb2 was visualized at the NMJ, in particular surrounding active zones (Brp) (Figure 1(B-B')).

Orb2 and Brat localizes in CNS

In larval brains, Orb2 is also widely expressed in the nervous system, including the ventral nerve cord (Figure 1(C)). We took advantage of the binary expression system UAS/Gal4 (Brand & Perrimon, 1993) and used a specific line (*D42-Gal4*) which express the transcription factor Gal4 in ventral nerve cord motor neurons (reported by *UAS-CD8 GFP*, Figure 1(D)) (Sanyal, 2009). Our experiments show Orb2 protein localization in D42 positive cells (1(C',D')) confirming the relationship between Orb2 and motor neurons.

Brat is critical for neuron proliferation control during brain development (Bello *et al.*, 2006). In third instar larva brain Brat is present in ventral nerve and optic lobes (1(E)).

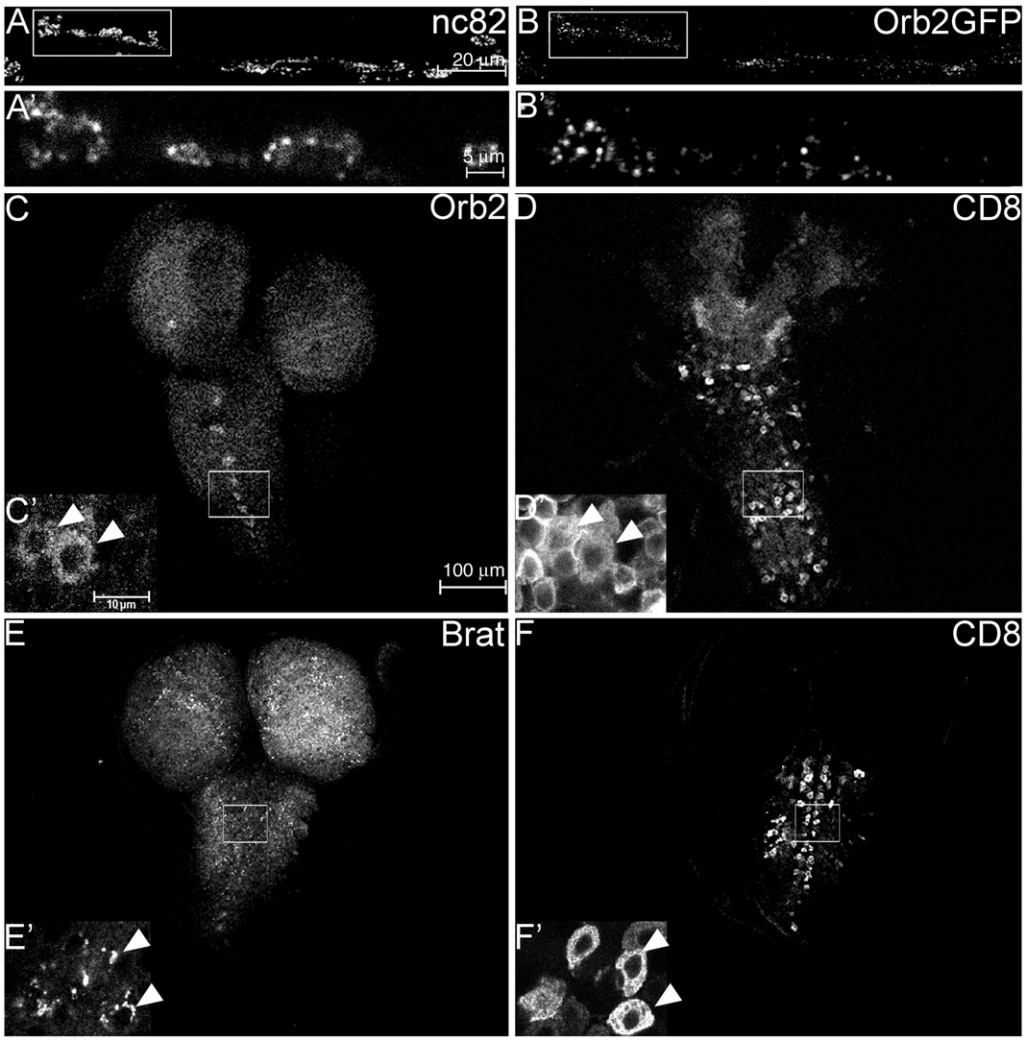

Figure 1. Orb2 localizes in the NMJ and brain. (A,B) Confocal image of larval NMJ. (A) Active zones marked with nc82 antibody (labeling Bruchpilot). (B) Orb2 GFP detected with anti-GFP (scale bar: 20 µm). (A′) Magnification of synaptic boutons showing Brp. (B′) Magnification of NMJ reveals that Orb2 is localized beneath active zones (scale 5 µm). (C) Confocal image of larval brain expressing CD8GFP under D42 promoter stained with anti-Orb2. (C′) Magnification of ventral ganglia cells expressing Orb2. (D) Confocal image of larva brain D42 > CD8GFP showing GFP expression. (D′) Magnification of D42 > CD8GFP cells from the ventral ganglia. (E) Larva brain D42 > CD8GFP stained with anti-Brat. (E′) Magnification of ventral ganglia cells. (F) D42 > CD8GFP labeling positive D42 cells (scale bar 100 µm. (F′) Magnification of ventral ganglia D42 cells (scale bar: 10 µm).

Furthermore we observe D42 cells of ventral cord (1(F)) express Brat protein (1(E',F')).

Orb2 is required for NMJ formation

Orb2 is locally expressed in mature synapses and it undergoes conformational change upon serotonin or octopamine stimuli in adult brain (Majumdar *et al.*, 2012).

To increase or attenuate Orb2 gene expression in motor neurons we used *UAS-Orb2* (upregulation) or *UAS-Orb2 RNAi* (knockdown) under the control of D42 promoter.

We quantified the number of active zones (nc82 + foci) in control (*UAS-LacZ*) and experimental NMJs (see material and methods). To avoid experimental variability due to rearing conditions, each assay is compared to its own internal control.

There was no significant effect on synapse number, morphology or shape in NMJs overexpressing *Orb2* (Figure 2(A–C)). However, *Orb2* knockdown yielded a significant decrease in synapse number in NMJ (Figure 2(D–F)). To discard that synapse number reduction was due to a general effect on neuronal size, we quantified the volume of the NMJs. The results indicate that the volume of the NMJs is not affected upon up or downregulation of *Orb2* (Supplementary Figure 1(A–C)).

These data suggest that Orb2 is necessary but not sufficient for synaptogenesis and motor neuron morphology during NMJ development.

Orb2 regulates brat expression

Orb2 is a translational regulator (Mastushita-Sakai *et al.*, 2010) and its protein includes RNA recognition domains, as other members of CPEB family, which allows binding to specific mRNAs (Hake, Mendez, & Richter, 1998) and control translation. It has been described that Orb2 binds to mRNA related with neuronal growth and synapse formation, among others (Mastushita-Sakai *et al.*, 2010). This binding and consequent activation of mRNA translation depends on Orb2conformational state. Oligomeric forms act as an activators and monomers as a repressors (Khan *et al.*, 2015).

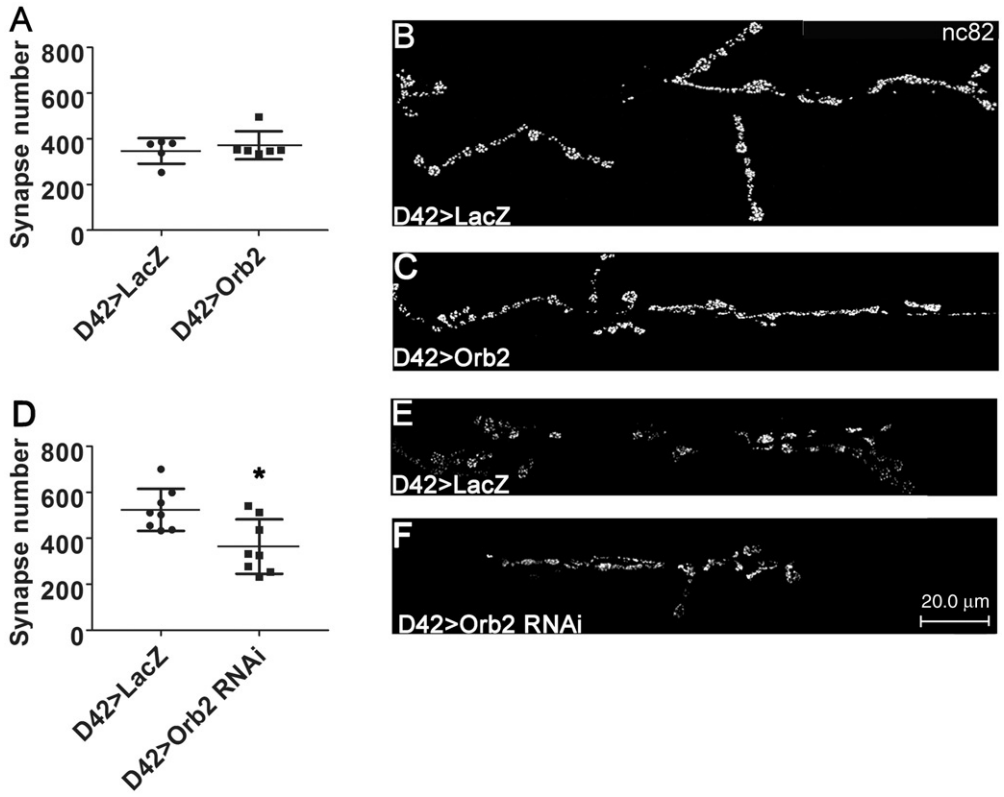

Figure 2. Orb2 is necessary to determine synapse number and NMJ morphology. (A) Synapse number quantification in NMJs after *Orb2* upregulation. (B,C) Confocal images of NMJ after *Orb2* downregulation and respective control (*UAS-LacZ*). (D) Synapse number quantification in NMJs after *Orb2* downregulation. (E,F) Confocal images of NMJ after *Orb2* downregulation and respective control (*UAS-LacZ*). Active zones are marked with nc82 antibody (scale bar: 20 µm) *T*-test ($^*p < .005$) ($n = 8$).

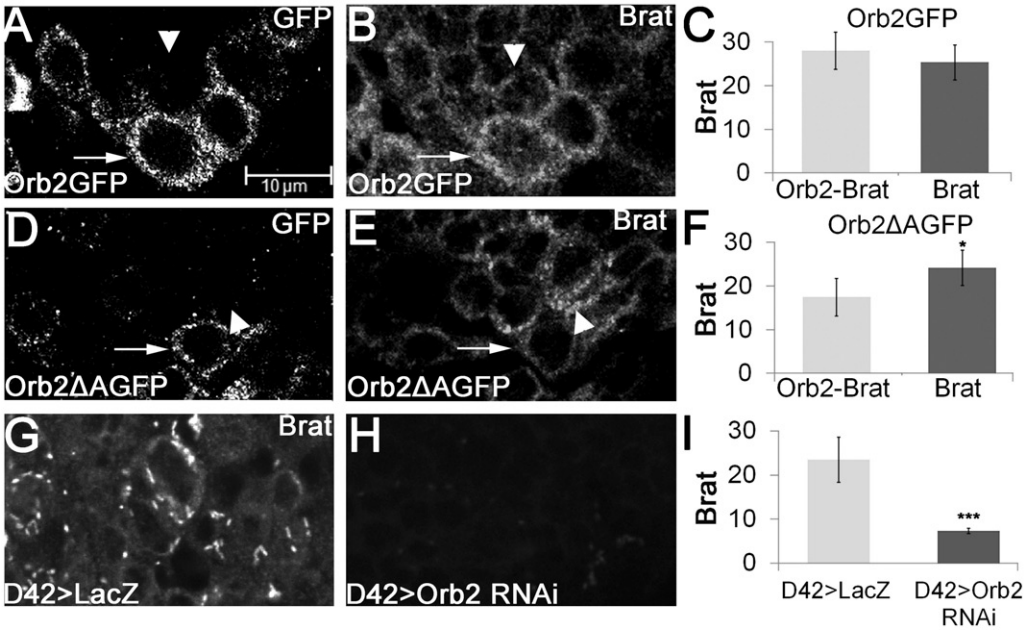

Figure 3. Orb2 represses expression of *Brain Tumor*. (A) 63x magnification confocal image of Orb2GFP cells of ventral ganglion stained with anti-GFP.(B) Orb2GFP cells stained with anti-Brat. (C) Quantification of fluorescence intensity in cells Orb2GFP ($n = 10$, n.s). (D) $Orb2^{\Delta AGFP}$ cells stained with anti-GFP. (E) $Orb2^{\Delta AGFP}$ of ventral ganglion stained with anti-Brat. Arrows show cells expressing Orb2 and Brat. Arrowheads mark cells only expressing Brat. (F) Quantification of fluorescence intensity in cells $Orb2^{\Delta AGFP}$ ($n = 10$, $p < .005$). Control cells expressing LacZ (G), and Orb2 RNAi (H) stained with anti-Brat. (scale bar: 10 µm (I) Quantification of fluorescence intensity in cells of the ventral nerve cord expressing *Lacz or Orb2 RNAi* ($n = 10$, $p < .001$).

To determine if Orb2 regulates *Brat* translation, we performed larval brains immunostaining in Orb2 GFP background and $Orb2^{\Delta AGFP}$, which eliminates A isoform blocking oligomerization process. Brat accumulates in the cytoplasm of cells in the optic lobes and ventral nerve cord of larval brains similar to Orb2 (Supplementary Figure). Neurons expressing Orb2GFP and Brat (3(A–C)) show similar levels of Brat protein (arrows) than cells expressing only

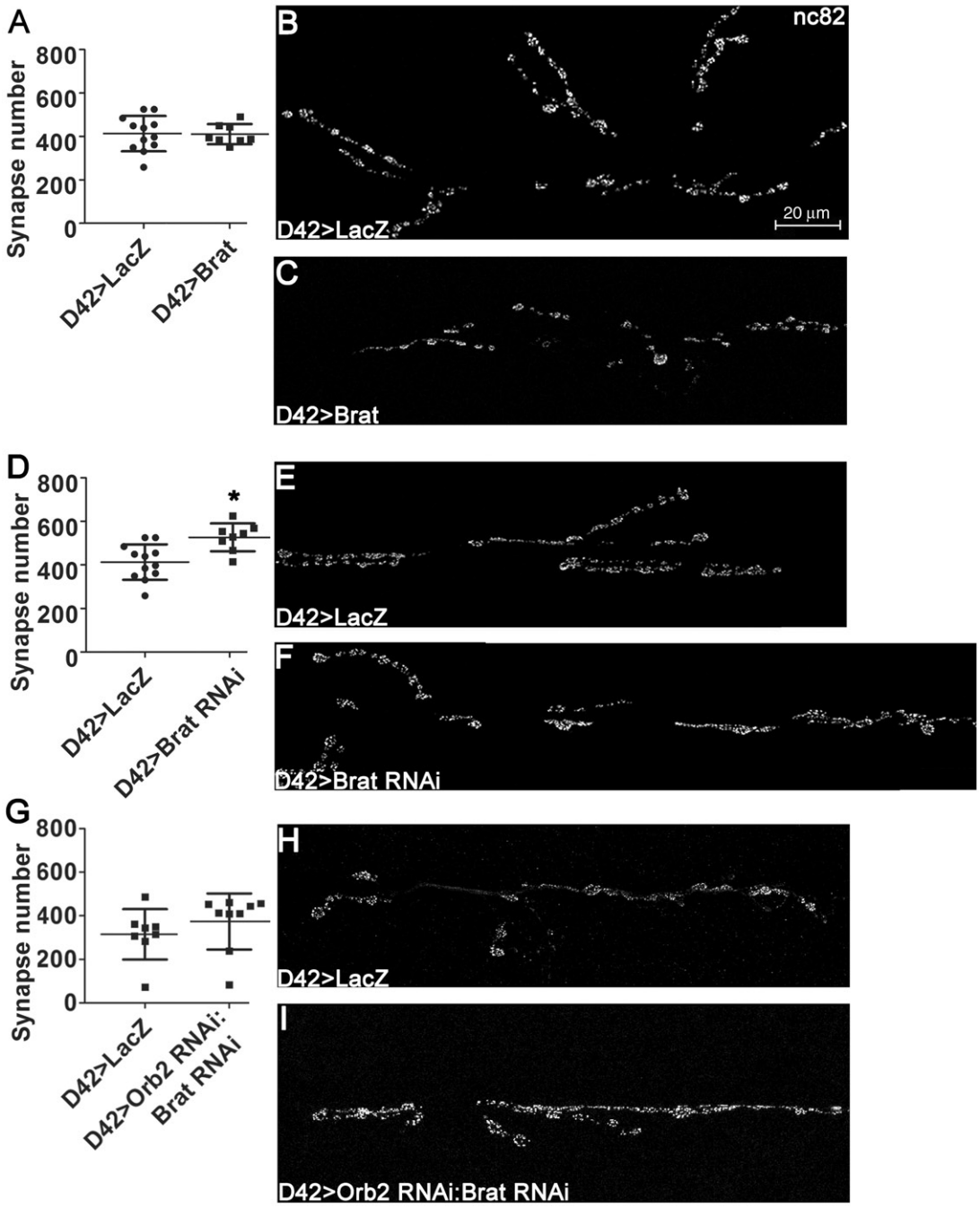

Figure 4. Brat is necessary to determine synapse number and morphology. (A) Synapse number quantification in NMJs after *Brat* upregulation (n.s). (B,C) Confocal images of NMJ after *Brat* upregulation and respective control (*UAS-LacZ*). (D) Synapse number quantification in NMJs after *Brat* downregulation ($p < .005$). Confocal images of NMJ after *Brat* downregulation and respective control (*UAS-LacZ*) (E–F). (G) Synapse number quantification after *Orb2 and Brat* downregulation (n.s). (H,I) Confocal images of NMJ after *Orb2 and Brat* downregulation and respective control. Active zones are marked with nc82 antibody (Bruchpilot) (scale 20 µm) ($n = 8$).

Brat (arrow heads). Cells expressing Orb2 lacking A isoform ($Orb2^{\Delta AGFP}$) (3(D–F)) shows a significant reduction in Brat protein in $Orb2^{\Delta AGFP}$ cells (arrows) and cells expressing only Brat (arrow heads). Orb2 downregulation in neurons (3(G–I)) reveal a significant decrease in Brat protein. These results suggest that Orb2 conformational state modulate total Brat protein synthesis (Figure 3).

Brat is required for NMJ formation and proliferation

Brat is a translational repressor involved in cell proliferation during development. Given that Orb2 represses *Brat* synthesis we explored whether or not Brat is necessary for the correct formation of active zones. As previously described *Brat* was up or down regulated specifically in motor neurons.

First we evaluated the effect of *Brat* overexpression in NMJs. We could not detect significant changes in the number of active zones (Figure 4(A–C)) nor in total volume (Supplementary Figure 1(E–G)).

Nevertheless, *Brat* knockdown in presynaptic neurons induced a significant increase in the number of active zones (Figure 4(D–F)) despite the volume of the NMJ is comparable to control (Supplementary Figure 1(E)). We observed

changes in NMJ morphology characterized by satellite boutons instead of the 'beads on a chain' wild-type pattern (Supplementary Figure 1(F)), in concordance with previous studies (Shi *et al.*, 2013). These results suggest that Brat is critical for the development and proper arborization of the NMJ in third instar larvae. However, higher levels of Brat are not sufficient to reduce synapse number. To evaluate the contribution of Orb2 and Brat together, we combined *Orb2 RNAi* and *Brat RNAi* under D42 promoter. The results show no significant differences in synapse number when compared to control NMJ. This result suggests that Brat absence counteracts *Orb2 RNAi* anti-synaptogenic effect. Furthermore, NMJ expressing both *Orb2 RNAi* and *Brat RNAi* showed similar morphology and volume compared with controls (Supplementary Figure 1(H–J)).

Brat and Orb2 induce transcriptional changes of synaptic genes

Synapse formation is triggered by interactions between specific molecules on the pre-and postsynaptic cells (Biederer & Stagi, 2008; Jordan-Alvarez, Santana, Casas-Tinto, Acebes, & Ferrus, 2017). In this context Brp and Syb are central players involved in the correct development and function of the NMJ. Syb is involved in neurotransmitter secretion, vesicle docking and synaptic transmission at NMJ (Littleton, 2000; Poskanzer, Marek, Sweeney, & Davis, 2003).

Brat and *Orb2* downregulation affects NMJ arborization and active zones establishment, we studied if the transcription levels of synaptic genes such as *Brp* or *Syb* were altered. In order to do that, we analyzed their mRNA expression by real-time qPCR. To explore NMJ vesicle trafficking state and neurotransmitter release after *Orb2 RNAi* and *Brat* RNAi expression, we analyzed *Syb* and *Brp* mRNA levels. Real-time qPCR results revealed no significant changes.

Due to we observed significant changes in synapse number associated to Brp protein in NMJ down-regulating *Orb2* or *Brat* we studied transcription levels by qPCR (Figure 5).

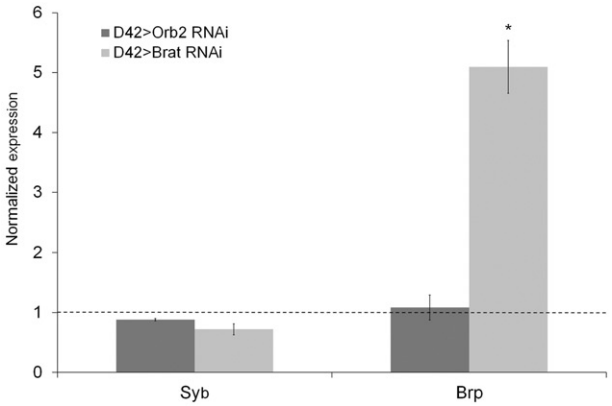

Figure 5. Expression of synaptic genes upon *Brat* or *Orb2* knockdown. Real-time PCR normalized data. *Brp and Syb* transcription levels from *D42 > LacZ, D42 > Orb2 RNAi* and *D42 > Brat RNAi* larval extracts. Data normalized to control samples expressing *LacZ*. *T*-test $p < .0005$ ($n = 3$).

The results showed that elimination of Orb2 does not affect *Brp* transcription. Brat down-regulation induces an increase *Brp* transcription levels which support the changes observed in number of active zones of NMJ (Figure 2).

In conclusion, Orb2 and Brat are affecting to the proper development of active zones, Orb2 modulates Brat translation while Brat regulates *Brp* transcription.

Discussion

How synapses are built and the genetic relationship between partners involved in synapse formation is poorly understood. Our data propose a molecular mechanism where Brat and Orb2 genetically interact and modulate the expression of synaptic proteins for the correct development of the NMJ. Orb2 is a regulator of translation of specific mRNAs after synaptic stimulation. Its role in the adult brain as a key player controlling learning and memory has been widely studied (Hervas *et al.*, 2016; Kruttner *et al.*, 2012; Kruttner *et al.*, 2015). However, little is known about Orb2 role during nervous system development. We have explored the role of Orb2 in NMJ and brain development through the regulation of *Brat*. We demonstrate that Orb2 plays a central role during NMJ development. Although Orb2 downregulation reduces synapse number, Orb2 upregulation is not sufficient to generate new active zones. Orb2 protein can adopt different conformational states (Majumdar *et al.*, 2012). Upon synaptic stimulation Orb2 changes its conformational state and interacts with target mRNAs. It is possible that synapse stimulation and Orb2 conformational changes are necessary to induce synaptogenesis. Therefore, *Orb2* upregulation would require additional events to yield synaptic changes.

Orb2 directly activates translation of other synaptic proteins as neuroligin, branchless or synaptobrevin (Mastushita-Sakai *et al.*, 2010). These data are compatible with real-time qPCR results that show no significant changes in *Syb* or *Brp* transcription after Orb2 reduction. Moreover, we observe a reduction in the number of synaptic spots labeled with Brp. Our hypothesis suggests that Orb2 is activating or repressing mRNA translation of a set of synaptic proteins involved in synaptic formation and stabilization. Orb2 down-regulation might be affecting some of these proteins and as a consequence induces a reduction in the NMJ active zones represented by a decrease in Brp spots. Further experiments and deeper analysis of mRNA partners of Orb2 and its relation with Brp might be done to elucidate this question.

Besides, Orb2 interacts with *Brat mRNA* (Mastushita-Sakai *et al.*, 2010). Orb2 can activate or repress translation depending on the conformational state (Khan *et al.*, 2015). We have provided evidences that Orb2 repress Brat translation, possibly through its monomeric form (Khan *et al.*, 2015).

In conclusion, we have shown that *Brat* downregulation increases the number of active zones. However, *Brat* upregulation does not affect synapse number. Given that Brat (as Orb2) is a repressor of translation in combination with other factors, Nanos and Pumilio (Menon, Andrews, Murthy, Gavis, & Zinn, 2009), it is plausible that Brat alone may not

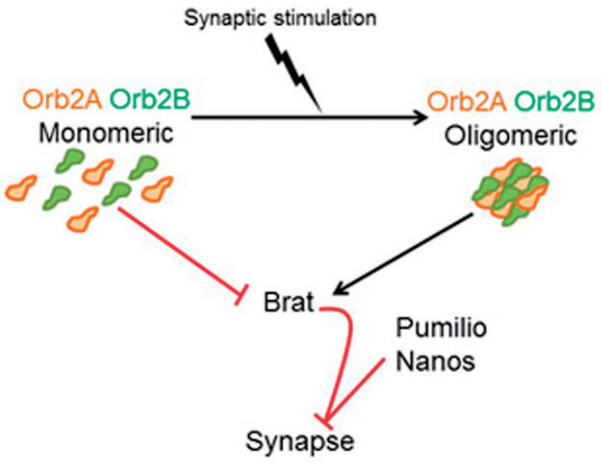

Figure 6. Schematic representation of Orb2 and Brat role in NMJs. Cartoon representing (1) Orb2 conformational change upon synaptic stimulation, (2) the postulated signaling cascade regulated by Orb2 conformers and (3) the proposed contribution for synapse formation.

suffice to have a significant effect on synaptic genes (Figure 6). Volume is not affected by Brat or Orb2 modifications, suggesting at least two different signaling pathways, one related with growth and other with synapse formation and stabilization. This hypothesis correlates with qPCR results where we alter transcription levels of genes related with active zones formation (*Brp*) but not with genes related with vesicle trafficking (*Syb*).

These evidences suggest that the increase in synapse number is not sufficient to properly build an NMJ. Moreover, *Brat* or *Orb2* regulation is not enough to induce an effect in NMJ formation. Proteins related with synaptic transmission, trafficking and other factors are involved and NMJs showing an increase in synapse number, branches and boutons can show otherwise defects in synapse transmission and vesicle trafficking (Shi *et al.*, 2013).

We propose that both proteins regulate a set of transcription factors which, in turn, modulate the expression of other genes. In conclusion, the architecture of an NMJ includes a collection of interrelated players which are in equilibrium to maintain motor neuron integrity.

Acknowledgments

We thank anonymous reviewers for critiquing the manuscript. We are grateful to J. Knoblich and N. Sonenberg for kindly sending me Brat antibody. Thanks to K. Keleman lab to providing us the Orb2GFP and Orb2$^{\Delta AGFP}$. We also want to thank the Vienna Drosophila Resource Centre, the Bloomington Drosophila stock Centre and the Developmental Studies Hybridoma Bank for supplying fly stocks and antibodies, and FlyBase for its wealth of information. ES was supported by a FPI grant from the Spanish Ministerio de Economía y competitividad. SC-T holds a Ramon y Cajal contract RyC 2012–11410. Research has been funded by grant BFU2015–65685P from the Spanish Ministry of Economy and Consejo Superior de Investigaciones CientÃficas.

Disclosure statement

No potential conflict of interest was reported by the authors.

Funding

ES was supported by a FPI grant [grant no. BES-2013-062725] from the Spanish Ministerio de Economía y competitividad. SC-T holds a Ramon y Cajal contract RyC 2012–11410. Research has been funded by grant [grant no. BFU2015–65685P] from the Spanish Ministry of Economy and Consejo Superior de Investigaciones CientÃficas.

ORCID

Elena Santana http://orcid.org/0000-0002-2444-9908
Sergio Casas-Tintó http://orcid.org/0000-0002-9589-9981

References

Aberle, H., Haghighi, A.P., Fetter, R.D., McCabe, B.D., Magalhaes, T.R., & Goodman, C.S. (2002). Wishful thinking encodes a BMP type II receptor that regulates synaptic growth in Drosophila. *Neuron*, *33*, 545–558. doi:10.1016/S0896-6273(02)00589-5

Bello, B., Reichert, H., & Hirth, F. (2006). The brain tumor gene negatively regulates neural progenitor cell proliferation in the larval central brain of Drosophila. *Development*, *133*, 2639–2648. doi:10.1242/dev.02429

Biederer, T., & Stagi, M. (2008). Signaling by synaptogenic molecules. *Current Opinion in Neurobiology*, *18*, 261–269. doi:10.1016/j.conb.2008.07.014

Brand, A.H., & Perrimon, N. (1993). Targeted gene expression as a means of altering cell fates and generating dominant phenotypes. *Development*, *118*, 401–415.

Cantera, R., Kozlova, T., Barillas-Mury, C., & Kafatos, F.C. (1999). Muscle structure and innervation are affected by loss of Dorsal in the fruit fly, Drosophila melanogaster. *Molecular and Cellular Neuroscience*, *13*, 131–141. doi:10.1006/mcne.1999.0739

Fouquet, W., Owald, D., Wichmann, C., Mertel, S., Depner, H., Dyba, M., … Sigrist, S.J. (2009). Maturation of active zone assembly by Drosophila Bruchpilot. *Journal of Cell Biology*, *186*, 129–145. doi:10.1083/jcb.200812150

Fulga, T.A., & Van Vactor, D. (2008). Synapses and growth cones on two sides of a highwire. *Neuron*, *57*, 339–344. doi:10.1016/j.neuron.2008.01.016

Hafer, N., Xu, S., Bhat, K.M., & Schedl, P. (2011). The Drosophila CPEB protein Orb2 has a novel expression pattern and is important for asymmetric cell division and nervous system function. *Genetics*, *189*, 907–921. doi:10.1534/genetics.110.123646

Hake, L.E., Mendez, R., & Richter, J.D. (1998). Specificity of RNA binding by CPEB: requirement for RNA recognition motifs and a novel zinc finger. *Molecular and Cell Biology*, *18*, 685–693. doi:10.1128/MCB.18.2.685

Hervas, R., Li, L., Majumdar, A., Fernandez-Ramirez Mdel, C., Unruh, J.R., Slaughter, B.D., … Carrion-Vazquez, M. (2016). Molecular basis of Orb2 amyloidogenesis and blockade of memory consolidation. *PLOS Biology*, *14*, e1002361. doi:10.1371/journal.pbio.1002361

Jordan-Alvarez, S., Santana, E., Casas-Tinto, S., Acebes, A., & Ferrus, A. (2017). The equilibrium between antagonistic signaling pathways determines the number of synapses in Drosophila. *PLoS One*, *12*, e0184238. doi:10.1371/journal.pone.0184238

Keleman, K., Kruttner, S., Alenius, M., & Dickson, B.J. (2007). Function of the Drosophila CPEB protein Orb2 in long-term courtship memory. *Nature Neuroscience*, *10*, 1587–1593. doi:10.1038/nn1996

Khan, M.R., Li, L., Perez-Sanchez, C., Saraf, A., Florens, L., Slaughter, B.D., … Si, K. (2015). Amyloidogenic oligomerization transforms Drosophila Orb2 from a translation repressor to an activator. *Cell*, *163*, 1468–1483. doi:10.1016/j.cell.2015.11.020

Kimura, S., Sakakibara, Y., Sato, K., Ote, M., Ito, H., Koganezawa, M., & Yamamoto, D. (2015). The Drosophila lingerer protein cooperates with Orb2 in long-term memory formation. *Journal of Neurogenetics*, *29*, 8–17. doi:10.3109/01677063.2014.917644

Kruttner, S., Stepien, B., Noordermeer, J.N., Mommaas, M.A., Mechtler, K., Dickson, B.J., & Keleman, K. (2012). Drosophila CPEB Orb2A mediates memory independent of Its RNA-binding domain. *Neuron*, *76*, 383–395. doi:10.1016/j.neuron.2012.08.028

Kruttner, S., Traunmuller, L., Dag, U., Jandrasits, K., Stepien, B., Iyer, N., … Keleman, K. (2015). Synaptic Orb2A bridges memory acquisition and late memory consolidation in Drosophila. *Cell Reports*, *11*, 1953–1965. doi:10.1016/j.celrep.2015.05.037

Littleton, J.T. (2000). A genomic analysis of membrane trafficking and neurotransmitter release in Drosophila. *Journal of Cell Biology*, *150*, F77–F82. doi:10.1083/jcb.150.2.F77

Lloyd, T.E., Verstreken, P., Ostrin, E.J., Phillippi, A., Lichtarge, O., & Bellen, H.J. (2000). A genome-wide search for synaptic vesicle cycle proteins in Drosophila. *Neuron*, *26*, 45–50. doi:10.1016/S0896-6273(00)81136-8

Lloyd, V. (2000). Parental imprinting in Drosophila. *Genetica*, *109*, 35–44. doi:10.1023/A:1026592318341

Majumdar, A., Cesario, W.C., White-Grindley, E., Jiang, H., Ren, F., Khan, M.R., … Si, K. (2012). Critical role of amyloid-like oligomers of Drosophila Orb2 in the persistence of memory. *Cell*, *148*, 515–529. doi:10.1016/j.cell.2012.01.004

Marques, G., Bao, H., Haerry, T.E., Shimell, M.J., Duchek, P., Zhang, B., & O'connor, M.B. (2002). The Drosophila BMP type II receptor wishful thinking regulates neuromuscular synapse morphology and function. *Neuron*, *33*, 529–543. doi:10.1016/S0896-6273(02)00595-0

Mastushita-Sakai, T., White-Grindley, E., Samuelson, J., Seidel, C., & Si, K. (2010). Drosophila Orb2 targets genes involved in neuronal growth, synapse formation, and protein turnover. *Proceedings of the National Academy of Sciences of the United States of America*, *107*, 11987–11992. doi:10.1073/pnas.1004433107

Menon, K.P., Andrews, S., Murthy, M., Gavis, E.R., & Zinn, K. (2009). The translational repressors Nanos and Pumilio have divergent effects on presynaptic terminal growth and postsynaptic glutamate receptor subunit composition. *Journal of Neuroscience*, *29*, 5558–5572. doi:10.1523/JNEUROSCI.0520-09.2009

Mozer, B.A., & Sandstrom, D.J. (2012). Drosophila neuroligin 1 regulates synaptic growth and function in response to activity and phosphoinositide-3-kinase. *Molecular and Cellular Neuroscience*, *51*, 89–100. doi:10.1016/j.mcn.2012.08.010

Poskanzer, K.E., Marek, K.W., Sweeney, S.T., & Davis, G.W. (2003). Synaptotagmin I is necessary for compensatory synaptic vesicle endocytosis in vivo. *Nature*, *426*, 559–563. doi:10.1038/nature02184

Sanyal, S. (2009). Genomic mapping and expression patterns of C380, OK6 and D42 enhancer trap lines in the larval nervous system of Drosophila. *Gene Expression Patterns*, *9*, 371–380. doi:10.1016/j.gep.2009.01.002

Shi, W., Chen, Y., Gan, G., Wang, D., Ren, J., Wang, Q., … Zhang, Y.Q. (2013). Brain tumor regulates neuromuscular synapse growth and endocytosis in Drosophila by suppressing mad expression. *Journal of Neuroscience*, *33*, 12352–12363. doi:10.1523/JNEUROSCI.0386-13.2013

Wagh, D.A., Rasse, T.M., Asan, E., Hofbauer, A., Schwenkert, I., Durrbeck, H., … Buchner, E. (2006). Bruchpilot, a protein with homology to ELKS/CAST, is required for structural integrity and function of synaptic active zones in Drosophila. *Neuron*, *49*, 833–844. doi:10.1016/j.neuron.2006.02.008

8. Discussion

In this work we underlie the relevance of a precise signaling equilibrium between molecules and mechanisms for building functional neuromuscular junctions. The three independent studies that compose this PhD project have in common their final read-out, the number of synapses. First, we induced gain or loss of function conditions for specific genes which are functionally related with PI3K in various signaling contexts. Second, we studied how Ric8/Frq binding changes synapse number and neurotransmitter release probability in response to Ca^{+2} surges. Finally, we studied whether the conformational state of Orb2 regulates, directly or indirectly, NMJ formation or stabilization. Under all these conditions, we observed changes in the NMJ that depict a scenario of dynamic signaling equilibrium to determine synapse number according to functional status of the cell.

Ying and Yang of the synapse

We uncovered a pathway for triggering synaptogenesis based on PI3K signaling, and a similar pathway that prevents synaptogenesis. Experiments combining pro- and anti-synaptogenic components of these pathways evidence their specificity and establish their hierarchical order.

Despite synapse number is constantly changing, values fluctuate within a normalcy range. Either the lack or the excess of synapses throughout the nervous system lead to lethality. Thus, a delicate equilibrium between pro and anti-synaptogenic signals becomes critical to control synapse number fluctuations.

Several of the tested signals appear ineffective on their own, but yield a phenotype when in combination with certain partners. These cases illustrate the complexity of functional interactions between signals of these pathways. Examples include the signaling crosspoint of Bsk/JNK or the transcriptional complex AP-1. It is plausible that these cases may rely on allosteric sites in the targeted proteins.

Many of the proteins analyzed are also involved in proliferation/growth or in differentiation. Therefore, we can envision different scenarios where cell size and synapse number are not causally related.

Thus, we have encountered genotypes that elicit overgrown NMJ, but with normal or reduced number of synapses, as well as genotypes with the opposite phenotype. Both situations are viable within a range of values, and our hypothesis on the equilibrated signaling suggests a compensatory effect that could represent a strategy to maintain synaptic homeostasis.

The current study is focused on the neuromuscular junction and one could question whether motor neurons and central neurons undergo the same signaling to determine their number of synapses. Muscles are single cells where Ca^{+2} signaling diffuse from a specific contact point (the post-synapsis) through the entire muscle. Thus, the exact location of the synapse may not influence the performance of the muscle. By contrast, accurate innervation might be more important in neurons of the central brain. That is, the geometry of the connectivity of central neurons may matter, but not so in the case of motor neurons. After all, the morphology of identified NMJs is far more variable than that of central neurons.

The magnitude of the synapse number changes elicited by the factors tested here are mostly within the range of 20-50%, these changes induce viable flies but are them significant to induce behavioral changes?

Indeed, previous studies from our group have shown that increments or decrements of synapse number in central neurons of the olfactory centers cause detectable changes in olfactory perception. These changes may include the transformation of an attractive response to a repulsive one for a given odorant and at a given concentration [5].

Therefore, it seems that our findings on larval motor neurons on the signaling equilibrium may be extrapolated to neurons in the CNS.

Does the number of synapses correlate with transmission efficiency?

In this work we describe a novel mechanism which explores the interaction between Frq2 and Ric8 depending upon Ca^{+2} surges. Our experiments, based on x-ray crystallography and direct binding assays, demonstrate the specificity of the interaction.

Thus, Ric8 binds to Frq2, not to Frq1, despite the two Frq proteins are 95% identical. The specificity for Frq2 results from key amino acids which regulate site accessibility to Ric8 in the Frq2 binding pocket.

At the NMJ, Frq2 exhibits opposite phenotypes over synapse number and transmission [98]. In our experiments, we demonstrate that Ric8 displays an effect as well, but contrary to Frq2, yields a similar impact over both neuronal features.

The downregulation of Ric8 leads to decrease in synapse number, whereas this phenotype requires Frq2 overexpression. Epistasis assays suggest that the binding induces the negative regulation of Frq2 over Ric8. Our observations sustain a hypothesis where Frq2 and Ric8 bind in the absence of Ca^{+2}. Ca^{+2} surges induce a conformational change of Frq2, which releases Ric8 to act as a guanyl exchange factor (GEF). That is, free Ric8 activates G alfa protein signaling cascade which is involved in synapse regulation and transmission, albeit in opposite directions.

These proteins regulate signaling responses by sensing changes in free Ca^{2+} and then transmitting the signal towards other functional levels. It might be possible that, as Ric8, Frq2 interacts with other partners following the release of Ric8 to play its effect over synaptic transmission.

The mechanisms by which Frq2 or G proteins, such Gs, display opposite effects over synapse number and release probability remain unknown. This might be a strategy to maintain the homeostasis at the NMJ. As for synapse number, transmission also fluctuates within a normalcy range. Either lack or excess of firing yields to neuron impairments. Different strategies can be used to maintain the equilibrium. Here, Frq2 could reduce release sites to maintain transmission levels in an optimal range.

Regarding Ric8 and transmitter release, we find that the number of synapses remains unaltered even though the release probability in these boutons does change. This apparent contradiction can be understood attending to the functional properties of the synaptic protein Bruchpilot (Brp). Super-resolution microscopy studies of Brp in single boutons [125] have revealed two different states of organization, clustered or free. Brp clustering correlates with an increase in the probability of neurotransmitter release. It would be desirable to

analyze the clustering/free ratio of Brp in the boutons with genetic manipulation of Ric8.

Hereto, the field has considered different neuronal types attending to their arborizations, ion channel endowment, neurotransmitter used, etc. It is likely, however, that future studies on synapse biology will have to incorporate quantitative data and local distribution of protein components of the synapse. This would render the synapse, rather than the neuron, as the true unit of neural physiology.

Local translation at the synapse

In our previous studies we induced genetic manipulations which up or downregulate specific proteins. This is a relatively slow process which requires transcription, translation and transport of proteins to specific points.

Learning and memory uses local translation at the synapse as a strategy to induce rapid changes. Here, we asked whether this mechanism operates in developing structures as well.

At the larval NMJ, modulation of Orb2 or its target Brat induces changes in the number of synapses. Whereas Orb2 downregulation decrease synapse number, lack of Brat have the opposite effect. This result indicates that Orb2 is pro-synaptogenic and Brat is anti-synaptogenic.

It is important to note that both proteins change the number of synapses but not the volume of the neuron. Therefore, we conclude that Orb2 and Brat determine active zones specification but not cell growth.

Although Brat has been reported as a negative regulator of cell proliferation, we do not observe this effect in our experiments. One possible explanation involves the temporal window of our experiments and the targeted cells.

Previous studies only showed oversized brains in which the Brat downregulation was targeted to proliferative cells. In fact, post-mitotic drivers, such as Elav-Gal4, with Brat mutants yield normal sized brains [126]. Our experiments using the post-mitotic driver D42-Gal4 support this evidence.

Hence, we postulate that Brat exhibits a dual function, modulator of proliferation (early stages) and synapse determinant (late stages). We also hypothesize that Orb2 regulates Brat translation. The experiments with Orb2 mutants, which inhibit oligomerization, reveal the functional relationship between both proteins.

9. Final remarks

We study the NMJ because of its relative simplicity, but this thesis research project provides information about the remarkable signaling complexity achieved in a motor neuron.

Here, we describe three new and independent mechanisms that control synapse number and activity. Furthermore, we describe the functional hierarchy of signals that compose two pathways, one pro- and other anti-synaptogenesis. Both pathways are cell autonomous.

Most likely, we have explored only a part of the pathways involved. For example, we are still far from knowing how these pathways in the synapse are connected with, or respond to, the environment.

Beyond the complexity of the mechanisms and their interactions, our findings describe a scenario in which the equilibrium between the pro- and the anti-synaptogenic signals maintain the homeostasis of the neuron.

Here we demonstrate how two major aspects of the neuron integrity are intimately linked, the number of synapses and the probability of release of neurotransmitter. Hence we must consider the combination of immunostaining and morphology analysis with electrophysiology or calcium imaging to accurately set the functionality of the neuron.

Deviations from the equilibrium often lead to pathologies such as the Fragile X and the Down syndromes where the number of synapses is in excess and, consequently, the activity per synapse tends to decrease.

Conversely, the loss of just about 16% of the inhibitory synapses in the frontal cortex seems to mark the difference between health and schizophrenia. Even poorly known disorders such as depression, anxiety, obsessive-compulsive mania or post-traumatic syndrome could result from a mild imbalance of synapse number and activity.

Understanding these mechanisms may shed light in the study of these pathological situations and how to correct them.

The study of specific proteins and their interactions begin to open the door to develop novel pharmacological treatments. As a proof of concept, recent work from our group has identified a small molecule from the phenothiazine group that inhibits the interaction between Frq2 and Ric8a. Administration of that drug to a genetic fly model of Fragile X reduces the abnormally high number of synapses to the point of restoring normal associative learning.

10. Future perspectives

In this work we study the molecular basis of formation and stabilization of synapses in a basal situation. Although we manipulate the NMJ to displace it from normalcy, we analyze these changes in a controlled environment. It is worth noting that our cells are constantly struggling against stress. Accumulation of reactive oxygen species (ROS) or misfolded proteins leads to cell destabilization. Moreover, external factors such heat or cold are perceived as stressors and induce cellular changes. In the context of neurons, these aggressions could affect synaptic connections and neuron integrity. Our next goal will be to study how stress conditions can affect the NMJ. If environmental stress change synapses, our aim will be to use the mechanisms described here to maintain neuron homeostasis in these situations.

11. Conclusions

- PI3K signaling pathway modulates the number of synapses at the NMJ.
- To establish functional NMJs, a delicate equilibrium between pro and anti-synaptogenic signals is required.
- Ric8 and Frq2 antagonistically regulate synapse number and neurotransmitter release.
- Frq2 binding affinity for Ric8 depends on Ca^{+2} surges and triggers the signaling cascade to control both neuronal features.
- While synapse number results from the negative regulation of Ric8 by Frq2, the mechanism to regulate neurotransmitter release deviates from this interaction.
- Orb2 and Brat modulate synapse formation but not cell growth at the NMJ.
- Orb2 conformational change is required for Brat local translation in neurons.
- The two major aspects of neuronal function, synapse number and transmission fluctuate within a normalcy range controlled by different signaling pathways.
- NMJ formation and maintenance require proteins involved in two mechanisms, cell growth and synapse determination.

12. Bibliography

1. Gan, W.B., et al., *Synaptic dynamism measured over minutes to months: age-dependent decline in an autonomic ganglion.* Nat Neurosci, 2003. **6**(9): p. 956-60.
2. Middei, S., M. Ammassari-Teule, and H. Marie, *Synaptic plasticity under learning challenge.* Neurobiol Learn Mem, 2014. **115**: p. 108-15.
3. Appelbaum, L., et al., *Circadian and homeostatic regulation of structural synaptic plasticity in hypocretin neurons.* Neuron, 2010. **68**(1): p. 87-98.
4. Beramendi, A., et al., *Neuromuscular junction in abdominal muscles of Drosophila melanogaster during adulthood and aging.* J Comp Neurol, 2007. **501**(4): p. 498-508.
5. Acebes, A., et al., *Synapse loss in olfactory local interneurons modifies perception.* J Neurosci, 2011. **31**(8): p. 2734-45.
6. Lacor, P.N., et al., *Abeta oligomer-induced aberrations in synapse composition, shape, and density provide a molecular basis for loss of connectivity in Alzheimer's disease.* J Neurosci, 2007. **27**(4): p. 796-807.
7. Benes, F.M. and S. Berretta, *GABAergic interneurons: implications for understanding schizophrenia and bipolar disorder.* Neuropsychopharmacology, 2001. **25**(1): p. 1-27.
8. Zeng, L.H., N.R. Rensing, and M. Wong, *The mammalian target of rapamycin signaling pathway mediates epileptogenesis in a model of temporal lobe epilepsy.* J Neurosci, 2009. **29**(21): p. 6964-72.
9. Dictenberg, J.B., et al., *A direct role for FMRP in activity-dependent dendritic mRNA transport links filopodial-spine morphogenesis to fragile X syndrome.* Dev Cell, 2008. **14**(6): p. 926-39.
10. Weitzdoerfer, R., et al., *Fetal life in Down syndrome starts with normal neuronal density but impaired dendritic spines and synaptosomal structure.* J Neural Transm Suppl, 2001(61): p. 59-70.
11. Gustafsson, B., et al., *Long-term potentiation in the hippocampus using depolarizing current pulses as the conditioning stimulus to single volley synaptic potentials.* J Neurosci, 1987. **7**(3): p. 774-80.
12. Castillo, P.E., *Presynaptic LTP and LTD of excitatory and inhibitory synapses.* Cold Spring Harb Perspect Biol, 2012. **4**(2).
13. Knight, D., et al., *Presynaptic plasticity and associative learning are impaired in a Drosophila presenilin null mutant.* Dev Neurobiol, 2007. **67**(12): p. 1598-613.
14. Handley, M.T., et al., *Structural and functional deficits in a neuronal calcium sensor-1 mutant identified in a case of autistic spectrum disorder.* PLoS One, 2010. **5**(5): p. e10534.
15. Thomas, B.J. and D.A. Wassarman, *A fly's eye view of biology.* Trends Genet, 1999. **15**(5): p. 184-90.
16. Hochner, B., et al., *Action-potential duration and the modulation of transmitter release from the sensory neurons of Aplysia in presynaptic facilitation and behavioral sensitization.* Proc Natl Acad Sci U S A, 1986. **83**(21): p. 8410-4.
17. McIntire, S.L., E. Jorgensen, and H.R. Horvitz, *Genes required for GABA function in Caenorhabditis elegans.* Nature, 1993. **364**(6435): p. 334-7.

18. Wullimann, M.F., L. Puelles, and H. Wicht, *Early postembryonic neural development in the zebrafish: a 3-D reconstruction of forebrain proliferation zones shows their relation to prosomeres.* Eur J Morphol, 1999. **37**(2-3): p. 117-21.
19. Brand, A.H. and N. Perrimon, *Targeted gene expression as a means of altering cell fates and generating dominant phenotypes.* Development, 1993. **118**(2): p. 401-15.
20. Keegan, L., G. Gill, and M. Ptashne, *Separation of DNA binding from the transcription-activating function of a eukaryotic regulatory protein.* Science, 1986. **231**(4739): p. 699-704.
21. Ma, J. and M. Ptashne, *A new class of yeast transcriptional activators.* Cell, 1987. **51**(1): p. 113-9.
22. Landgraf, M., et al., *The origin, location, and projections of the embryonic abdominal motorneurons of Drosophila.* J Neurosci, 1997. **17**(24): p. 9642-55.
23. Schmid, A., A. Chiba, and C.Q. Doe, *Clonal analysis of Drosophila embryonic neuroblasts: neural cell types, axon projections and muscle targets.* Development, 1999. **126**(21): p. 4653-89.
24. Ruiz-Canada, C. and V. Budnik, *Introduction on the use of the Drosophila embryonic/larval neuromuscular junction as a model system to study synapse development and function, and a brief summary of pathfinding and target recognition.* Int Rev Neurobiol, 2006. **75**: p. 1-31.
25. Jan, L.Y. and Y.N. Jan, *Properties of the larval neuromuscular junction in Drosophila melanogaster.* J Physiol, 1976. **262**(1): p. 189-214.
26. Johansen, J., et al., *Stereotypic morphology of glutamatergic synapses on identified muscle cells of Drosophila larvae.* J Neurosci, 1989. **9**(2): p. 710-25.
27. Prokop, A., et al., *Presynaptic development at the Drosophila neuromuscular junction: assembly and localization of presynaptic active zones.* Neuron, 1996. **17**(4): p. 617-26.
28. Hall, Z.W. and J.R. Sanes, *Synaptic structure and development: the neuromuscular junction.* Cell, 1993. **72 Suppl**: p. 99-121.
29. Burns, M.E. and G.J. Augustine, *Synaptic structure and function: dynamic organization yields architectural precision.* Cell, 1995. **83**(2): p. 187-94.
30. Dittman, J.S. and W.G. Regehr, *Calcium dependence and recovery kinetics of presynaptic depression at the climbing fiber to Purkinje cell synapse.* J Neurosci, 1998. **18**(16): p. 6147-62.
31. Stevens, C.F. and J.F. Wesseling, *Activity-dependent modulation of the rate at which synaptic vesicles become available to undergo exocytosis.* Neuron, 1998. **21**(2): p. 415-24.
32. Borst, A., *Periodic current injection (PCI)--a new method to image steady-state membrane potential of single neurons in situ using extracellular voltage-sensitive dyes.* Z Naturforsch C, 1995. **50**(5-6): p. 435-8.
33. Geppert, M., et al., *Synaptotagmin I: a major Ca2+ sensor for transmitter release at a central synapse.* Cell, 1994. **79**(4): p. 717-27.
34. Katz, B. and R. Miledi, *The timing of calcium action during neuromuscular transmission.* J Physiol, 1967. **189**(3): p. 535-44.

35. Menon, K.P., R.A. Carrillo, and K. Zinn, *Development and plasticity of the Drosophila larval neuromuscular junction.* Wiley Interdiscip Rev Dev Biol, 2013. **2**(5): p. 647-70.
36. Mendoza, C., et al., *Novel isoforms of Dlg are fundamental for neuronal development in Drosophila.* J Neurosci, 2003. **23**(6): p. 2093-101.
37. Sink, H. and P.M. Whitington, *Location and connectivity of abdominal motoneurons in the embryo and larva of Drosophila melanogaster.* J Neurobiol, 1991. **22**(3): p. 298-311.
38. Shishido, E., M. Takeichi, and A. Nose, *Drosophila synapse formation: regulation by transmembrane protein with Leu-rich repeats, CAPRICIOUS.* Science, 1998. **280**(5372): p. 2118-21.
39. Kose, H., et al., *Homophilic synaptic target recognition mediated by immunoglobulin-like cell adhesion molecule Fasciclin III.* Development, 1997. **124**(20): p. 4143-52.
40. Taniguchi, H., et al., *Functional dissection of drosophila capricious: its novel roles in neuronal pathfinding and selective synapse formation.* J Neurobiol, 2000. **42**(1): p. 104-16.
41. Packard, M., et al., *The Drosophila Wnt, wingless, provides an essential signal for pre- and postsynaptic differentiation.* Cell, 2002. **111**(3): p. 319-30.
42. Miech, C., et al., *Presynaptic local signaling by a canonical wingless pathway regulates development of the Drosophila neuromuscular junction.* J Neurosci, 2008. **28**(43): p. 10875-84.
43. Fouquet, W., et al., *Maturation of active zone assembly by Drosophila Bruchpilot.* J Cell Biol, 2009. **186**(1): p. 129-45.
44. Kittel, R.J., et al., *Bruchpilot promotes active zone assembly, Ca2+ channel clustering, and vesicle release.* Science, 2006. **312**(5776): p. 1051-4.
45. Kaufmann, N., et al., *Drosophila liprin-alpha and the receptor phosphatase Dlar control synapse morphogenesis.* Neuron, 2002. **34**(1): p. 27-38.
46. Ohtsuka, T., et al., *Cast: a novel protein of the cytomatrix at the active zone of synapses that forms a ternary complex with RIM1 and munc13-1.* J Cell Biol, 2002. **158**(3): p. 577-90.
47. Carrillo, R.A., et al., *Presynaptic activity and CaMKII modulate retrograde semaphorin signaling and synaptic refinement.* Neuron, 2010. **68**(1): p. 32-44.
48. Tessier, C.R. and K. Broadie, *Drosophila fragile X mental retardation protein developmentally regulates activity-dependent axon pruning.* Development, 2008. **135**(8): p. 1547-57.
49. Schuster, C.M., et al., *Genetic dissection of structural and functional components of synaptic plasticity. II. Fasciclin II controls presynaptic structural plasticity.* Neuron, 1996. **17**(4): p. 655-67.
50. Liu, Z., et al., *Distinct presynaptic and postsynaptic dismantling processes of Drosophila neuromuscular junctions during metamorphosis.* J Neurosci, 2010. **30**(35): p. 11624-34.
51. Afroz, S., et al., *Synaptic pruning in the female hippocampus is triggered at puberty by extrasynaptic GABAA receptors on dendritic spines.* Elife, 2016. **5**.

52. Sherwood, N.T., et al., *Drosophila spastin regulates synaptic microtubule networks and is required for normal motor function.* PLoS Biol, 2004. **2**(12): p. e429.
53. Collins, C.A., et al., *Highwire restrains synaptic growth by attenuating a MAP kinase signal.* Neuron, 2006. **51**(1): p. 57-69.
54. Marques, G. and B. Zhang, *Retrograde signaling that regulates synaptic development and function at the Drosophila neuromuscular junction.* Int Rev Neurobiol, 2006. **75**: p. 267-85.
55. Schuster, C.M., et al., *Genetic dissection of structural and functional components of synaptic plasticity. I. Fasciclin II controls synaptic stabilization and growth.* Neuron, 1996. **17**(4): p. 641-54.
56. Eaton, B.A. and G.W. Davis, *LIM Kinase1 controls synaptic stability downstream of the type II BMP receptor.* Neuron, 2005. **47**(5): p. 695-708.
57. Chang, F., et al., *Involvement of PI3K/Akt pathway in cell cycle progression, apoptosis, and neoplastic transformation: a target for cancer chemotherapy.* Leukemia, 2003. **17**(3): p. 590-603.
58. Nelson, C.M. and C.S. Chen, *Cell-cell signaling by direct contact increases cell proliferation via a PI3K-dependent signal.* FEBS Lett, 2002. **514**(2-3): p. 238-42.
59. Foukas, L.C., et al., *Activity of any class IA PI3K isoform can sustain cell proliferation and survival.* Proc Natl Acad Sci U S A, 2010. **107**(25): p. 11381-6.
60. Morgensztern, D. and H.L. McLeod, *PI3K/Akt/mTOR pathway as a target for cancer therapy.* Anticancer Drugs, 2005. **16**(8): p. 797-803.
61. Berns, K., et al., *A functional genetic approach identifies the PI3K pathway as a major determinant of trastuzumab resistance in breast cancer.* Cancer Cell, 2007. **12**(4): p. 395-402.
62. Samuels, Y. and V.E. Velculescu, *Oncogenic mutations of PIK3CA in human cancers.* Cell Cycle, 2004. **3**(10): p. 1221-4.
63. Karar, J. and A. Maity, *PI3K/AKT/mTOR Pathway in Angiogenesis.* Front Mol Neurosci, 2011. **4**: p. 51.
64. Martin-Pena, A., et al., *Age-independent synaptogenesis by phosphoinositide 3 kinase.* J Neurosci, 2006. **26**(40): p. 10199-208.
65. Arnes, M., et al., *Amyloid beta42 peptide is toxic to non-neural cells in Drosophila yielding a characteristic metabolite profile and the effect can be suppressed by PI3K.* Biol Open, 2017. **6**(11): p. 1664-1671.
66. Cuesto, G., et al., *GSK3beta inhibition promotes synaptogenesis in Drosophila and mammalian neurons.* PLoS One, 2015. **10**(3): p. e0118475.
67. Gorczyca, M., C. Augart, and V. Budnik, *Insulin-like receptor and insulin-like peptide are localized at neuromuscular junctions in Drosophila.* J Neurosci, 1993. **13**(9): p. 3692-704.
68. Keshishian, H., et al., *Cellular mechanisms governing synaptic development in Drosophila melanogaster.* J Neurobiol, 1993. **24**(6): p. 757-87.
69. Tokoro, T., et al., *Localization of the active zone proteins CAST, ELKS, and Piccolo at neuromuscular junctions.* Neuroreport, 2007. **18**(4): p. 313-6.

70. Wagh, D.A., et al., *Bruchpilot, a protein with homology to ELKS/CAST, is required for structural integrity and function of synaptic active zones in Drosophila.* Neuron, 2006. **49**(6): p. 833-44.
71. Kittel, R.J., et al., *Active zone assembly and synaptic release.* Biochem Soc Trans, 2006. **34**(Pt 5): p. 939-41.
72. Kurdyak, P., et al., *Differential physiology and morphology of motor axons to ventral longitudinal muscles in larval Drosophila.* J Comp Neurol, 1994. **350**(3): p. 463-72.
73. Lnenicka, G.A. and H. Keshishian, *Identified motor terminals in Drosophila larvae show distinct differences in morphology and physiology.* J Neurobiol, 2000. **43**(2): p. 186-97.
74. Quick, M.W., *The role of SNARE proteins in trafficking and function of neurotransmitter transporters.* Handb Exp Pharmacol, 2006(175): p. 181-96.
75. Chen, Y.A. and R.H. Scheller, *SNARE-mediated membrane fusion.* Nat Rev Mol Cell Biol, 2001. **2**(2): p. 98-106.
76. Schoch, S., et al., *SNARE function analyzed in synaptobrevin/VAMP knockout mice.* Science, 2001. **294**(5544): p. 1117-22.
77. Katz, B. and R. Miledi, *Spontaneous and evoked activity of motor nerve endings in calcium Ringer.* J Physiol, 1969. **203**(3): p. 689-706.
78. Berridge, M.J., M.D. Bootman, and H.L. Roderick, *Calcium signalling: dynamics, homeostasis and remodelling.* Nat Rev Mol Cell Biol, 2003. **4**(7): p. 517-29.
79. Long, A.A., et al., *Presynaptic calcium channel localization and calcium-dependent synaptic vesicle exocytosis regulated by the Fuseless protein.* J Neurosci, 2008. **28**(14): p. 3668-82.
80. Yang, S.N., Y.G. Tang, and R.S. Zucker, *Selective induction of LTP and LTD by postsynaptic [Ca2+]i elevation.* J Neurophysiol, 1999. **81**(2): p. 781-7.
81. Zundorf, G. and G. Reiser, *Calcium dysregulation and homeostasis of neural calcium in the molecular mechanisms of neurodegenerative diseases provide multiple targets for neuroprotection.* Antioxid Redox Signal, 2011. **14**(7): p. 1275-88.
82. Zamponi, G.W. and K.P. Currie, *Regulation of Ca(V)2 calcium channels by G protein coupled receptors.* Biochim Biophys Acta, 2013. **1828**(7): p. 1629-43.
83. Herlitze, S., et al., *Modulation of Ca2+ channels by G-protein beta gamma subunits.* Nature, 1996. **380**(6571): p. 258-62.
84. Bean, B.P., *Neurotransmitter inhibition of neuronal calcium currents by changes in channel voltage dependence.* Nature, 1989. **340**(6229): p. 153-6.
85. Raingo, J., A.J. Castiglioni, and D. Lipscombe, *Alternative splicing controls G protein-dependent inhibition of N-type calcium channels in nociceptors.* Nat Neurosci, 2007. **10**(3): p. 285-92.
86. Suh, B.C., K. Leal, and B. Hille, *Modulation of high-voltage activated Ca(2+) channels by membrane phosphatidylinositol 4,5-bisphosphate.* Neuron, 2010. **67**(2): p. 224-38.
87. Kammermeier, P.J., V. Ruiz-Velasco, and S.R. Ikeda, *A voltage-independent calcium current inhibitory pathway activated by muscarinic*

agonists in rat sympathetic neurons requires both Galpha q/11 and Gbeta gamma. J Neurosci, 2000. **20**(15): p. 5623-9.
88. Yanez, M., J. Gil-Longo, and M. Campos-Toimil, *Calcium binding proteins.* Adv Exp Med Biol, 2012. **740**: p. 461-82.
89. Lisman, J., H. Schulman, and H. Cline, *The molecular basis of CaMKII function in synaptic and behavioural memory.* Nat Rev Neurosci, 2002. **3**(3): p. 175-90.
90. Pongs, O., et al., *Frequenin--a novel calcium-binding protein that modulates synaptic efficacy in the Drosophila nervous system.* Neuron, 1993. **11**(1): p. 15-28.
91. Nef, S., et al., *Identification of neuronal calcium sensor (NCS-1) possibly involved in the regulation of receptor phosphorylation.* J Recept Signal Transduct Res, 1995. **15**(1-4): p. 365-78.
92. Dason, J.S., et al., *Frequenin/NCS-1 and the Ca2+-channel alpha1-subunit co-regulate synaptic transmission and nerve-terminal growth.* J Cell Sci, 2009. **122**(Pt 22): p. 4109-21.
93. Saab, B.J., et al., *NCS-1 in the dentate gyrus promotes exploration, synaptic plasticity, and rapid acquisition of spatial memory.* Neuron, 2009. **63**(5): p. 643-56.
94. Nakamura, T.Y., et al., *Possible Signaling Pathways Mediating Neuronal Calcium Sensor-1-Dependent Spatial Learning and Memory in Mice.* PLoS One, 2017. **12**(1): p. e0170829.
95. Koh, P.O., et al., *Up-regulation of neuronal calcium sensor-1 (NCS-1) in the prefrontal cortex of schizophrenic and bipolar patients.* Proc Natl Acad Sci U S A, 2003. **100**(1): p. 313-7.
96. D'Onofrio, S., et al., *Modulation of gamma oscillations in the pedunculopontine nucleus by neuronal calcium sensor protein-1: relevance to schizophrenia and bipolar disorder.* J Neurophysiol, 2015. **113**(3): p. 709-19.
97. Bahi, N., et al., *IL1 receptor accessory protein like, a protein involved in X-linked mental retardation, interacts with Neuronal Calcium Sensor-1 and regulates exocytosis.* Hum Mol Genet, 2003. **12**(12): p. 1415-25.
98. Romero-Pozuelo, J., et al., *Chronic and acute alterations in the functional levels of Frequenins 1 and 2 reveal their roles in synaptic transmission and axon terminal morphology.* Eur J Neurosci, 2007. **26**(9): p. 2428-43.
99. Martin, K.C. and A. Ephrussi, *mRNA localization: gene expression in the spatial dimension.* Cell, 2009. **136**(4): p. 719-30.
100. Bassell, G.J. and S.T. Warren, *Fragile X syndrome: loss of local mRNA regulation alters synaptic development and function.* Neuron, 2008. **60**(2): p. 201-14.
101. Kiebler, M.A. and G.J. Bassell, *Neuronal RNA granules: movers and makers.* Neuron, 2006. **51**(6): p. 685-90.
102. Majumdar, A., et al., *Critical role of amyloid-like oligomers of Drosophila Orb2 in the persistence of memory.* Cell, 2012. **148**(3): p. 515-29.
103. Ashley, C.T., Jr., et al., *FMR1 protein: conserved RNP family domains and selective RNA binding.* Science, 1993. **262**(5133): p. 563-6.
104. Narayanan, U., et al., *S6K1 phosphorylates and regulates fragile X mental retardation protein (FMRP) with the neuronal protein synthesis-dependent mammalian target of rapamycin (mTOR) signaling cascade.* J Biol Chem, 2008. **283**(27): p. 18478-82.

105. Muddashetty, R.S., et al., *Reversible inhibition of PSD-95 mRNA translation by miR-125a, FMRP phosphorylation, and mGluR signaling.* Mol Cell, 2011. **42**(5): p. 673-88.
106. Darnell, J.C., et al., *FMRP stalls ribosomal translocation on mRNAs linked to synaptic function and autism.* Cell, 2011. **146**(2): p. 247-61.
107. Kim, E.Y., et al., *Drosophila CLOCK protein is under posttranscriptional control and influences light-induced activity.* Neuron, 2002. **34**(1): p. 69-81.
108. Brennecke, J., et al., *bantam encodes a developmentally regulated microRNA that controls cell proliferation and regulates the proapoptotic gene hid in Drosophila.* Cell, 2003. **113**(1): p. 25-36.
109. Enright, A.J., et al., *MicroRNA targets in Drosophila.* Genome Biol, 2003. **5**(1): p. R1.
110. Picao-Osorio, J., et al., *MicroRNA-encoded behavior in Drosophila.* Science, 2015. **350**(6262): p. 815-20.
111. Caygill, E.E. and L.A. Johnston, *Temporal regulation of metamorphic processes in Drosophila by the let-7 and miR-125 heterochronic microRNAs.* Curr Biol, 2008. **18**(13): p. 943-50.
112. Siegel, G., et al., *A functional screen implicates microRNA-138-dependent regulation of the depalmitoylation enzyme APT1 in dendritic spine morphogenesis.* Nat Cell Biol, 2009. **11**(6): p. 705-16.
113. Karr, J., et al., *Regulation of glutamate receptor subunit availability by microRNAs.* J Cell Biol, 2009. **185**(4): p. 685-97.
114. Beveridge, N.J., et al., *Schizophrenia is associated with an increase in cortical microRNA biogenesis.* Mol Psychiatry, 2010. **15**(12): p. 1176-89.
115. Wang, D., et al., *Targeting of microRNA-199a-5p protects against pilocarpine-induced status epilepticus and seizure damage via SIRT1-p53 cascade.* Epilepsia, 2016. **57**(5): p. 706-16.
116. Hake, L.E. and J.D. Richter, *CPEB is a specificity factor that mediates cytoplasmic polyadenylation during Xenopus oocyte maturation.* Cell, 1994. **79**(4): p. 617-27.
117. Huang, Y.S., et al., *CPEB3 and CPEB4 in neurons: analysis of RNA-binding specificity and translational control of AMPA receptor GluR2 mRNA.* EMBO J, 2006. **25**(20): p. 4865-76.
118. Si, K., S. Lindquist, and E.R. Kandel, *A neuronal isoform of the aplysia CPEB has prion-like properties.* Cell, 2003. **115**(7): p. 879-91.
119. Si, K., et al., *A neuronal isoform of CPEB regulates local protein synthesis and stabilizes synapse-specific long-term facilitation in aplysia.* Cell, 2003. **115**(7): p. 893-904.
120. Mastushita-Sakai, T., et al., *Drosophila Orb2 targets genes involved in neuronal growth, synapse formation, and protein turnover.* Proc Natl Acad Sci U S A, 2010. **107**(26): p. 11987-92.
121. Khan, M.R., et al., *Amyloidogenic Oligomerization Transforms Drosophila Orb2 from a Translation Repressor to an Activator.* Cell, 2015. **163**(6): p. 1468-83.
122. Kruttner, S., et al., *Drosophila CPEB Orb2A mediates memory independent of Its RNA-binding domain.* Neuron, 2012. **76**(2): p. 383-95.
123. Xu, S., et al., *The CPEB protein Orb2 has multiple functions during spermatogenesis in Drosophila melanogaster.* PLoS Genet, 2012. **8**(11): p. e1003079.

124. Hafer, N., et al., *The Drosophila CPEB protein Orb2 has a novel expression pattern and is important for asymmetric cell division and nervous system function.* Genetics, 2011. **189**(3): p. 907-21.
125. Ehmann, N., et al., *Quantitative super-resolution imaging of Bruchpilot distinguishes active zone states.* Nat Commun, 2014. **5**: p. 4650.
126. Shi, W., et al., *Brain tumor regulates neuromuscular synapse growth and endocytosis in Drosophila by suppressing mad expression.* J Neurosci, 2013. **33**(30): p. 12352-63.